THE UNIVERSITY *of* EDINBURGH

Biochemical determinants of CDK1 phosphorylation of cell cycle substrates using mass spectrometry-based phospho-proteomics

Aymen al-Rawi

A thesis presented for the degree of Doctor of Philosophy

The Institute of Cell Biology

University of Edinburgh

October 2022

Acknowledgements

I would like to begin this thesis by expressing my utmost gratitude to my two supervisors Dr Tony Ly and Professor William C. Earnshaw, to whom I owe everything that I learnt throughout my PhD, from the basics of working in a laboratory up to writing research grants. Words cannot express how much I shall miss working with them. I would also like to extend this to my thesis committee members Professor Adele Marston and Dr Julie Welburn for their valuable guidance during my PhD, and to Professor JP Arulanandam for all the collaborations that we had with his group.

I would also like to thank the past and current members of the Ly Laboratory Dr Van Kelly, Dr Ananya Kar, Dr Rona Sharp, David Lewis, Edward Kay, Juan Valverde, Rene Rivera, Catriona Liggett, Verena Banschbach, Yixin Wang, Susanne Zimbelmann, Ease Liu, Sarah Chandler, Melanie Lim, Keerthi Sivan and Ioanna Demetriou for making this journey seem so easy. I am also grateful for all the valuable advice from Dr Kumiko Samejima, Dr Lucy Remnant, Dr Bram Prevo, Dr Maria Abad, and from members of Professor Julian Blow's and Dr Constance Alabert's laboratories.

Finally, I would like to express my gratitude to the Darwin Trust for generously funding my PhD at the University of Edinburgh. Without their support, none of the work that I am about to present here would have been possible. I would also like to thank the postgraduate office advisors Karen Woodcock and Helena Sim for all their support, especially during the time that I spent at the University of Dundee.

This thesis is dedicated to my parents Dania and Saad, to my brother Ahmed, to my aunts Iman and Fitnah, and …

to my dear friend Muhanad al-Qaisy (1949 – 2021).

Aymen al-Rawi.

Declaration

By signing this:

I declare that the thesis has been composed by myself and that the work has not be submitted for any other degree or professional qualification. I confirm that the work submitted is my own, except where work which has formed part of jointly-authored publications has been included. My contribution and those of the other authors to this work have been explicitly indicated below. I confirm that appropriate credit has been given within this thesis where reference has been made to the work of others.

Some of the work presented in chapters 3-6 either was previously published or has been submitted for publication. A full description of my contribution to the three scientific papers that featured this work is described in the Appendix.

Aymen al-Rawi

Date: 14 October 2022

Abstract and summary

Abstract

The cell cycle is a complex series of events that results in one parental cell dividing into two daughter cells. Division only occurs when cells have successfully replicated their DNA, to create progeny each with a copy of their genome. Protein phosphorylation is one mechanism that regulates the cell cycle. Kinases such as the polo-like family, the Auroras, and the Cyclin dependent kinases (CDKs) along with phosphatases, such as PP2A and PP1, form dynamic regulatory circuits that activate and inactivate substrate proteins through reversible phosphorylation of targeted residues. CDK1 is the main regulator of protein phosphorylation in mitosis, carrying out hundreds of these phosphorylations. Monomeric CDK1, however, is inactive and requires either a Cyclin A or Cyclin B partner to gain activity. Progressive expression and degradation of the two Cyclins determine the activity of CDK1 during the cell cycle. Besides, the Cyclin partner was suggested to mediate CDK1 substrate choice. This role, however, has always been a point of debate. Cks1 is another element in CDK1 complexes with even less understood role in substrate phosphorylation. My project aimed to characterise these substrates based on their dependency on CDK1 activity, its Cyclin partner, and the presence of a Cks1 in its complex, in order to understand how the temporal ordering of their phosphorylation is maintained throughout the cell cycle. To achieve that, I developed an *in vitro* kinase assay through which I phosphorylated fixed and permeabilized cells using recombinant CDK1 in complex with different subunits and assessed their phospho-proteome using mass spectrometry. Results revealed that both CDK1 activity and its Cyclin partner determine the substrate to be targeted for phosphorylation. The presence of Cks1, on the other hand, increased the number of phosphorylated residues on the targeted substrates. This data also unveiled the ability of CDK1 to phosphorylate sites lacking the +1 Proline in its S/TPXK/R consensus motif in the presence of either Cyclin A2 or

Cks1 in its complexes. This non-Proline directed phosphorylation uncovered new details of the mechanism by which CDK1 maintains the temporal ordering of substrates phosphorylation. The data here also reveals CDK1 phosphorylation of mitotic sites for which an upstream kinase has not been reported.

Summary (non-technical)

There are several processes that cells need to maintain in order to stay alive. These include energy production, self-defence, and division. Division of cells occurs through a complex process known as the cell cycle. It ensures that older cells of different tissues and organs are replaced by newer ones once they reach the end of their lifespan. The cell cycle is driven by a combination of enzymes that work together to initiate and terminate the events of this process. Furthermore, cells exert mechanisms by which they tightly control the functions of these enzymes. This is to ensure that the cell cycle only occurs when needed and to maintain its integrity. Dysregulations of these mechanisms can result in abnormal accumulation of cells and cancer. One of the major enzymes that drive the cell cycle is called CDK1. In this thesis, I aimed to expand on what is currently known about the regulation of CDK1 in cells. To do this, I developed a novel experimental system that involved a combination of biochemical approaches and comprehensive data analysis. As a result, I was able to uncover new details of the mechanisms by which cells ensure that CDK1 is only functional when it should be. This thesis extends our understanding of how the cell cycle is regulated in our cells.

Table of contents

List of figures

Chapter 1:

Thesis introduction

1.1 General overview of the cell cycle

Cells are the simplest units of life. Whether making up multicellular organisms or living on their own as a unicellular organism, all cells need to maintain basic processes to survive. These include metabolism, protein synthesis, immunity, and reproduction. In eukaryotic cells, clonal reproduction is achieved via a complex process called the *cell cycle*[1]. Here, cells undergo four phases with distinct morphological phenotypes: G1, S, G2 then M. During these phases, a cell replicates its DNA, condenses it into chromosomes, segregates these chromosomes, then physically divides into two daughter cells (Figure 1.1). In the presence of both growth factors and external cues, the cell cycle begins by initiating transcription and protein synthesis for components that are essential for division[2], such as ribosomes[3]. This occurs in the first gap (G1) phase. Furthermore, a group of proteins that include ORC, Cdc6 and Cdt1 load components of the minichromosome maintenance (MCM) complex onto chromatin, all creating a pre-replication complex[4]. The loading of MCMs stops as cells progress into the DNA synthesis (S) phase[5]. The transition from G1 to S marks the beginning of DNA replication[6]. During S phase, components of the pre-initiation complex, such as Cdc45, MCM10 and PCNA, are assembled on the DNA[7]. This complex creates replication forks that allow DNA Polymerase to replicate the DNA and results in cells having two identical sets of chromosomes. When this process is complete, cells exit S phase and enter the second gap (G2) of the cell cycle. By this point, cells are described to have a DNA content of 4N instead of the pre-replication 2N, where N is the number of complete sets of chromosomes. As well as DNA replication, S phase also involves duplication of the centrioles – ninefold symmetric structures that form the nucleating centres of what will become the spindle poles in M phase.

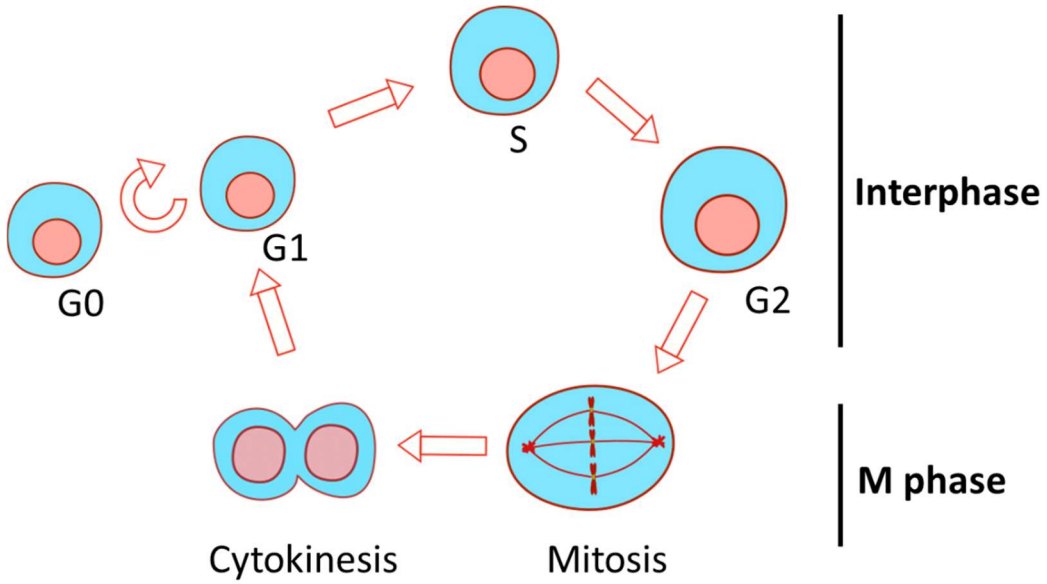

Figure 1.1: The somatic cell cycle phases.

In G2, cells continue to grow and synthesise more components before entering the subsequent M phase. Up until the end of G2, cells are described to be in *interphase* (Figure 1.1).

During M phase, first the DNA is condensed into chromosomes and segregated in *mitosis*, then the cytoplasm is divided to produce two identical daughter cells during *cytokinesis*[1,8] (Figure 1.1). The condensation of replicated DNA into chromosomes facilitates the segregation of sister chromatids by reducing their complexity. Coinciding with DNA condensation, the nuclear envelope of the cell breaks down, allowing components of both nucleoplasm and cytoplasm to mix. In addition, the two pairs of centrioles separate and create pericentriolar matrices that convert them into centrosomes residing at the two poles of the cell. One advantage of the nuclear envelope breakdown is that it allows the spindle microtubules that emanate from these centrosomes to capture the chromosomes during prometaphase[9,10]. This binding is critical for proper alignment of these chromosomes at the centre of the cell during metaphase, which is the mitotic subphase that proceeds chromosomal segregation.

The association of the spindle microtubules with chromosomes in prometaphase requires the establishment of a very complex, multi-subunit protein structure known as the kinetochore[11]. The assembly of the kinetochore does not occur on random areas of chromosomes, however. Instead, it is established on epigenetically defined regions known as the centromeres[12]. Here, components of the constitutive centromere associated network (CCAN), bind the centromere directly, while NUF2 and NDC80, which are components of the outer kinetochore, bind microtubules. In addition, the outer kinetochore bears disordered regions, which as well as being domains for signalling and functional regulation, provide structural flexibility[13]. Both points allow the kinetochore to serve as a flexible linker of chromosomes to microtubules in mitotic cells.

The establishment of a proper metaphase plate requires each of the two sister chromatids of a chromosome to associate with microtubules emanating from the opposite pole to that associated with the other one. Once this happens, cells initiate the segregation of their chromosomes by pulling apart the sister chromatids towards the spindle poles. This marks the beginning of anaphase and is achieved through the depolymerising and shrinking of microtubules, which are now tightly bound to the centromeres through the kinetochore. Once the chromatids reach the opposite poles, nuclear envelopes begin to form around them[14], and cells begin to undergo extensive cytoskeletal reorganisations to create a contractile ring that eventually cleaves their cytoplasm during cytokinesis[15]. This represents the very last mitotic subphase and is known as telophase.

Cytokinesis is characterised by de-condensation of chromosomes, polarisation of cells and perhaps most importantly, contraction of the cytoskeletal fibres that make up the contractile ring. This last step causes parental cells to be ‘pinched off’, each creating two daughter cells. It also marks the end of the cell cycle. The new daughter cells will either be in G1 phase for another round of division, or enter a quiescent state known as G0[16] (Figure 1.1). Whether cells are in G1 or G0 depends on

numerous factors, including the presence of DNA damage and the availability of nutrients and external stimuli. A full illustration of M phase events is in Figure 1.2.

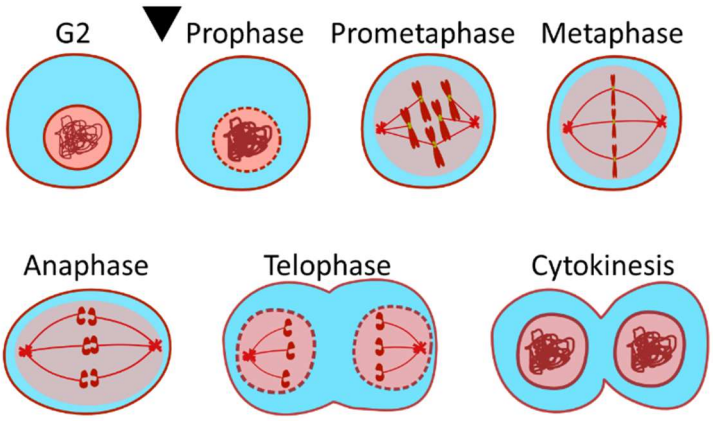

Figure 1.2: cellular re-organisations during G2 and M phases. The black arrow represents the beginning of M phase.

Frequent cell divisions create potential for errors in genome duplication and segregation[17,18]. These errors can have catastrophic consequences, not only for the cell, but the whole organism. An example of this is carcinogenesis. The latter is a term describing the transformation of a healthy growing cell into a cancerous one. So, how does a cell prevent such errors from occurring? Cells create a system through which they can tightly control the transitions from one major event to the next. This system relies on setting up *checkpoints* across the cell cycle[19]. From the description above, one can conclude that there are two major events that need to happen for successful completion of a cell cycle. The initiation of DNA replication that occurs during S phase and the equal distribution of this replicated DNA between the two daughter cells during M phase. Indeed, checkpoints exist during the cell cycle to ensure faithful occurrence of each of these events. The first is during the transition from G1 to S phase, and it prevents cells from prematurely replicating their DNA[20]. A G2 checkpoint then ensures the absence of major DNA replication errors[21]. And last, but not least, is a mitotic spindle assembly checkpoint (SAC), which guarantees faithful attachments between the microtubules and the kinetochore when chromosomal segregation happens[22]. A substantial body of literature has

linked several types of cancers to dysregulation of these checkpoints[23]. Furthermore, chemotherapeutic drug agents have been developed to target these checkpoints. Both Palbociclib and Abemaciclib are examples of drugs that were developed to target the G1/S transition and were approved for clinical use by the United States Food and Drug Administration[24]. In addition, Alvocidib (or Flavopiridol), which prevents M phase entry, is under clinical trial for treatment of lymphomas and solid tumours[25].

Successful cell divisions do not only require damage-free replicated DNA and faithfully segregated chromosomes, but also maintenance to the order in which these events occur. Segregation of DNA before its replication will produce two daughter cells with completely different genomes. Similarly, the occurrence of cytokinesis before the chromosomes have properly aligned in metaphase will cause uneven distribution of genetic material. Therefore, it is important for cells ensure that all the molecular events described above occur in the right order. The initiation and regulation of all the cell cycle events described above are mainly carried out by two families of enzymes known as the Cyclin dependent kinases (CDKs) and protein phosphatases 1 (PP1) and 2A (PP2A). This raises a question about the molecular mechanisms that allow these enzymes to trigger the right event at the right time. Indeed, several elegant studies where abundance or activity of CDKs and protein phosphatases were altered have reported severe phenotypes, resulting from dysregulation of cell cycle events ordering[26-28].

So far, I have presented the different events that occur during a human somatic cell cycle and raised a question about the molecular mechanisms that allow CDKs, PP1 and PP2A to regulate the ordering of this process. In this chapter, I will begin by briefly describing one of the most common biochemical interactions occurring in a dividing cell. I will then shift my focus to CDKs, PP1 and PP2A, and present one of the most common techniques that current cell cycle studies have intensively utilised, in the last part of this chapter. Finally, I will end the chapter by describing a model

substrate for this study and by stating the aim of this thesis and any potential impact that it may have on our understanding of the human cell cycle.

1.2 Cell cycle control

Progression through the cell cycle can be attributed to the molecular changes that accompany that process. Structural components, such as the kinetochore and microtubules, and enzymes that carry out catalysis, like *kinases*, are examples of proteins important for cell division. Perhaps the latter are of particular significance for this study to highlight. Kinases are a group of proteins that add phosphate groups to targeted substrates[29]. Because of its negative charge, this phosphate group can induce changes in the three-dimensional structure of the substrate, leading to an impact on its function. In human cells, there are 518 putative protein kinases expressed[30], all sharing a central catalytic domain. Since their discovery in the 1950s, the importance of these enzymes in different cellular processes has been extensively studied, including cell division. Substrate *phosphorylation* by protein kinases is central to the regulation of cell cycle progression[31]. For example, crossing the G1/S border and S phase entry is associated with phosphorylation of the protein Retinoblastoma (RB) by the kinases CDK4 and 6[32]. This phosphorylation promotes S phase entry by reducing the inhibitory effect that RB exerts on the transcription of genes essential for DNA replication. Similarly, for DNA replication to happen, the kinase DDK phosphorylates subunits of the pre-initiation complex, which allows the elongation of the nascent, replicating DNA to occur[33]. In mitotic cells, phosphorylation of the kinetochore proteins determines the extent of their attachment to spindle microtubules[34]. Kinases are also involved in checkpoint activation. For example Aurora B activity is required for the recruitment of Mps1 to the kinetochore[35]. Phosphorylation of Knl1 and Mad1 by Mps1 then leads to the inactivation of the anaphase promoting complex/Cyclosome (APC/C)[36,37], which prevents chromosomal segregation, holding the cell in metaphase. What makes all

these phosphorylation reactions suitable for regulating dynamic processes required for cell division is the fact that they are reversible.

1.2.1 Cell cycle kinases are counteracted by phosphatases

The reversibility in phosphorylation of cell cycle-related proteins is an important factor for creating and maintaining a *temporal order* for the events of this process[38]. What this means is that through phosphorylation and *dephosphorylation* of substrates, cells are able to control the initiation and termination of their division events. Dephosphorylation of substrates is carried out by another group of enzymes called *phosphatases*[39,40]. Just like phosphorylation, dephosphorylation can also be activating or inhibitory, depending on the context. Two types of serine/threonine phosphatases are considered the main regulators of the human cell cycle, PP1 and PP2A. Both PP1 and PP2A are holoenzymes comprised of catalytic and regulatory subunits. PP1 has more than 200 possible interactors that provide it with substrate specificity[41]. PP2A holoenzyme, on the other hand, is a heterotrimer comprised of a catalytic subunit termed C, a scaffolding subunit A and either a B55 or B56 regulatory subunit[42]. Both PP1 and PP2A-B55 are inactivated during mitosis, as their activity cause dephosphorylation of substrates that lead to mitotic exit (Reviewed by Holder et al.[43]). For example, removal of the Mps1-induced phosphorylation from Knl1 by PP2A-B55, promotes the activation of APC/C, allowing anaphase to take place[44]. Distinct mechanisms regulate the activities of PP1 and PP2A-B55 during M phase. CDK1 driven phosphorylation of a C terminal site inactivates PP1[45]. This is then reversed by autocatalytic activity that removes the inhibitory phosphate at mitotic exit[46]. PP2A-B55, on the other hand, is inactivated by the MASTL/Greatwall-ENSA/ARPP19 pathway[47]. Here, the kinase MASTL/Greatwall phosphorylates its substrates ENSA and ARPP19, which then compete with phosphorylated mitotic substrates in binding to PP2A-B55. Reactivation of PP2A-B55 at mitotic exit occurs when PP1 inactivates MASTL/Greatwall by removing CDK1-induced phosphorylation

from it[48]. Contrary to PP1 and PP2A-B55, PP2A-B56 remains active during mitosis, where its activity is required for correcting erroneous kinetochore-microtubule attachments[44]. Furthermore, phosphorylation of PP2A-B56 substrates by the mitotic kinase CDK1 is required for its high affinity interactions with them. Both the regulation PP1, PP2A-B55 and PP2A-B56 by different pathways and their dependency on each other for activation create the ordered dephosphorylation of substrates that succeed chromosomal segregation[43].

The interplay between kinases and phosphatases is important for ordering substrates phosphorylation during the cell cycle[49]. Here, a balance in the counteracting actions of kinases and phosphatases creates a steady state where the phosphorylation of a particular substrate is also balanced. In this state, some of the copies of that substrate are phosphorylated, while the rest are dephosphorylated. What tends to happen for a certain cell cycle event to be initiated is a decline in the activity of one side. This leads the substrate copies to be dominated by the action of the other side. The existence of such a balance is not only essential for creating a system that can be tightly controlled by the cell, but also for the way that transitions between different cell cycle phases occur, which are described to be 'switch-like'[50]. For example, PP1 and PP2A regulation of the phosphatase CDC25C causes rapid exit from interphase and entry to M phase [51,52]. In contrast, dephosphorylation of multiple sites on the kinase Wee1, prevents cells from entering M phase, whereas their phosphorylation inactivates this kinase and promotes a 'switch-like' mitotic entry[53]. From all these examples, it is clear that this interplay between kinases and phosphatases is not only on the targeted substrate, but also on each other. The latter, creates feedback loops between these enzymes, where their activities impact each other, either in a positive or a negative way. These loops also contribute to the rapid transitions between cell cycle phases[54].

1.2.2 Regulation of kinase and phosphatase activities towards cell cycle substrates

The feedback loops are not the only mechanism by which cells control the activities of kinases and phosphatases. Instead, other layers of regulation exist. Targeted degradation of these enzymes is one example. Phosphorylation of Wee1 (as discussed in section 1.2.1) promotes proteasomal degradation[55]. Thus, both phosphorylation and degradation are important for inactivating Wee1 to promote entry into mitosis. The addition of multiple phosphates on the N-terminal part of this protein creates 'phospho-degrons' where components of the SCF ubiquitin Ligase complex can dock. This docking promotes the ubiquitination of Wee1, which targets this kinase for degradation by the proteasome. Degradation of kinases and phosphatases is not necessarily mediated by 'phospho-degrons', instead, it can also be mediated by other sequences, such as D boxes and ABBA motifs[56]. Also, degradation-mediated inactivation does not necessarily target the catalytic subunit of kinase or phosphatase itself, but it can target proteins that associate with these enzymes. To elaborate on the last point, many kinases and phosphatases exist in complexes with partner proteins. These partner proteins activate the enzymes and can be themselves the target for degradation. For example, the kinase DDK requires association with a Dbf4 partner to be activated. Degradation of that subunit by the APC/C through a D box in metaphase leads to inactivation of DDK[57].

Whether through phosphorylation or degradation, the examples above suggest that protein kinases and phosphatases need to be inactivated in order to prevent their actions on the cellular substrates. This, however, is not completely true. Cells contain multiple kinases and phosphatases that are active at a time and yet, high selectivity in their interactions with cell cycle substrates still exist. If kinases share the same catalytic domain, where does this substrate selectivity come from? There are several factors that determine this. One is that selectivity can be substrate encoded. Here, the catalytic domain of the kinase contains a disordered loop known as the activation segment[58]. The sequences of this loop are highly variable between kinase families,

leading to variable substrate amino acid sequence preferences. What this does is create a preferred *motif* for each kinase that is specifically present on its substrates. For example, the mitotic kinase Aurora B phosphorylates motifs where basic residues exist on the N-terminal side of the *phospho-acceptor site*[59-61]. In contrast, the cell cycle regulator Polo-like kinase 1 (PLK1), prefers the presence of acidic residues in the regions flanking the phospho-acceptor site[62]. This is also true for protein phosphatases as PP1 docks on RVXF and SILK/GILK motifs[63] whereas PP2A-B55 prefers phosphorylated Threonine flanked by basic residues[64]. One issue with a system that completely relies on this is that although different kinase and phosphatase families have different activation loops, members of the same family usually share the same or very similar sequences. The kinases Aurora A and Aurora B are example of that. Here, the substrate specificity cannot be explained by T-loop specificity only, instead, the selectivity comes from the other components of the kinase complex. For example, Aurora B is a part of the chromosome passenger complex (CPC), which also includes Borealin, Survivin and the scaffolding inner centromere protein (INCENP)[65-67]. Aurora A, on the other hand, exist in complexes with TPX2[66]. The presence of these subunits impacts the subcellular localisation of these two kinases, bringing them near their specific substrates. Furthermore, even in the presence of all family members in the same cellular compartment, these subunits can still give higher selectivity of one member for a set of substrates over the other. For example, the Survivin subunit of the CPC contains a phospho-adaptor pocket, through which this complex can dock on phosphorylated Histone H3, giving Aurora B access to sites that are not accessible to Aurora A[68]. The crosstalk between all these mechanisms as well as the temporal regulation of the non-catalytic partners of protein kinases allow cells to determine which substrate to be phosphorylated and when. This in turn creates a system where phosphorylation of substrates can be ordered in a way that promotes cell cycle events to occur how it was described in section 1.1. The same is true for phosphatases as different pools of PP1 and PP2A gain their substrate specificity through their regulatory subunits[41]. The mechanisms

by which cells control the activity of kinases and phosphatases towards substrates are summarised in Figure 1.3.

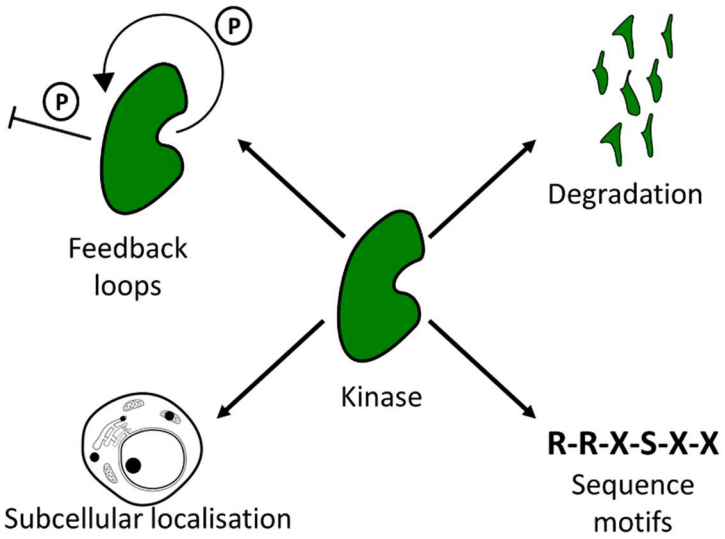

Figure 1.3: Cellular mechanisms for regulating the activities of protein kinases and phosphatases on substrates.

The net phosphorylation, or the *phospho-proteome*, that controls the activities of kinases and phosphatases described earlier increases with cell cycle progression[69]. The importance of this increase for DNA replication and then for mitotic entry was evident in the literature[70]. The bulk of this cell cycle related phospho-proteome is attributed to the CDKs, perhaps the most important of which is CDK1.

1.2.3 Cyclin-CDK phosphorylation regulates the order of cell cycle events

The CDKs represent a large family of protein kinases with 21 members identified so far. Phosphorylation by these proteins is essential for many cellular processes, including transcription of genes, and activation of each other[71]. In the human somatic cell cycle, phosphorylation of substrates by four of these CDKs, namely CDK1, 2, 4 and 6, is directly involved in initiating the division events described in section 1.1[72]. For example, the phosphorylation of RB by CDK4/6 is associated with progression

through G1 phase[2]. Similarly, DNA replication requires activation of CDK2[73]. Also, for M phase entry, a rise in CDK1 activity above a certain threshold is necessary[74,75]. Albeit all their functional specialisations, all CDKs share a similar requirement to gain catalytic activity, and this is a *Cyclin* partner[76]. Just like CDKs, the Cyclins also belong to a large family of proteins, and four members form complexes with and activate the cell cycle related CDKs. However, in contrast to CDKs, which are constitutively expressed during the cell cycle, their Cyclin partners are characterised by their dynamic expression and degradation[72,76]. Cyclin E activates CDK2 and reaches its peak expression at the G1/S border before being degraded in S phase[8]. Cyclin D, on the other hand, is expressed across the entire cell cycle and can form complexes with either CDK4 or CDK6. In contrast, levels of Cyclin A and B peak during G2 and mitosis. Cyclin A is both expressed and degraded earlier than Cyclin B. Early degradation of Cyclin A in prometaphase stabilises kinetochore-microtubule interactions[77] whereas Cyclin B destruction causes chromosomes to segregate during anaphase. Another contrast between Cyclin A and Cyclin B is that the former can be the activating partner of both CDK1 and CDK2 whereas the latter only forms complexes with CDK1. Expression levels of the four Cyclins are illustrated in Figure 1.4A. The advantage of this system is that it allows cells to control the activity of the four CDKs without having to modulate the expression or degradation of the catalytic subunit. Furthermore, distinct signalling pathways regulate the activities of different Cyclin-CDK complexes. Cyclin B-CDK1 is inhibited by Wee1 and Myt1 induced phosphorylation on residues T14 and Y15. Dephosphorylation of these by CDC25 phosphatases reactivates the complex allowing G2/M transition[78]. In addition, all CDK1 and CDK2 complexes can be inhibited by high affinity interaction with the CIP/KIP family of CDK inhibitors. In contrast, CIP/KIP members promote the activation of CDK4 and CDK6 by facilitating their complex formation with Cyclin D[79]. The Cyclin D-CDK4/6 complexes are then inhibited by the INK4 family of CDK inhibitors. Modulation of CDK activity by INK4 or CIP/KIP occurs either through preventing their association with Cyclin partners or by forming inactive ternary

complexes with them[80] (Reviewed by Besson et al.[81]). The expression times of Cyclins A, E, D, and B during the cell cycle, their CDK partners, and their regulatory mechanisms are summarised in Figure 1.4B. Beside this, inspired by budding and fission yeast cells, which both only express a single CDK that resembles the human CDK1, experiments questioning the redundancy of CDKs revealed that under certain condition, these kinases can compensate for each other. For example, Santamaria et al. reported through mouse knockout experiments that out of the four CDKs, CDK1 is the only essential member for cells survival[82]. In addition, a recent paper by Lau et al. showed that CDK2 can compensate for the other CDKs if expressed to levels comparable to those of CDK1[83]. In both reports, CDK1 and 2 were able, across the cell cycle, to form complexes with all the Cyclins that would otherwise be with the absent CDKs. Both this redundancy and the peak expression timing stress the point that the substrate specificity of CDK may come from the Cyclin partner.

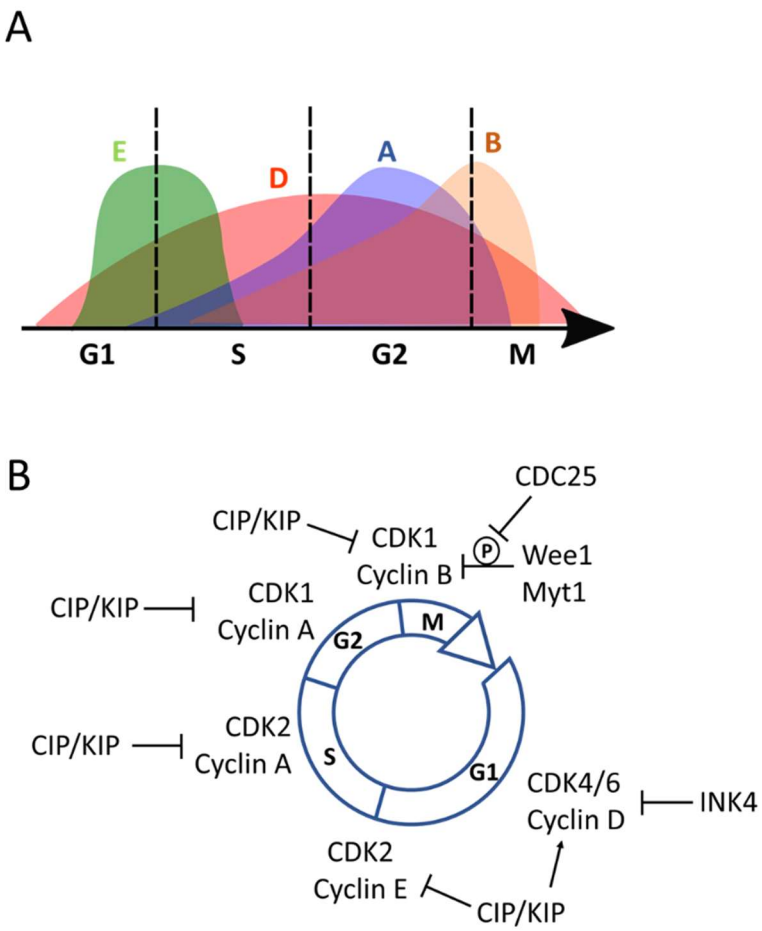

Figure 1.4: Cyclin-CDK complexes and their regulatory pathways in a human somatic cell cycle. (A) Expression levels of Cyclins A, B, D, and E during the cell cycle. (B) Different Cyclin-CDK complexes and their regulators.

1.2.4 Qualitative and quantitative models explain the temporal ordering of substrates phosphorylation during the cell cycle

The role of Cyclins in how CDKs choose their substrates has always been a point of debate. What initiated these discussions is the fact that during the cell cycle, CDK activity increases in a way that matches that of the phospho-proteome. This led some to suggest a *quantitative* model for substrates phosphorylation by the CDKs[84]. In this model, the temporal ordering of substrates phosphorylation by CDKs is solely driven by the quantitative changes in their activity occurring during the cell cycle. What this implies is that substrates in the late cell cycle phases require higher CDK activity to be phosphorylated than those in the earlier ones. These variable requirements create distinct thresholds of activity that the CDKs need to surpass to be able to initiate the different cell cycle events, and that the later in the cell cycle the event is, the higher the threshold will be. For example, the CDK activity required for DNA replication to happen is lower than that needed for mitotic entry. But what is the role of Cyclins in all of this? In the quantitative model, the Cyclins exist to activate the CDKs. This model is supported by elegant experiments by Coudreuse and Nurse on fission yeasts[70]. In their report, the expression of Cyclin B fused to analogue-sensitive CDK1 (CDK1-as) in cells lacking all the other Cyclins was sufficient to drive all their division events, as long as this chimera was present with the right activity. Furthermore, the activity of this fusion protein that was required to initiate DNA replication was lower than that for M phase entry. In higher eukaryotes like humans, both the complexity of the genome, which contains several isoforms of each of the four Cyclins, and the CDK-independent roles that some of these have, like Cyclin E[85], prevented the replication of the exact same experiment. Having said that,

it was evident that the expression of Cyclin B in human cells depleted of Cyclin A can partially rescue the division deficiencies resulting from that depletion[86].

The dissimilarity between the four Cyclins expressed in human cells is much more substantial than those among the fission yeast ones. In humans, the Cyclin partner does not only allow cells to control the activity of CDKs through degradation. Instead, it also promotes other control mechanism described in section 1.2.2. One of these is the subcellular localisation of CDKs. For Cyclin E, the presence of a nuclear localisation signal relocates the CDKs into that compartment when in complex them[87]. In contrast, Cyclin B carries nuclear exclusion signal that retains the activity of Cyclin B-CDK1 to the cytoplasm, ensuring that it only phosphorylates nuclear proteins during M phase[88], after the nuclear envelope has broken down. More than one Cyclin type can be the partner that activates a particular CDK (Figure 1.4). For example, CDK1 can form stable complexes with either Cyclin A or Cyclin B. All these points led some to suggest an alternative model to the quantitative one, where the Cyclins are central to determining the substrate selectivity of CDKs[89]. This model is termed *qualitative* and is based on experiments by Loog and Morgan in which they phosphorylated recombinant budding yeast S and M phase substrates *in vitro* with either Clb2-Cdk1 (M phase Cyclin-CDK1) or Clb5-Cdk1 (S phase Cyclin-CDK1)[90]. What these experiments demonstrated is a clear preference by the Clb5-Cdk1 complex to phosphorylate the S phase substrates. In support of this, a report by Pagliuca et al. also revealed distinct interactomes for different human Cyclin-CDK complexes *in vivo*[91]. This distinctiveness, however, was less pronounced between the complexes that were coexisting at the same time during cell cycle, making it difficult to conclude whether the substrate selectivity here was coming exclusively from the Cyclin partner or the expression levels and subcellular localisation. Based on all of this, it is possible to conclude that while both the qualitative and quantitative models originated from experiments on yeast cells, and that each have its supportive and contradictory arguments, the complexity of upper eukaryotes presents a challenge to replicating similar investigations in human cells.

1.2.5 The phospho-adaptor Cks1 is a component of some Cyclin-CDK complexes

The Cyclins are not the only proteins that can form stable complexes with CDKs and have essential roles in cell division. CDKs can also associate with another family of proteins called the Cyclin dependent kinase subunit (Cks)[92]. In human cells, two paralogues, named Cks1 and Cks2, make up this family. Both proteins fold to create a positively charged pocket[93] (Figure 1.5). The cationic nature of this pocket suggested that it may be involved in Cyclin-CDK docking onto anions, such as Aspartates and Glutamates, or even on phosphorylated residues. This was investigated through dot blot arrays on peptides bearing different amino acid sequences[94]. Through these, it was clear that the cationic pocket of, at least the budding yeast homologue of Cks1, docks on phosphorylated Threonines. Furthermore, the respective mutagenesis of Cks1's Lysine 11 and Arginine 71 to Glutamate and Alanine creates a phospho-binding mutant version of this protein[95,96]. The next obvious question was whether its docking onto these Threonines *in vivo* involves phosphorylation by Cdk1. Just like the kinases described in section 1.2.2, CDKs have a preferred sequence motif on their substrates that they specifically target. This motif is comprised of a phospho-acceptor Serine or Threonine next to a Proline on the C terminal side (+1 Proline), and sometimes a basic residue three amino acids downstream (+3 basic) – S/TPXK/R[97]. In the dot blot arrays, the presence of a Proline nearby seemed to improve the binding of Cks1 to the phosphorylated Threonine. So, does Cks1 dock on CDK phosphorylated residues? And, perhaps more importantly, why? In experiments carried out by Koivomagi et al., the phosphorylation of a truncated version of the budding yeast Cdk1 inhibitor Sic1 on Threonine 48 (T48) *in vitro* required both the phosphorylation of Threonine 33 (T33), as well as the presence of a Cks1 subunit in the recombinant Cyclin-Cdk1 complex that they phosphorylated with[98]. Furthermore, the distance between these two sites, which both resided on a disordered region, was also a determining factor, as adding or removing amino acids from that sequence abolished the phosphorylation of T48[99]. This showed that Cdk1 phosphorylates the priming T33 site, which in turn provides a docking platform for

Cks1. This docking then promotes the phosphorylation of T48. What was remarkable about T48 though is that it lacked the +1 Proline in its sequence motif. Through these experiments, it was evident that Cks1 enhances the phosphorylation of low affinity, and perhaps *non-canonical*/*non-Proline*, sites by positioning Cdk1 in close proximity to them. The significance of this phosphorylation *in vivo* was that it caused Sic1 to be phosphorylated on multiple sites. This *multisite* phosphorylation was critical for the degradation of Sic1 and entry into the cell cycle. In consistency with these findings in budding yeast, depletion of Cks1 and 2 in human cells reduces the multisite phosphorylation of APC/C, arresting these cells in mitosis[100].

A combination of multisite phosphorylation and Cks1 can lead to different outcomes, based on the identity of the targeted protein. In some cases, this combination causes the stabilisation of the substrate. The binding of Cks1 on Cdc6 phosphorylated on multiple sites is a good example[101]. Here, Cks1 shields a phospho-degron on Cdc6, preventing its ubiquitination and degradation by the proteasome. Also, Cks1 can inhibit the function of CDK substrates without causing their degradation. For example, docking of Cks1, along with a phospho-binding pocket in Cyclin B, onto phosphorylated Separase inhibits the activity of that protein[102]. This is important for creating timely segregation of chromosomes in mitotic cells, since Separase promotes the separation of sister chromatids. Beside all of this, Cks1 can also have CDK-independent roles in cells. For example, in budding yeasts, Cks1 localises to the open reading frame of *GAL1*, a gene that encodes a protein involved in Galactose metabolism[103]. This localisation is important for efficient transcription, as it mediates the recruitment of the proteasome to this region, which promotes mRNA elongation by RNA polymerase II, allowing rapid transcription of *GAL1*[104]. A similar mechanism was suggested for the expression of the APC/C activator Cdc20, which is impaired in the absence of Cks1[100]. The impact of Cks1 depletion on both the multisite phosphorylation of APC/C mentioned in section 1.2.5, and the transcription of Cdc20, result in cells arresting in prometaphase due to failure to establish proper metaphase plates. This arrest is due to the stabilisation of Cyclin A, which needs to be degraded

by the APC/C^{Cdc20} in prometaphase for cells to create stable kinetochore-microtubule attachments[77,105].

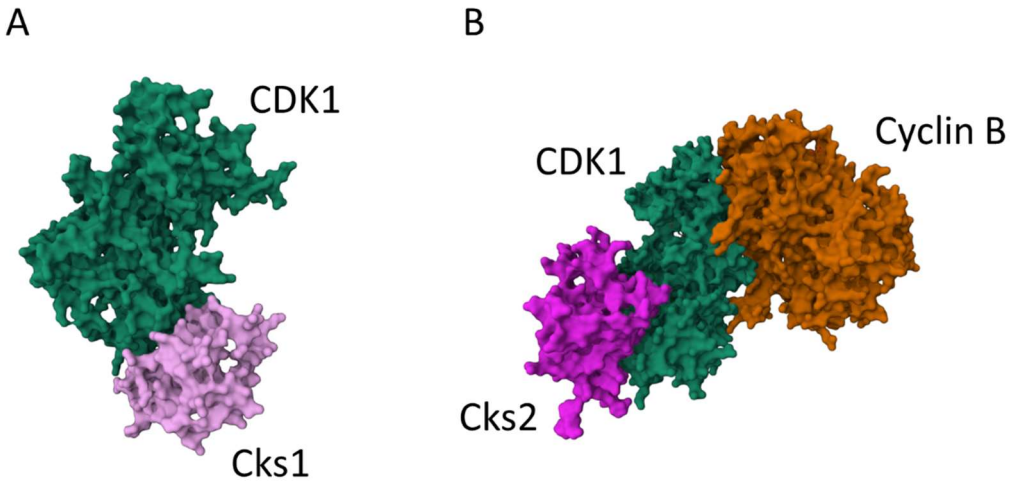

Figure 1.5: Crystal structures of CDK1 in complex with Cks proteins. Recombinant CDK1-Cks1 complex (A) and Cyclin B-CDK1-Cks2 (B) reported by Brown et al.[93]

All the findings presented in the last sections regarding the roles of Cks1 and 2 in CDK-mediated phosphorylation were based on experiments on individual substrates. In addition, most of these were carried out on budding yeasts or on proteins normally expressed in these cells. A comprehensive, proteome-wide analysis of how these two paralogues impact the phosphorylation of substrates by CDKs in human cells is still missing from the literature.

1.2.6 Study of cell cycle phosphorylation using mass spectrometry

Whether investigating the Cyclins or Cks1, several techniques were historically used to reach the conclusions presented earlier. Depending on the nature of the question, combinations of genetic engineering, biochemical assays and imaging tools were, and perhaps still, the gold standard methods for these investigations. In the most recent years, remarkable advances in *mass spectrometry* were made[106]. This is particularly

true for the field of phospho-proteomics. The invention of the Orbitrap by Makarov led to significant improvement in both the quality and quantity of data that this method can generate[107]. These advances added mass spectrometry to the list of techniques used for cell cycle investigations. The advantage here is that one can visualise proteome-wide changes occurring in the cell. Furthermore, it makes it possible to determine the cellular compartments in which these changes are happening. In a classic data dependent acquisition run carried out in an Orbitrap mass spectrometer, cellular proteins are initially digested into *peptides* using a protease. These peptides are then loaded onto a liquid chromatography (LC) column and eluted with a mobile phase to create a gradient that can be electro-sprayed into a mass spectrometer. This electrospray process is particularly important, not only because it turns that liquid gradient into a gas state, which is essential for a peptide to fly in the mass spectrometer, but also because the high voltage of the electro-spray induces its ionisation. The pH of the LC gradient determines the charge of these ions and is chosen based on the type of sample to be analysed. In the case of peptides, it is always acidic, as it produces ions with positive charges. The abundance of these ions in the sample, which reflects the quantity of the proteins that they belong to, is then calculated using Fourier Transform mass spectrometry (FTMS)[108]. This step is called the MS^1 scan and is carried out in the Orbitrap of the mass spectrometer. The peptides analysed during this step are termed *precursor ions*. Next, the amino acid sequences, or the *identities*, of these precursor ions are determined. This is done by colliding them with gas molecules to produce *fragments* that are then analysed in a second, MS^2 scan, usually by FTMS. Both MS scans described here provide qualitative and quantitative information about the individual components of a sample.

The complexity of these samples, which are usually generated from cell lysates, however, makes it impossible to identify every precursor ion eluted. Therefore, a few precursor ions, usually the most abundant ones, from each MS^1 scan are selected for MS^2 analysis. For that reason, cell digests are usually separated by more than one

fractionation method before analysing them on a mass spectrometer, as this reduces their complexity, allowing more peptides to be identified. The data that are generated from both the MS^1 and MS^2 scans are in the form of mass to charge (m/z) ratios and are usually analysed by matching them with theoretical data that are either real, such as the human proteome, or decoy. This matching then produces scores that can be used to eliminate false positives from datasets.

1.2.7 Cell cycle discoveries through mass spectrometry-based investigations

A great body of what is known about the cell cycle control by protein kinases and phosphatases was uncovered in experiments that had utilised mass spectrometry in combination with other approaches. For example, Ly et al. demonstrated, using peptide digests from G1, S, G2 and M phase populations separated by fluorescent antibody cell sorting (FACS), that the cell cycle progression associates with an increase in the phospho-proteome[69]. Olsen et al. showed that phosphorylation of some of these sites reaches full occupancy during mitosis[106]. Also, the motifs bearing many of the mitotic sites were unveiled in the report of Dephoure et al.[109] Furthermore, the kinases and phosphatases targeting some of these motifs for phosphorylation or dephosphorylation were discovered in phospho-proteomic screens by both Kettenbach et al.[60] and Cundell et al.[64] Mass spectrometry was also an important tool for localising the sites phosphorylated by Cdk1 on Sic1 in the experiments of Koivomagi et al. described in section 1.2.5[98]. Beside phospho-proteomics, affinity purification mass spectrometry was used to reveal the interactors of many cell cycle proteins kinases and phosphatases, including those reported by Pagliuca et al. described in section 1.2.4[110]. Finally, the kinetics of chromatin localisation for mitotic proteins during prophases, including those for kinases and phosphatases, were uncovered by Samejima et al., using a novel, mass-spectrometry-based method[111].

1.2.8 Phosphorylations on the NDC80 tail regulate mitotic progression

As it was described in section 1.1, the kinetochore is assembled on centromeres to act as a linker between the spindle and mitotic chromosomes. The kinetochore can be divided into either inner or outer compartments. While the CCAN makes up the inner compartment, three proteins form the outer kinetochore: Knl1, Mis12 and NDC80 (together known as the KMN network; Reviewed by Musacchio and Desai[11]). Knl1 contains the MELT sequences where Mps1 phosphorylation drives SAC signalling[112]. Mis12 and NDC80, on the other hand, form the contacts with CENP-C and CENP-T of the CCAN[113,114]. Interaction with the spindle is achieved through the contacts that the NDC80 complex makes with microtubules.

The NDC80 complex is a heterotetramer, comprised of SPC24, SPC25, NUF2 and NDC80/Hec1 (hereafter NDC80). SPC24 and SPC25 subunits make the contacts with Mis12 and CENP-T[114] whereas NUF2 and NDC80 bind spindle microtubules. The structure of the NDC80 subunit features a coiled coil region for oligomerisation, a calponin homology (toe) domain, and an 80 amino acids-long disordered region known as the tail, both at the N-terminus. Both the toe domain and the tail are involved in microtubules binding (Reviewed by Wimbish and DeLuca[13]). The positive charge of the tail created by its many Lysine residues forms a salt bridge with Glutamate patches on microtubules surface. During the event of an erroneous attachment, mitotic progression is halted due to SAC activation. For it to continue, the salt bridge forming the erroneous attachment needs to be destabilised. Here, Aurora kinases phosphorylate multiple sites on the tail. The negative charges of the added phosphates disrupt the salt bridge, allowing microtubules to move freely. Stable attachments are re-established again when protein phosphatases dephosphorylate the tail residues. Although Aurora A and B are the known kinases to disrupt such erroneous attachments for NDC80, we have recently shown that CDK1 can also phosphorylate at least one site on that tail[115]. Mutagenesis of this site

compromises the ability of cells to correct kinetochore-microtubule attachment errors.

In addition to binding microtubules, the NDC80 subunit is also involved in binding of the Ska complex, which acts as a crosslinker, providing further stability to kinetochore-microtubule attachments[116]. The toe domain of this subunit also plays a role in promoting SAC signalling by providing a platform for Mps1 in the absence of end-on microtubule attachments (Reviewed by Nilsson[117]). All the above makes NDC80 an attractive model substrate to study how kinase-phosphatase crosstalk regulates mitotic progression. This is especially true when considering the number of sites phosphorylated on NDC80 in proteomics studies with no previously identified roles[118].

1.3 Aims of this study

From the description of how the four members of the CDK family control progression through the cell cycle presented in section 1.2, it is evident that the complexity of human cells still presents a major challenge in obtaining a comprehensive understanding of how each of the qualitative and quantitative models contribute to the temporal ordering of substrates phosphorylation by CDKs. Similarly in that sense, the lack of any reports investigating how Cks1 and 2 affect the phosphorylation for hundreds of substrates by CDK makes it difficult to know why these subunits should stably exist in the complexes of CDK1, 2, 4 and 6 across the entire cell cycle. In this study, I aimed to develop a method that would allow me to investigate these two questions. I shall describe this method in chapter 3 of this thesis. In chapters 4 and 5, this method is used investigate how changing the Cyclin partner of CDK1, titrating its activity, and adding a Cks1 subunit to its complexes affect its phosphorylation of substrates. I chose CDK1 because it is the master-regulator of mitosis in human cells, and up until this moment, the evidence has shown that the endogenous activity of this kinase alone is sufficient to phosphorylate all the cell cycle substrates that would

otherwise be phosphorylated by the other three CDKs[82]. Depletion of Cyclin A and Cyclin B produce distinct phenotypes[86,119]. This, along with structural difference between these two Cyclins, such as the hydrophobic patch of Cyclin A[120] and the phospho-binding pocket in Cyclin B[102], makes it interesting to question how the Cyclin subunit impacts the substrate selectivity of CDK1. Cks1 was studied, owing to the structural similarity between Cks1 and Cks2. From these experiments, I was able to uncover a novel mechanism by which CDK1 may control the temporal ordering of its substrates' phosphorylation in the cell cycle. Finally, I attempted to reproduce the results using orthogonal approaches in chapter 6 and chose one substrate as an example to follow up on in future investigations.

Chapter 2:

Methodology

2.1 Cell culture

For the *in vitro* phosphorylation assays, TK6 cells[121] were seeded at 80,000 cells/ml in 400 ml of Rowell Park Memorial Institute (RPMI) medium supplemented with 10% foetal bovine serum (FBS) and Glutamax and left to grow for 48 hours undisturbed. Cells were then centrifuged at 300 g for 4 mins at room temperature and resuspended in 30 ml Dulbecco's phosphate-buffered saline (DPBS). After another round of centrifugation, cells were fixed and permeabilized as described in section 2.3. For the *in vivo* investigations, HeLa cells either expressing CDK1-as[122] or carrying a Flip Recombinase target (FRT) locus[123] were seeded at 30% density in Dulbecco's modified Eagle medium (DMEM) supplemented with 10% FBS, Glutamax and pyruvate. Once at 80% confluency, cells were washed twice with DPBS and detached by 10 min incubation with 0.25% Trypsin protease. Trypsin was then inhibited by resuspending the detached cells in complete medium. Both TK6 and HeLa cells were maintained at 37°C and in the presence of 5% CO2.

2.2 FRT clones with inducible expression of NDC80-GFP

To generate HeLa FRT cell line stably expressing mCherry-Tubulin and conditionally expressing NDC80-GFP mutant, 50 ng of mCherry-β-Tubulin plasmid were mixed with 500,000 cells in 11 µl volume and loaded into a Neon electroporator according to the manufacturer's instructions. To transfect the cells on this apparatus, 2 pulses of 35 msec were carried out at 1005 V. Cells were then placed in 0.5 ml complete medium at 37°C in a 24-well plate. FACS was then used to sort 96 mCherry-positive single cells into a 96-well plate. To select the most compatible cells with time-lapse imaging, 96 subclones of these cells were arrested in prometaphase with 100 µM of Monastrol and then released into complete medium supplemented with 40 µM MG132. Fluorescent microscopy was used to image the cells at both prometaphase and metaphase and three individual colonies were selected and pooled for downstream preparations (hereafter, simply HeLa FRT mCherry-Tubulin). To generate inducible

expression of NDC80-GFP, the HeLa FRT mCherry-Tubulin cells from above were transfected with a DNA construct expressing short interfering – RNA (siRNA)-resistant NDC80 tagged at the C-terminus with Green Fluorescent Protein (GFP). To generate NDC80 mutants, the QuickChange kit was used according to the manufacturer's instructions. Briefly, 50 ng of NDC80-GFP plasmid was mixed with 1 ng of dNTP mixture in a 50 µl QuickChange reaction buffer and 2.5 U of *pfu* Ultra HF DNA polymerase in the presence of 125 ng of forward and reverse primers carrying one of following complementary sequences:

S76A: CAACTTGGTATATTTTCCGCTTCTGAGAAAATCAAGGACC

S76/77A: CAACTTGGTATATTTTCCGCTGCTGAGAAAATCAAGGACC

S76D: CAACTTGGTATATTTTCCGATTCTGAGAAAATCAAGGACC

S76/77D: CAACTTGGTATATTTTCCGATGATGAGAAAATCAAGGACC

T31A: CAAGGCCTCTATGCCCCTCAAACCAAAGAGAAACC

T31D: CAAGGCCTCTATGACCCTCAAACCAAAGAGAAACC

Polymerase chain reaction (PCR) was then performed to amplify mutagenized plasmids. The reaction involved 1 cycle of DNA denaturation at 95°C for 30 sec followed by 18 cycles of: 30 sec denaturation at 98°C, 1 min mutagenized primer annealing at 55°C, then 8 min extension at 68°C. To remove methylated DNA from the PCR product, samples were incubated with 10 U of *DpnI* for 1 hour at 37°C. To propagate the mutagenized plasmids, XL1 Blue super-competent *Escherichia coli* (*E. coli*) cells were transformed with 10 µl of the PCR product. Briefly, cells were incubated with the plasmids for 30 min on ice, heat shocked at 42°C for 45 sec, then left to recover for 2 min on ice before 1 hour agitation with SOC medium at 37°C. Transformed cells were then streaked on Luria-Bertani (LB) agar plates supplemented with 200 µg/ml Ampicillin and left to grow at 37°C overnight. Three selected bacterial colonies from each plate were inoculated separately into 25 ml of LB medium and left to grow at 37°C overnight. To purify the plasmids from these

cells, PureLink™ HiPure Plasmid Midiprep Kit was used according to manufacturer's instructions. The ratio of absorbances at 260/280 nm was measured with a nanopore and used as a readout to the purity of these plasmids and Sanger sequencing was performed to check the presence of the desired mutations. Electroporation of HeLa cells with each mutant was carried out using the same parameters used when generating the mCherry clones except that the cells were co-transfected with OG44 Flp Recombinase plasmid to recombine the NDC80-GFP sequences into the FRT locus. To select the transfected cells in cultures, 300 µg/ml Hygromycin was added to the cultures 24 hours post electroporation and cells were left to grow for 3 weeks until reaching 80% confluency. Aliquots of these cells were frozen in FBS supplemented with 10% di-methyl sulphoxide (DMSO) and stored in liquid nitrogen vapor. To test the expression of NDC80-GFP, HeLa cultures were grown in complete medium supplemented with 1 µg/ml Doxycycline (Dox) for 16 hours to induce the expression of the protein then 2 million cells from these were lysed in 70 µl cell extraction buffer (CEB; 1 mM HEPES, 10 µM EDTA, 2% SDS, 1x cOMPLETE protease inhibitor cocktail and 1x Roche phosphatase inhibitor cocktail) and sonicated for 1 min at 10% amplitude. Proteins were denatured at 70°C for 10 min, then 25 mM tris carboxyethyl phosphine (TCEP) was added. Samples were then mixed with lithium dodecyl sulphate (LDS)-based sample buffer, heated at 70°C for 10 min and loaded onto a 4-12% NuPAGE Bis-Tris gel. SDS-polyacrylamide gel electrophoresis (PAGE) was performed for 2 hours at 150 V in NuPAGE MES buffer. Protein bands in the gel were visualised by western blotting for 2 hours at 200 mA onto a 0.2 µm pore-sized nitrocellulose membrane in NuPAGE transfer buffer supplemented with 20% methanol. Membranes were then briefly washed with deionised water to remove the methanol and blocked for 1 hour at room temperature with tris-buffered saline (TBS; 50 mM Tris-HCl, 150 mM NaCl; pH 7.5) supplemented with 5% milk. After a brief wash with TBS, membranes were probed overnight at 4°C with anti-NDC80 (1:1000) and anti-GAPDH (1:2500) antibodies for loading control. Membranes were then washed three times with TBS supplemented with 0.1% Tween (TBS-T) and incubated

for two hours with secondary antibodies conjugated to either IRDye-680RD or IRDye-800CW at room temperature. Bands were visualised using Li-Cor CLx Odyssey scanner and the presence of ~100 kDa band, i.e., 27 kDa larger than the endogenous NDC80 band, on the membrane was used as a readout for successful expression.

2.3 Cell fixation and centrifugal elutriation

To use TK6 cells as substrates for *in vitro* investigations, samples described in section 2.1 were fixed for 10 mins at room temperature with 1% formaldehyde diluted in DPBS. Cells were then washed once with DPBS and permeabilized at -20°C for at least 24 hours in 90% methanol. To collect G1 and G2/M cells, methanol was washed off by centrifugation and pellets were resuspended in 5 ml MES-buffered saline supplemented with 1% FBS (MBS-F; pH 6.0). Asynchronous cells were then loaded into an elutriation chamber spinning at 2100 rpm and trapped there by MBS-F flowing at a 15 ml/min rate in the opposite direction. G1, S, and G2/M cells were collected into 50 ml falcon tubes by gradually increasing the flow rate up to 35 ml/min. Fractions were then centrifuged and pellets were resuspended either in DPBS alone or in the presence of a 1x Roche phosphatase inhibitor cocktail depending on the experiment. Representative samples from each fraction were stained with 50 µg/ml propidium iodide supplemented with 50 µg/ml RNAse A and flow cytometry was used to assess the cell cycle population in each fraction based on their DNA content, where 2N cells were considered G1 and those with 4N were G2&M. To collect mitotic cells, TK6 cells were grown in complete medium supplemented with S-trityl L-Cysteine (STLC) for 16 hours. Prometaphase cells were then harvested (Section 2.1) and fixed as described above.

2.4 Protein expression and purification

For the experiments where the *in vitro* phosphorylation of fixed cells was being optimised, a recombinant active Aurora B was expressed and purified from bacterial cells as described[115]. To express a complex with high activity, *E. coli* Rosetta cells were co-transformed with His-SUMO-Aurora B (55-344) and the C-terminus of INCENP (835-903). Both plasmids are kind gifts from the Jeyaparakash Arulanandam group at the University of Edinburgh. Transformed cells were selected by their ability to grow on LB agar plates supplemented with 50 μg/ml of Kanamycin, and 100 μg/ml of both Spectinomycin and Chloramphenicol. A single colony was then inoculated into 10 ml of LB medium and left to grow overnight at 37°C. Cells from this culture were then inoculated into 2 L of LB medium and grown at 37°C until reaching an optical density of 0.5. Temperature was then reduced to 18°C, and the expression was induced by growing these cells for 18 hours in the presence of 350 μM IPTG. Bacterial pellets from this culture were resuspended in lysis buffer (25 mM HEPES, 500 mM NaCl, 25 mM Imidazole, 2 mM β-mercaptethanol, 1 x cOMPLETE protease inhibitor cocktail and 50 U Benzonase; pH 7.5) and lysed in a bio-disruptor. Soluble proteins were then collected after a 50 min spin at 22,500 rpm at 4°C and affinity purification with nickel silica beads was performed to purify the recombinant His-SUMO-Aurora B-INCENP complex from the supernatant. To remove non-specifically bound proteins, beads were washed once with each of the lysis buffer, a chaperone buffer (25 mM HEPES, 1000 mM NaCl, 30 mM Imidazole, 50 mM KCl, 10 mM MgCl2, 2 mM ATP and 2 mM β-mercaptethanol; pH 7.5) and a low salt buffer (25 mM HEPES, 200 mM NaCl, 25 mM Imidazole and 2 mM β-mercaptethanol; pH 7.5). To elute the recombinant complex, the beads were placed for 2 hours at 4°C in elution buffer (25 mM HEPES, 200 mM NaCl, 500 mM imidazole, 2 mM β -mercaptethanol; pH 7.5) and the flow through containing the protein was collected. This process was repeated three times to collect as much protein as possible. The presence of the recombinant complex was assessed by SDS-PAGE followed Instant Blue staining of gels. Fractions containing the complex were pooled and desalted using 50 ml HiPrep 26/10

Sephadex G-25 fine resin-packed desalting column fitted on ÄKTA liquid chromatography instrument and fractionated in a dialysis buffer (25 mM HEPES, 200 mM NaCl and 2 mM β-mercaptethanol; pH 7.5). To cleave the His-SUMO tag, the protease SENP2 (a kind gift from the Jeyaparakash Arulanandam group at the University of Edinburgh) was added to the dialysis fractions containing the Aurora B complex and incubated overnight at 4°C. Representative samples were then analysed by SDS-PAGE and a decrease in the molecular weight was used as a readout for the cleavage. The complex was then concentrated into 300 µl volume using Ultra-4 Centrifugal Filter Unit and further purified using a 24 ml Superdex 75 10/300 gel filtration (GF) column for size exclusion chromatography (SEC). Fractions were collected in a GF buffer (25 mM HEPES, 200 mM NaCl, 4 mM Dithiothreitol [DTT] and 5% Glycerol; pH 7.5), snap frozen in liquid nitrogen and stored at -80°C until the kinase assays. This complex was also used in the paper by Kucharski et al.[115]

2.5 Kinase assays on fixed cells and western blotting

To induce *in vitro* phosphorylation of residues, 2 million fixed and permeabilized cells from the G1 or G2/M elutriation fractions in section 2.3 were placed in Eppendorf tubes and centrifuged at 15,000 g for 30 sec at 4°C. Tubes were then rotated continuously end-over-end for the times indicated and samples were spun again at the same speed for another 30 sec. This centrifugation method was used for all the subsequent preparation steps for samples with fixed cells. Pellets from these cells were resuspended and blocked with 40 mM Tris-HCl, supplemented with 5% Bovine Serum Albumin (BSA). While the samples were blocking, x2 reaction master-mix (40 mM tris, 0.5% BSA, 20 mM Adenosine triphosphate [ATP], recombinant CDK1 complexes [generous gifts from the Endicott laboratory in Newcastle University], x2 Roche phosphatase inhibitor cocktail; pH 7.5) was prepared on ice. After 10 mins, cells were pelleted and resuspended in 200 µl of 40 mM Tris-HCl, supplemented with 0.5% BSA. To start the phosphorylation reaction, 200 µl of the master-mix was added

to the cells and samples were placed at room temperature on a rotator for 40 mins, leaving 20 sec gaps between them. Reactions were then stopped by adding 500 µl of quenching buffer (40 mM Tris-HCl, 0.5% BSA, 11 mM EDTA). Two washes were carried out with this buffer before resuspending cells pellets in 300 µl of DPBS, supplemented with x1 Roche phosphatase inhibitor cocktail. For the reactions that involved prior dephosphorylation, G2/M cells pellets from the elutriation fractions of section 2.3 were resuspended in DPBS without the phosphatase inhibitor cocktail and counted by flow cytometry. Two million cells from these were then placed in Eppendorf tubes and centrifuged and pellets were resuspended in dephosphorylation reaction master-mix (HEPES-buffered saline, 0.5% BSA, 8 U of λ phosphatase, 10 mM $MnCl_2$; pH 7.5) and placed on a rotator at room temperature for 19 hours. To stop the reactions, cells were washed three times with DPBS then heat treated at 65°C for 30 min to inactivate the phosphatase. Cells were then blocked and phosphorylated as described above. Phosphorylations with Aurora B were carried out with the exact same protocol described above except that blocking and quenching buffer, and the kinase master-mix were made with DPBS instead of the 40 mM Tris-HCl and that reactions were performed at 37°C rather than at room temperature.

To check that these recombinant kinases had successfully induced *in vitro* phosphorylation, 200 µl of the 300 µl phosphorylated cells in DPBS prepared above were centrifuged and resuspended in 70 µl of CEB. Samples were then sonicated at 10% amplitude for 30 sec and their crosslinking by formaldehyde was reversed by heating at 95°C for 50 min. Protein extracts were briefly -centrifuged, reduced with 25 mM TCEP, mixed with x1 LDS sample buffer, and immunoblotted with anti-Alpha-Tubulin (1:5000) antibody either in combination with anti-H3-phospho-Serine10 (H3pS10, 1:1000) or anti-phospho(p)-SPXK/R (1:1000) antibody as described in section 2.2.

2.6 Sample preparation for (phospho-)proteomics analysis

100 µl of the 300 µl phosphorylated cells prepared in section 2.5 were centrifuged and pellets were resuspended in a Tryptic digestion buffer (100 mM triethyl ammonium bicarbonate [TEAB], 2 mM $MgCl_2$, 25-29 U Benzonase) and incubated at 37°C. After 30 min, 2.5 µl of Pierce Trypsin were added at 5 ng/µl concentration to the cells for in cell-digestion of cellular proteins and samples were vortexed and incubated overnight at 37°C shaking at 1200 rpm[124]. To ensure complete digestion, another round of Tryptic digestion was carried out with another 2.5 µg Trypsin for 4 hours and peptides were driedusing a SpeedVac. To clean up the samples before isobaric labelling with tandem mass tags (TMT), peptides were resuspended in 0.5% formic acid (pH < 3) and immobilised on C_{18} NEST micro-spin columns conditioned with absolute acetonitrile and equilibrated with 0.5% formic acid. Peptides on the columns were washed twice with 0.5% formic acid and eluted with 80% acetonitrile diluted in 0.5% formic acid. Peptides were then dried to remove solvent. TMTpro 16plex was used to label the peptides using a modification of the manufacturer's protocol. Briefly, dried peptides were resuspended in 60 µl of 100 mM TEAB and 0.25 mg TMTpro dissolved in 10 µl absolute acetonitrile were added to them and incubated for 1 hour at room temperature. Reactions were quenched by 15 min incubation at 37°C with 2.5 µl of 5% hydroxylamine and pooled into one tube. Labelled peptides were then dried and C_{18} desalting was carried out using Sep-Pak 50 mg columns as described above, except that an extra wash with 0.5% acetic acid was added to the protocol and that elution buffer was prepared with acetic acid instead of formic acid, both were to remove unbound TMT from the sample. Desalted peptides were then separated into two tubes (95% of the sample for phospho-proteomics and 5% for proteomics) and dried at 30°C. To enrich for phosphorylated peptides, digests were resuspended in 0.5 ml loading buffer (80% acetonitrile, 5% trifluoroacetic acid [TFA], 5% glycolic acid) and dissolved for 20 mins. Peptides were then immobilised for 20 mins on 3.2 mg of MagResyn titanium-IMAC beads pre-washed with 70% ethanol and equilibrated with loading buffer. To remove non-

specifically bound peptides, beads carrying the digests were washed for 2 mins once with buffer 1 (80% acetonitrile, 1% TFA) then twice with buffer 2 (10% acetonitrile, 1% TFA). Elution was carried out by dipping the beads twice for 15 mins in elution buffer 1 (1% ammonium hydroxide in water) and once for 1 hour in elution buffer 2 (50/50 mix of 1% ammonium hydroxide and acetonitrile [v/v]). A second round of phospho-enrichment was carried out by dipping a new batch of MagResyn titanium beads in the flow through of the first enrichment and peptides were pooled together and acidified with 0.5% formic acid then lyophilised to remove solvent from the sample. All the phospho-enrichment steps above were done at 25°C on a thermo-mixer shaking at 1200 rpm. Any residual magnetic beads from these phospho-enrichment steps were cleared by passing the phosphorylated peptides through a desalting NEST micro-spin C_{18} column as described above. Finally, for deep (phospho-)proteomics analysis, both phospho-enriched and the 5% sample for proteomics were fractionated on a 1 mm column packed with 13 µm sized C_{18} coated-BEH silica resin with buffer A (10 mM ammonium formate; pH 9.3) as a mobile phase. 16 fractions of these peptides were then eluted in a mobile phase with a gradient of 15 – 80% of buffer B (10/90 mixture of 10 mM ammonium formate; pH 9.3 and 100% acetonitrile [v/v]) diluted in buffer A (v/v). These fractions were dried at 30°C and stored at -20°C until data acquisition by mass spectrometry. All sample preparation steps described in this section were carried out in Protein LoBind tubes and high-performance liquid chromatography (HPLC) grade solvents.

2.7 Thio-phosphorylation assays on CDK1-as cells and affinity purification of peptides

For *in vivo* investigations of Cyclin A2 role in thio-phosphorylation of substrates by CDK1-as, ON-Target pool of siRNA either targeting the expression of *CCNA2* or carrying a scrambled (SCR) non-targeting sequence was mixed with RNAiMAX Lipofectamine in 6 ml of Opti-MEM. After 10 min incubation, RNA-Lipofectamine

complexes were added to a suspension of 3.5 million HeLa CDK1-as cells grown in complete medium as described in section 2.1 to a final siRNA concentration of 20 nM and 10 µM lipofectamine. After a 16 hours incubation, media was changed, and cells were arrested by adding 2 µM 1nm-PP1 (NM) for 18 hours. Cells were then detached by washes with DPBS and incubation with 0.25% Trypsin, both supplemented with 2 µM NM. To wash off NM, cells were placed in Eppendorf tubes and three rounds of 30 sec centrifugation at 5000 g and resuspension of pellets in DPBS were carried out. To induce thio-phosphorylation of CDK1-as substrates, cells were centrifuged, and pellets were resuspended in a permeabilization buffer (20 mM HEPES, 100 mM KOAc, 5 mM NaOAc, 2 mM MgOAc, 1 mM EGTA, 10 mM MgCl2, 500 µM DTT, 45 mg/ml Digitonin, 5 mM GTP, 0.2 mM ATP, 0.1 mM Bulky-ATP and 1x cOMPLETE protease inhibitor cocktail) for 20 mins at 21°C. Thio-phosphorylation reactions were stopped by adding 20 µM EDTA and a 15 min incubation with 1.5 mM p-nitro-benzyl mesylate (PNBM) was carried out at 21°C to alkylate thio-phosphorylated peptides (PNB-thio-phosphates). Protein lysates from these cells were prepared by resuspending pellets in 250 µl CEB followed by sonication at 10% amplitude for 1 min. Proteins in these lysates were denatured by heating at 70°C for 10 mins and their amount was estimated using bicinchoninic acid (BCA) assay, performed according to manufacturer's instructions. Expression of depleted proteins and successful thio-phosphorylation were assessed by western blotting of lysates with antibodies targeting Cyclin A2 (1:2000), Cyclin B1 (1:2000), CDK1 (1:2000) and thio-phospho-esters (ThioP; 1:4000) as described above.

To prepare samples for thio-phospho-proteomic analysis by mass spectrometry, a volume of cell lysates containing 500 µg of proteins was incubated for 10 min with 25 mM TCEP at 37°C. Cysteinyl thiols were then carbamidomethylated with 25 mM iodoacetamide for 1 hour in the dark. Proteins were precipitated by acetone. Acetone was removed after each wash by centrifugation at 15,000 g for 10 mins at 4°C. acetone precipitation was followed by a final wash with 90% ethanol and proteins were then dried for 20 mins at 30 °C to remove residual solvent. To carry

out Tryptic digestion, proteins were resuspended in 500 µl of 100 mM TEAB, supplemented with 2 mM $MgCl_2$ and incubated overnight with 12.5 µg of Trypsin to a 25 ng/µl concentration at 37°C. To ensure efficient digestion, proteins digests were subjected to a further 4-hour incubation with another round of treatment with 12.5 µg Trypsin. Samples were then desalted using Sep-Pak 50 mg C_{18} columns and eluted in 90% acetonitrile diluted in 0.5% formic acid. To increase the stoichiometry of peptides modified with PNB-thio-phosphates, 95% of the dried samples were resuspended in 400 µl of x1 PTM-Scan buffer and incubated with 5 µg of anti-ThioP antibody immobilized on 20 µg of protein G dyna magnetic beads for 1 hour at room temperature. Beads were then washed once with x1 PTM-Scan buffer then twice with DPBS, and thio-phosphorylated peptides were eluted by incubating beads with 400 µl of formic acid for 15 min at room temperature. To remove any residual beads from the sample, peptides were desalted with stage tips prepared in advance and eluted with 90% acetonitrile diluted in formic acid. Peptides were then dried and stored at -20°C until data acquisition by mass spectrometry. The other 5% of the samples was kept for total proteome analysis.

2.8 *In vitro* phosphorylation assays on recombinant substrates

To induce *in vitro* phosphorylation of recombinant, 100 nM of CDK1 was incubated for 40 min with either 500 nM recombinant full length PML isoform 4 (PML-IV) purified from *E.coli* cells by the Hay laboratory at University of Dundee, 500 nM Cyclin H-CDK7-MAT1 or 300 nM 'NDC80^{Broccoli}' (both purified by thse MRC-PPU reagents and services at University of Dundee). Reactions were carried out at 21°C in 150 µl of 40 mM Tris, supplemented with 10 mM ATP. Reactions were stopped by adding SDS to a final concentration of 2%. Total phosphorylation of recombinant proteins was then assessed by SDS-PAGE followed by Pro-Q Diamond staining according to manufacturer's instructions. Total protein bands in the gel were visualised by staining with Instant Blue. For mass spectrometry analysis, ~5 µg of

proteins from the reaction tubes above were reduced, alkylated, and precipitated as described in section 2.7. Tryptic digestion and desalting were then carried as described in section 2.7, except that proteins here were digested with 0.2 µg Trypsin at 0.66 ng/µl and that desalting of 2 µg of digests was carried out using two discs of stage C_{18} tips, where peptides were eluted in 80% acetonitrile diluted with 0.1% TFA. To remove residual SDS from samples, desalted peptides were resuspended in 50 mM ammonium bicarbonate, supplemented with 0.05% formic acid, and incubated with HiPPR resin columns according to manufacturer's instructions. Samples were then eluted, dried and frozen until data acquisition by mass spectrometry.

2.9 Immunoprecipitation of thio-phosphorylated NDC80

For *in vivo* investigations of NDC80 thio-phosphorylation by CDK1-as, 2-8 million HeLa CDK1-as cells thio-phosphorylated as described in section 2.7 were lysed for 30 min with 200 µl RIPA buffer (150 mM sodium chloride, 50 mM tris-hydrochloric acid, 1% Nonidet P-40 [v/v], 0.5% sodium deoxycholate [v/v], 0.1 % SDS [v/v]; pH 8) on ice. Lysates were then centrifuged at 15,000 g for 10 min at 4°C and soluble proteins in the supernatant were collected. To immuno-precipitate (IP) NDC80 or CENP-C, the supernatant was incubated on a rotator for 1 hour at 4°C with 2 µg of either anti-NDC80 or anti-CENP-C antibodies immobilised on magnetic dyna-protein G beads. To remove non-specific proteins, beads were washed three times with DPBS supplemented with 0.1% tween and proteins were eluted by 10 min incubation at 70°C with 10 µl CEB. Samples were then reduced with TCEP, diluted in LDS sample buffer, and immunoblotted with anti-ThioP, anti-NDC80, and anti-GAPDH antibodies as described in sections 2.2 and 2.7.

2.10 Data acquisition by mass spectrometry

In the experiments of chapters 3 and 5, data of the HPLC fractions prepared in section 2.6 were acquired by a Dionex Ultimate 3000 HPLC-coupled Tribrid Fusion Lumos mass spectrometer. Peptides were loaded onto a 75 µm × 50 cm EASY-Spray column with 2 µm sized particles on an EASY-Spray source and operated constantly at 50°C in 0.1% formic acid mobile phase at a flow rate of 0.3 µl/min. Peptides were then fractionated by subjecting them to a mobile phase with 120 min gradient of 2 to 40% of buffer C (80% acetonitrile in 0.1% formic acid) in 0.1% formic acid followed by a steep increase to 95% in 11 min both at 0.25 µl/min. This gradient of peptides was then sprayed into the front end of a mass spectrometer with 2.2 kV at ion capillary temperature of 280°C with a maximum cycle time of 3 sec. To quantitate the precursor ions, MS^1 scans in an Orbitrap were carried out at 120,000 resolutions and a maximum injection time of 50 msec. To identify the sequences of these ions, MS^2 scans were performed on the top 10 most abundant ions with +2 to +6 charge in the MS^1 380-1500 m/z scan window. Selected precursor ions were then fragmented at 28% energy in a HCD cell and scanned on a linear ion trap with a maximum injection time of 50 msec. To eliminate the ratio compression of TMTpro reporters, the top 5 precursors from each of these MS^2 scans were selected for a synchronous precursor selection (SPS)-MS^3 run[125]. These MS^2-generated precursors were fragmented in HCD cell at 55% collision energy and scanned in an Orbitrap at a resolution of 55,000 with a 90 msec maximum injection time. For normalisation, the data of a total proteome samples was acquired in parallel using the exact same method, except that the MS^2 fragmentation was at carried out in a CID chamber at 35% normalised collision energy.

In the experiments of chapter 4, peptide fractions prepared in section 2.6 for both phospho-proteomic and total proteomic analysis were loaded on a trap 100 µm × 2 cm, PepMap nanoViper C_{18}, 5 µm, 100 Å column fitted on a Dionex Ultimate 3000 RS system for 3 min in 0.1% TFA mobile phase. Online fractionation of these peptides

was then carried out in analytical 75 µm × 50 cm, PepMap RSLC C_{18}, 2 µm, 100 Å column by subjecting them to a mobile phase with 5% to 35% gradient of buffer C in 0.1% formic acid for 130 min, followed by a steep increase to 98% for 22 min, both at a flow rate of 0.3 µl/min. Peptides were then sprayed into a Tribrid Fusion mass spectrometer with a cycle time of 3 sec. The MS^1, MS^2 and SPS-MS^3 scans were carried out as described above, except that the maximum injection time was 70 msec for MS^2 and 110 msec for SPS-MS^3, and that the MS^3 fragmentation was at 58% HCD. Identification of phosphorylated peptides by the MS^2 scan also included setting an expected neutral loss that matches the m/z of a phosphate group (98 m/z) for these experiments. Identical method was used to acquire data from the label-free thio-phosphorylated peptides described in section 2.7, except that it lacked both the SPS-MS^3 scan and the neutral loss set up in the MS^2.

Data acquisition for *in vitro* experiments in chapter 6 and those with sequential phosphatase then kinase reactions were carried out in an Orbitrap Eclipse mass spectrometer. The peptides loading and online fractionation parameters were identical to those used for the Tribrid Fusion mass spectrometer described in the paragraph above. The MS^1, MS^2 and SPS-MS^3 scans parameters matches those used to acquire the data on the Tribrid Fusion Lumos described, except that the precursor ions selected for MS^2 fragmentation also included those with +7 charge.

The PML-IV peptides from section 2.8 were loaded onto the same system described for chapter 4 samples. Online fractionation was carried out using a 47 min gradient, where peptides were subjected to a mobile phase with a buffer C gradient of 5% to 98% in 38 min. Data were acquired in a Tribrid Fusion mass spectrometer for 35 min using identical method to that used for the label-free thio-phosphorylated peptides, except that the dynamic exclusion duration of precursor ions was 45 sec instead of 70 sec and that the MS^2 maximum injection time was 50 msec.

To process the data, raw files were analysed using MaxQuant software[126], version 1.6.14. Phospho.STY.txt, Evidence.txt and ProteinGroups.txt files were produced by

matching the raw data to the human reference proteome including reviewed and unreviewed sequences (UniProt, accessed 2017). *In silico* analysis was carried out using the R language. Reverse hits were eliminated from any downstream analysis. To normalise for mixing errors, reporter intensities were normalized by histone protein abundances. TMTpro reporter ion intensities of each phosphorylated site for a particular condition from the Phospho.STY.txt file was divided by the combined Histones' intensities for that condition from the ProteinGroups.txt file. The fold change in phosphorylation for each site was then calculated against that in a control sample, where cells were incubated with a kinase dead Cyclin B-CDK1^{D146N}+Cks1 (D146N), and those with at least 2-fold increase in phosphorylation were considered significantly changed for downstream analysis. To compare different conditions, the phosphorylation intensities of each site in these conditions were scaled using the following equation: $(X- \bar{X})/SD$, where X is the fold change of the site at a particular condition, $\bar{X}$ is the average fold change across all conditions for that site, and SD is the standard deviation of these fold change values. For the CDK1 activity experiments described in chapter 4, the fold change values for sites were not scaled. Instead, a 'cap', by which the fold change value for any site with more than 6.5 increase in phosphorylation was converted to 6.5. Using this, *in silico* saturation was induced on the dataset.

For clustering analysis, scaled fold changes were plotted on a heat map and the Ward agglomeration algorithm was used to separate them into groups based on their phosphorylation patterns across the different conditions. Clusters containing sites with interspersed missing values were eliminated from downstream analysis. To perform motif enrichment analysis, the amino acid sequences flanking the phospho-acceptor residues in the Sequence.window column of the Phospho.STY.txt table for the most common isoform of each protein were inserted into the online tool WebLogo[127]. For comparative enrichment analysis, IceLogo was used to plot figures for sequence enrichments in a positive dataset relative to that in a background dataset[128]. DAVID Bioinformatics (https://david.ncifcrf.gov) was used to perform

gene ontology (GO) analysis. The *p*-values from Fisher's test and the enrichment fold change cut offs were reduced to allow all functions for each set to be reported in the results table and compared. GraphPad prism software was used create heat maps plotting the fold change in GO enrichment of functions. To perform the multisite phosphorylation analysis, the Modification.window column of the PhosphoSTY.txt file was used to identify the location of phosphorylated residues within the protein sequence. The data of this column were separated so that the sequence of each protein is in a row of an Excel sheet and that each cell of that row represents an individual residue. Residues with no phosphate group were represented by a value of 0 and those that were phosphorylated were assigned a value of 1. The number of cells with a value of 1 in a particular row was used to plot the multisite phosphorylation status of proteins in different conditions, while their location relative to a central phosphorylated site were plotted on a bar chart to represent any proximity enrichment relative to one another.

Raw mass spectrometry data acquisition files of samples from thio-phosphorylation assays were processed initially with ProteoWizard software to convert them into mzML files. FragPipe software was then used to process this data and match them to the human proteome sequences[129]. STY file containing residues modified by p-nitro-benzyl-phosphate was used to calculate the fold change of siCCNA2 against siSCR. Sites with 0.5-fold change or less in their phosphorylation intensity were considered significantly affected by Cyclin A2 depletion. GraphPad Prism was used to plot the pie charts for this analysis.

2.11 Reagents table

Antibodies			
Name	**Manufacturer**	**Catalogue number**	**Final concentration**
Rabbit anti-Human phospho-SPXK motif	Cell Signalling Technologies	2325S	1:1000
Rabbit anti-Human thio-phospho-ester (ThioP) for IP	Abcam	ab133473	5 µg
Rabbit anti-Human thio-phospho-ester (ThioP) for WB	Abcam	ab92570	1:4000
Rabbit anti-human Cks1	Thermo-Fisher Scientific	36-6800	1:500
Rabbit anti-human Cks2	Abcam	ab155078	1:1000
Rabbit anti-human Cyclin A2	Abcam	ab32386	1:2000
Mouse anti-human Cyclin B1	Cell Signalling Technologies	4118S	1:2000
Mouse anti-human GAPDH	Santa Cruz Biotechnology	sc-365062	1:2500
Mouse anti-human α-Tubulin	Sigma-Aldrich	CP06-100UG	1:5000
Mouse anti-human H3pS10	Cell Signalling Technologies	29237S	1:1000
Mouse anti-human NDC80	Santa Cruz Biotechnology	sc-515550	WB: 1:1000/IP: 2 µg
Guinea pig anti-human CENP-C	Caltag and Medsystems	PD030	IP: 5 µl

Columns/instruments:		
Name	**Manufacturer**	**Catalogue number**
Elutriation chamber	Beckman-Coulter	356943
Sep-Pak 50 mg C_{18} columns	Waters	WAT054955
NEST micro-spin C_{18} columns	Harvard Apparatus	74-4601
HPLC 1 mm, 13 µm BEH resin C_{18} columns	Waters	186002346
24 ml Superdex 75 10/300 gel filtration column	Cytiva	29148721
53 ml Sephadex G-25 HiPrep 26/10 desalting column	Cytiva	10470505

Chemicals			
Name	**Manufacturer**	**Catalogue number**	**Final concentration**
Propidium Iodide (PI)	Sigma-Aldrich	P4864-10ML	50 µg/ml
Diamidino phenylindole (DAPI)	Sigma-Aldrich	D9542-10MG	5 µg/ml
1-NM-PP1 (NM)	Sigma-Aldrich	529581-1MG	2 µM
S-trityl-L-Cysteine (STLC)	Sigma-Aldrich	164739-5G	25 µM
Adenosine triphosphate (ATP)	Sigma-Aldrich	A2383-5G	10 mM/0.2 µM
N-Phenyl-ATP-γ-S (Bulky ATP)	Biolog	P 044	0.1 µM
Guanosine triphosphate (GTP)	Sigma-Aldrich	G8877-10MG	5 µM
Dithiothreitol (DTT)	Sigma-Aldrich	D0632-1G	500 µM
Tris carboxyethyl phosphine (TCEP)	Thermo-Fisher Scientific	PG82080	25 mM
Iodoacetamide	Sigma-Aldrich	I1149-5G	25 mM
Triethylammonium bicarbonate (TEAB)	Sigma-Aldrich	T7408-100ML	100 mM

Tandem mass tag (TMTpro) 16 plex	Thermo-Fisher Scientific	A44520	0.25 mg
Hydroxyl amine	Thermo-Fisher Scientific	90115	5%
Acetonitrile	Thermo-Fisher Scientific	A955-1	80-99.9%
Methanol	Fisher Scientific	11976961	20-90%
Formic acid	Thermo Fisher Scientific	28905	0.5-2%
Acetic acid	Thermo Fisher Scientific	A11350	0.50%
Trifluoroacetic acid (TFA)	Sigma-Aldrich	302031	0.1-5%
ammonium hydroxide	Sigma-Aldrich	338818-100ML	1%
Ammonium formate	Sigma-Aldrich	78314-100ML-F	10%
Glycolic acid	Sigma-Aldrich	420581-100ML	5%
PTM-Scan IAP buffer	Cell Signalling Technologies	9993	x1
cOMPLETE protease inhibitor cocktail	Sigma-Aldrich	11836170001	x1
Phosphatase inhibitor cocktail (PhosSTOP)	Roche	4906837001	x1
Trypsin protease	Thermo-Fisher Scientific	90058	1:20
Pierce HiPPR columns	Thermo-Fisher Scientific	88305	25 ul settled resin
Benzonase	EMD Millipore	70664-10KUN	5 U

Cell culture medium supplements			
Name	**Manufacturer**	**Catalogue number**	**Final concentration**
Dulbecco's Modified Eagle Medium (DMEM)	Life Technologies	10565018	x1
Roswell Park Memorial Institute (RPMI)	Life Technologies	61870010	x1
Opti-MEM (GlutaMAX)	Life Technologies	51985026	x1
Dulbecco's phosphate buffered saline (DPBS)	Life Technologies	14190250	x1
Foetal bovine serum	Life Technologies	10270106	1-10%
Trypsin, no phenol red	Thermo-Fisher Scientific	15090046	0.25%
Lipofectamine RNAiMAX	Invitrogen	11668019	10 nM
On-Target 4 Si-CCNA2 RNA duplex	Dharmacon	LQ-003205-00-0002	20 nM
On-Target non-targeting Si-SCR duplex	Dharmacon	D-001810-01	20 nM
PureLink™ HiPure Plasmid Midiprep Kit	Invitrogen	K210004	NA

Chapter 3:

Development of an *in vitro* kinase assay to study the phosphorylation dynamics of cell cycle substrates

3.1 Summary

Protein phosphorylation is one of the molecular mechanisms through which a cell maintains its faithful division. Protein kinases and phosphatases form complex dynamic circuits that determine the phosphorylation status of cellular substrates. One challenge when studying these enzymes, however, is the signalling complexity found in cells. This complexity makes it difficult to demonstrate identification of a direct substrate in cells. Therefore, *in vitro* kinase assays on either recombinant substrates or cells' lysates have been historically used for this purpose. However, the simplicity of assays on individual substrates prevents investigating global patterns in kinases-substrates interactions. Furthermore, the activity of other kinases in the lysates makes it challenging to identify the putative kinase behind phosphorylation events detected. In this chapter, I developed and optimised a method by which phosphorylation of substrates by a particular kinase can be characterised in whole cells where other kinases and phosphatases are inactive. This method involved incubation of fixed and permeabilized cells with recombinant kinases and a phosphate donor molecule. Titration of cells with recombinant active Aurora B and coupling this with mass spectrometry-based phospho-proteomics yielded quantitative changes in protein phosphorylation level across the proteome. Furthermore, it demonstrated an enrichment of the consensus amino acid sequence targeted by Aurora B. Results from this chapter present a new method to study protein phosphorylation *in vitro* that is highly sensitive to both the activity and composition of the recombinant kinase used.

3.2 Introduction

A central regulatory mechanism in cell cycle control is the reversible post-translational modification of proteins by phosphorylation. In mammalian cells, protein phosphorylation occurs on Serine, Threonine or Tyrosine residues in substrate proteins. The phosphate group changes the electrostatic character of the

acceptor amino acid residue, frequently resulting in conformational changes that affect the structure and function of the phosphorylated substrate. In cells, proteins are phosphorylated in a cell cycle regulated manner. This is the net output of the antagonistic activities between protein kinases and phosphatases[39]. Numerous negative and positive feedback loops have been shown, which help determine the temporal ordering of substrate phosphorylation[49]. Several other factors may contribute to that, too. One of these is the activity of the enzymes, which may be determined by phosphorylation of particular sites in that enzyme, such as the activation loop phosphorylation in kinases. The activity can also be gained from association with other non-catalytic subunits. For example, CDK1 is activated by forming a complex with either Cyclin A or B. Similarly, Aurora B association with- and phosphorylation of INCENP substantially increases its activity. Another important factor is the proximity of these enzymes to the targeted residue. PLK1 for example, localises, through its polo-binding domain, near its target residues[34]. Similarly, Survivin's docking on phosphorylated Histone 3 localises CPC at the centromere during mitosis, which is critical for maintaining faithful kinetochore-microtubule attachments[130].

Many methods have been developed to study such determinant factors of substrate phosphorylation by a particular kinase or dephosphorylation by a phosphatase, however the complexity of the system makes it extremely difficult to segregate indirect substrates from those that are direct. These methods involve investigating the dynamics and kinetics of phosphorylation either *in vitro* or *in cellulo* as well as the use of small molecule kinase inhibitors. Coupling these techniques with mass spectrometry allowed comprehensive assessment of protein phosphorylation during the cell cycle[60,69,109,131]. Despite these technical advances, each method still has its own limitations. For example, while assessing the phospho-proteomic signature of different cell cycle phases provides information about how the phosphorylation status of individual substrates changes with cell cycle progression, it does not identify the kinases responsible. Similarly, experiments where a recombinant kinase

is added to cell lysates fail to discriminate between direct and indirect substrates, since other kinases are still active in the background. Inhibitor based approaches on the other hand have the limitations of potential off-target effects on other kinases. Recently, our laboratory reported two mass spectrometry-based (phospho-)proteomic studies of the cell cycle from fixed and permeabilized cells[69,124]. In this chapter, I will present a method in which protein phosphorylation of substrates can be induced *in vitro* by recombinant kinases in these cells. The advantage of using such system is that the processes of fixation and permeabilization substantially compromise the activity of endogenous phosphatases in these cells while completely diminishing that of kinases. This means that unlike parallel experiments on lysates, phosphorylation detected post fixation and permeabilization can be exclusively attributed to the recombinant kinase added to the cell. Furthermore, this sort of analysis allows global assessment of substrates phosphorylation by that kinase since the crosslinking will preserve most of the targets in the cell.

3.3 Results

3.3.1 *In vitro* phosphorylation of Histone H3 by recombinant Aurora B can be induced in fixed cells

To investigate the possibility of using recombinant proteins to phosphorylate substrates in fixed and permeabilized cells *in vitro*, firstly, I fixed and permeabilized a suspension of TK6 cells. This is a human lymphoblast cell line that grows in suspension. We chose TK6 in this study both for its diploid karyotype and relatively small size[132]. The diploid karyotype makes them is less genetically transformed than other cell lines, like HeLa. Besides, TK6 growth in suspension means that they are less likely to aggregate during harvesting. Both this and their small size makes them more compatible with the elutriation method that will be described later in this chapter. The fixation by formaldehyde cross linking of cellular proteins is to inactivate protein kinases in these cells. Inactivation of kinases here means that any phosphorylation

event detected after incubation with the recombinant kinase is very likely to be a result of direct interaction between that kinase and the phosphorylated substrate. Permeabilization with methanol was performed to allow both the recombinant kinase and the phosphate group donor molecule, ATP, to penetrate the plasma membrane. The full protocol is presented in Figure 3.1A. Secondly, to induce protein phosphorylation in these cells, I expressed and purified a recombinant active Aurora B from bacterial cells. I chose this protein because it is the catalytic subunit of the CPC, a key regulator of protein phosphorylation in mitotic cells[65-67]. Aurora B has been demonstrated to phosphorylate Histone H3 on Serine 10, which is frequently used as a phospho-epitope marker for mitotic cells[133]. SEC of soluble proteins from bacterial lysates that were enriched for this protein showed a distinct peak that corresponded to the molecular weight of the active Aurora B kinase complex (Figure 3.1B, left panel, asterisk). SDS-PAGE of samples from the fractions that contained this peak showed two bands with molecular weights matching those of the two truncated subunits in the recombinant complex: INCENP$^{885-903}$ and Aurora B$^{55-334}$ (Figure 3.1B, right panel). No other protein bands could be observed in the lane, which suggests the major protein species in the preparation is the kinase desired. Next, I incubated the fixed cells prepared above with this complex and ATP. To assess if the recombinant Aurora B complex was able to *in vitro* phosphorylate these cells, I performed IF analysis with the H3pS10 antibody (Figure 3.1C). As Figure 3.1C shows, fixed cells treated with Aurora B and ATP have increased H3pS10 signal when compared to cells incubated with only ATP. These results demonstrate phosphorylation of cellular substrates by the added recombinant Aurora B.

Because the aim here is to use this assay in studies of protein phosphorylation dynamics, it is crucial to investigate the concentration dependence of kinase activity. This can be tested by titrating the cells with Aurora B and assessing the phosphorylation with H3pS10 afterwards. Western blotting analysis of lysates from fixed cells incubated with three different concentrations of Aurora B showed gradual increase in the signal intensity of the band corresponding to H3pS10 (Figure 3.1D).

This increase was proportional to the amount of the active Aurora B added. In contrast, the signal intensity of total Histone H3 and Alpha-Tubulin bands across the four samples were not changing. This shows that the increase in H3pS10 intensity was not due to an increase in sample loading. No band could be observed in the control sample, where no recombinant kinase was added. Taken together, these results show that it is possible to use recombinant Aurora B and ATP to induce protein phosphorylation in fixed and permeabilized cells and that this phosphorylation is dependent on the kinase concentration.

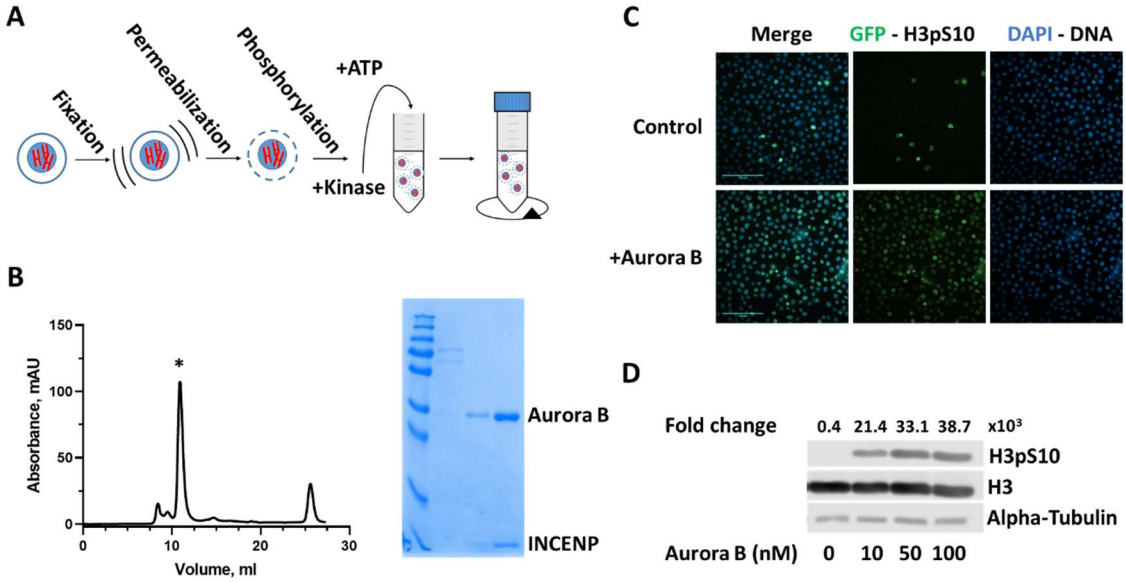

Figure 3.1: Protein phosphorylation in fixed and permeabilized cells. (A) Experimental workflow: Fixed and permeabilized cells are incubated with recombinant protein kinase and ATP to induce protein phosphorylation. (B) Purification of recombinant Aurora B to use it for testing the assay in (A). SEC profile for Aurora B^{55-334} co-expressed with truncated $INCENP^{885-903}$ in the left panel and gel from SDS-PAGE stained with Instant Blue for samples from the elution fractions of the large peak in the chromatogram (asterisk) in the right panel. (C) IF microscopy images of fixed cells after incubation with either the complex purified in (B) or only ATP (Control). (D) Western blotting of lysates from fixed cells titrated with

recombinant Aurora B. Numbers on top represent the row intensity values of underneath H3pS10 bands divided by 1000, quantitated by Emperia studio software.

3.3.2 Protein phosphatases retain some activity in cells after fixation and permeabilization

Because protein phosphorylation is a reversible modification, it is important to consider the activity of phosphatases, which carry out substrate dephosphorylation. A recent report suggested that enzymes in cells fixed with paraformaldehyde can retain some activity post-fixation[134]. In the experiments that I discussed in section 3.3.1, in addition to the formaldehyde fixation, I also added methanol to the cells, which as well as being a permeabilizer, is a fixative. This makes it less likely to retain any enzymatic activity than when fixing with formaldehyde alone. However, because I am planning to use this assay to study phosphorylation dynamics as it will be discussed in the next two chapters of this thesis, it was important to ensure that no endogenous phosphatase activity will interfere with the phosphorylation induced by the recombinant kinase here. This phosphatase interference is another major issue when using fresh cell extracts for this sort of investigation. To assess the activity of protein phosphatases in the fixed cells used here, I incubated these cells with the molecule p-nitro-phenyl phosphate (pNPP). This colourless molecule contains a phosphate group that is cleavable by all phosphatases, including Serine and Threonine. Upon the cleavage of this group, the colour of the molecule is yellow. The absorbance at 504 can thus be used to indirectly assess the phosphatase activity in a sample that contains pNPP. Results from this experiment have shown that incubation of pNPP with fixed cells for 19 hours at 30°C significantly increases absorbance when compared to control sample where no fixed cells were added (Figure 3.2B). This suggests that these cells retain some phosphatase activity even after formaldehyde fixation and methanol permeabilization. To investigate the possibility of supressing this activity, I incubated cells with either a titration of the Serine/Theonine

phosphatase inhibitor, Microcystin, or with the pan phosphatase inhibitor cocktail, PhosSTOP. Results revealed that albeit with a dose-dependent reduction in absorbance, the levels remained significantly higher in the samples contained Microcystin than the control (Figure 3.2A). This shows that even the maximum concentration of Microcystin used in this experiment did not inhibit the endogenous activity of phosphatases. In contrast to this, despite a marginal increase, absorbance levels were no longer significantly higher in the sample that included PhosSTOP when compared to the control. These results demonstrate that fixed cells retain some phosphatase activity and that this activity can be halted by treatment with PhosSTOP at the recommended concentration by the manufacturer. The duration of the reactions here, however, significantly exceeded that of the kinase assays (19 hr versus 40 min). Incubation of cells with pNPP for only 40 min did not yield any yellow colour in the sample, suggesting low residual activity of protein phosphatases in these cells (data not shown). Alternatively, this may be explained by the low sensitivity of pNPP, as 19-hour incubation with 1 U of λ Phosphatase only showed marginal increase in the signal.

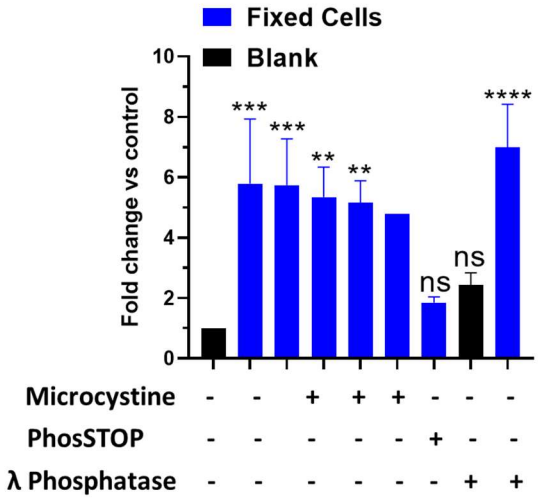

Figure 3.2: The activity of phosphatases in fixed cells. Bar chart showing the fold change in absorbance at 504 in fixed cells in the presence and absence of either a titration of microcystin, x1 PhosSTOP or λ Phosphatase compared to a blank sample

with only pNPP after a 19-hour incubation at 30°C. ns: no significance; ** p <0.01; *** p <0.001; **** p <0.0001.

3.3.3 Centrifugal elutriation to enrich G2 cells in the sample

In section 3.3.1, I showed that incubation of fixed and permeabilized cells with a recombinant version of the mitotic kinase Aurora B resulted in robust phosphorylation of an Aurora B substrate. The results of the fixed cell phosphorylation assay will crucially depend on the substrates present in the cell at the time of fixation. It is therefore important to consider whether the cells will have the appropriate substrates expressed. Even though Aurora B was reported to target substrates in interphase cells[135,136], most of its phosphorylations occur during M phase[65]. Hundreds of proteins undergo cell cycle regulated variation in protein abundance, peaking in G2 and M phase of the cell cycle. Asynchronous cultures of human cells will consist of primarily G1- and S-phase cells, which will have low to no expression of G2/M-phase peaking proteins. Thus, to ensure that appropriate substrates for Aurora B are available in fixed cells for phosphorylation, I chose to enrich for G2 cells and use them in the assay. An obvious method to use for this purpose would be the FACS, which produces cell cycle populations with minimum cross contamination, since one can rely on the expression of cell cycle markers to fractionate cells with this method. Having said that, the number of cells required for an *in vitro* phosphorylation assay experiment makes FACS impractical. For this reason, I used centrifugal elutriation to separate the cell cycle populations in the fixed culture. This is a method where cells are fractionated based on their size, which increases with cell cycle progression. However, centrifugal elutriation cannot discriminate between G2 phase cells and those in M[131]. Results showing the DNA content assessed by flow cytometry of fixed TK6 cells fractionated by this technique revealed clear separation of cells with 2N, 3N and 4N DNA content in some of the fractions, which respectively correspond to G1, S and G2/M (Figure 3.3A). Then,

based on this data, I pooled the fractions with 4N DNA content (Figure 3.3A, fractions 10-12) and stained a sample from this pool for the DNA and the mitotic marker H3pS10 to calculate the percentage of mitotic cells by flow cytometry. Results have shown than no more than 10% of the fixed cells in this pool are in mitosis (Figure 3.3B). This means that in the control samples of the phosphorylation assay, the stoichiometry of Aurora B targets that will be phosphorylated by the endogenous kinase before fixation will not exceed 10% when using these cells. Based on this data, centrifugal elutriation was used to enrich G2 phase and other cell cycle phases in all the experiments that involved *in vitro* kinase assays in later chapters of this thesis.

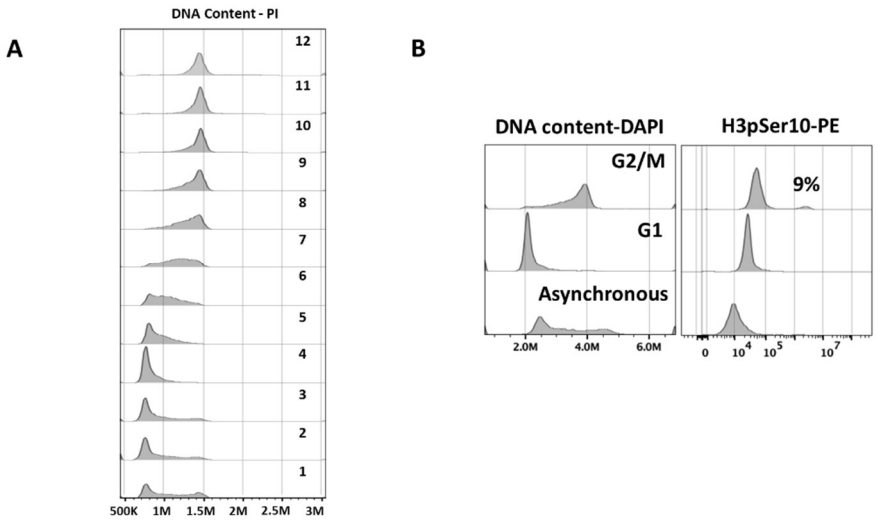

Figure 3.3: Centrifugal elutriation of fixed cells to separate cell cycle populations. (A) DNA content of fixed TK6 cells fractionated by centrifugal elutriation and evaluated by flow cytometry. Layers represent the different centrifugal elutriation fractions. Layer 1 is the original culture that was fractionated. (B) Flow cytometry analysis of the pool of fractions 2 (G1) or 10-12 (G2M) in (A) stained with DAPI and H3pSer10-PhycoErythrin (PE).

3.3.4 Quantitative Phospho-proteomics of fixed cells phosphorylated by Aurora B *in vitro*

Next, I wanted to apply this fixed cell kinase assay to investigate the substrates of Aurora B. To do that, I fixed and permeabilized a culture of TK6 cells and collected the G2/M populations using centrifugal elutriation. I then performed the *in vitro* phosphorylation assay described in section 3.3.1. with a titration of recombinant Aurora B and prepared peptide digests from the phosphorylated and control cells using the protocol previously reported by our laboratory[124] (Figure 3.4A). To enable comparison between multiple different samples, I labelled the peptide digests with TMT and pooled them into one sample. Channels from the same TMT set were used to label samples of the second replicate to increase the likelihood of identifying the same peptides and hence assess the reproducibility of their phosphorylation across the two biological replicates (Figure 3.4 B). Titanium immobilised affinity chromatography (Ti-IMAC) was used to enrich for phosphorylated peptides. Finally, to allow deep phospho-proteomic analysis, I used reverse phase liquid chromatography to fractionate the phosphorylated peptides before data acquisition by mass spectrometry. A detailed protocol for sample preparation is described in Figure 3.4A and chapter 2. To acquire the phospho-proteomic data, I used the SPS-MS^3 method[125]. Using this method improves the quantitation of TMT reporters since it minimises the interference between TMT ions labelling multiple peptides co-eluting at the same time.

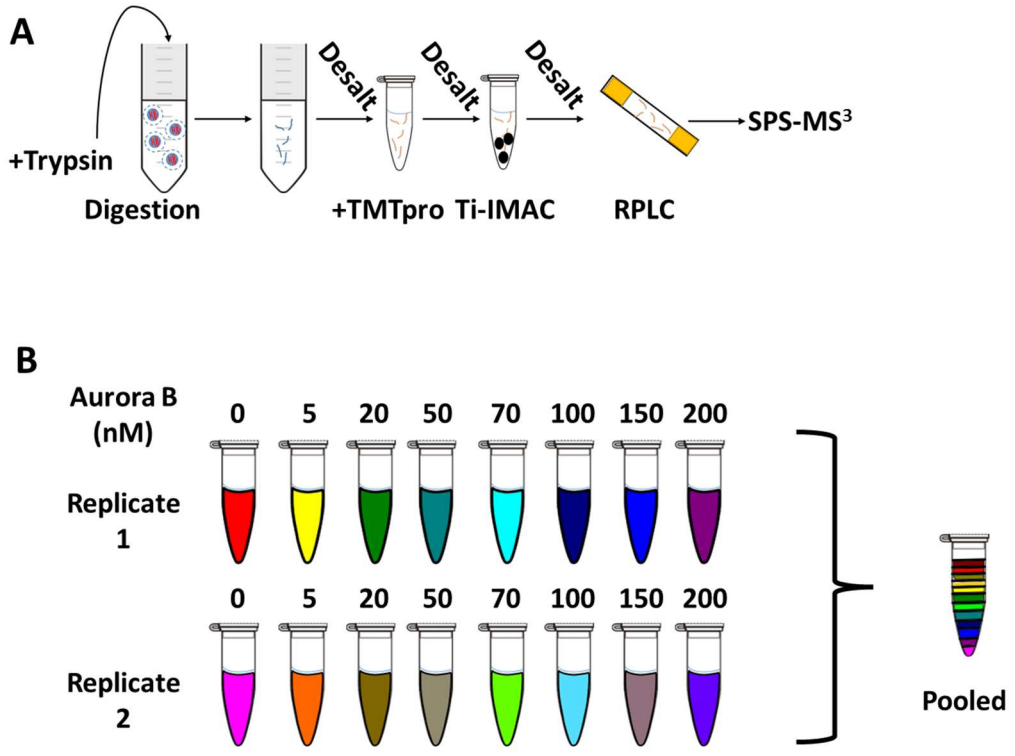

Figure 3.4: Phospho-proteomic analysis of fixed cells phosphorylated by Aurora B *in vitro*. (A) Schematic describing the sample preparation for mass spectrometry-based phospho-proteomic analysis. (B) Multiplexing samples with TMTpro for quantitative mass spectrometry-based phospho-proteomics. Fixed cells in (A) from two replicates were titrated with Aurora B at the concentrations indicated and labelled with the TMTpro channels 126-130^{N} (top row, first replicate) and 130^{C}-134^{N} (bottom row, second replicate) before being pooled together.

In this experiment, I identified and quantitated 13374 sites. Out of these, 362 sites showed at least 2-fold increase in their phosphorylation with *p* values < 0.05 (Student's *t* test) at 200 nM Aurora B concentration in the two biological replicates. Many of the induced phosphorylations were on proteins with known mitotic functions. These included TPX2, LMNA, Ki67, NUMA1, KIF21A. In addition, the Aurora B T-loop site Threonine 272 was also phosphorylated *in vitro*. Furthermore, recombinant Aurora B phosphorylated multiple sites on the scaffolding subunit of

the CPC, INCENP. When all phosphorylated sites that passed the fold change cut off were plotted on a heat map, their average phosphorylation in each sample was increasing in a way that was proportional to the amount of Aurora B added to that sample (Figure 3.5A and B). When looking at the individual sites of the heat map, however, their phosphorylation pattern was variable. This data reflects different propensities for these sites to Aurora B phosphorylation. Because this assay is performed on fixed cells, I did not expect to see a drop in phosphorylation at a higher concentration compared to a lower one. Having said that, some of the heat map sites show this kind of pattern in their phosphorylation profile (Figure 3.5A, bottom of the heat map). This is very likely to result from intensity readings missing from the phospho-proteomic dataset at these conditions. Despite of this, the vast majority of sites on the heat map do not fall into this category. Because of the *in vitro* nature of the assay, I expected a fraction of the sites phosphorylated here to be non-specific. For this reason, it was important to investigate the specificity of phosphorylation carried out by a recombinant Aurora B to the motif targeted by the endogenous counterpart. Studies using peptide arrays and small molecule inhibition have demonstrated that the consensus motif of Aurora B consists of a phospho-acceptor residue (Serine or Threonine) and one or more basic residues in the N-1 to N-3 positions, where N is the phospho-acceptor residue[60,61,137]. I performed motif enrichment analysis for the phosphorylated sites in the heat map and compared it to that in the rest of the phospho-proteome. Results have shown Arginine enrichment, mainly in position -2, but also in -1 and, to a lesser extent, in -3 and -4 (Figure 3.5C). These results demonstrate that recombinant Aurora B in the fixed cell kinase assay phosphorylated sites located in the established consensus amino acid sequence for Aurora B[60,137]. Taken together, the data from this experiment shows that fixed cells can be phosphorylated to different extents on sites that fall within the motif targeted by Aurora B *in vivo*.

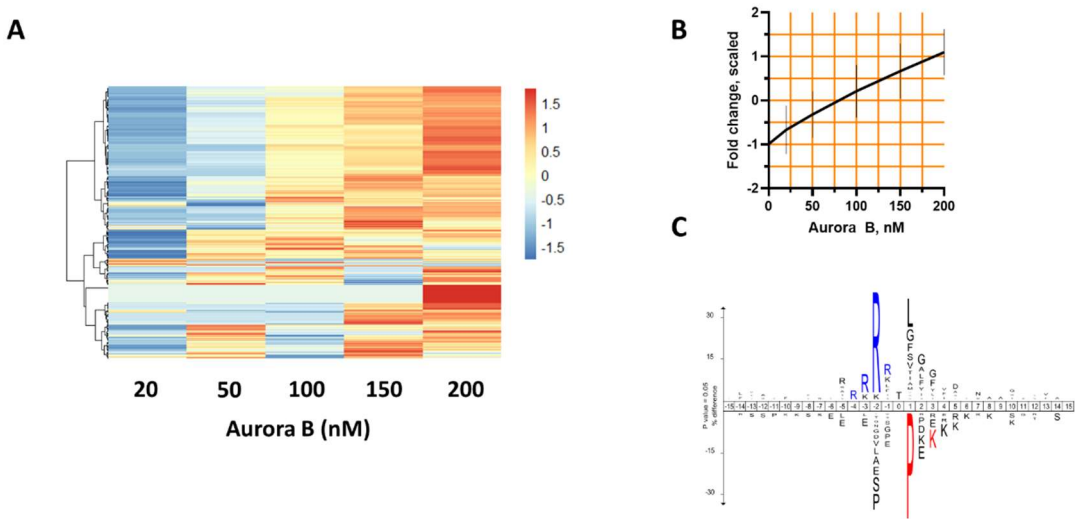

Figure 3.5: Concentration-dependent increase in the phosphorylation of sites within the Aurora motif. (A) Heat map representing the fold change in phosphorylation intensity of sites (rows) by the different concentrations (columns) of Aurora B against a control sample where no kinase was added. Data in each row were scaled to make them relative to each other. (B) Line plot representing the average phosphorylation of sites across the different concentrations of Aurora B in the heat map from (A). (C) IceLogo chart showing the sequence enrichment analysis of sites from (B) on the top panel when compared to that of the rest of the phospho-proteome at the bottom.

3.4 Discussion

In this chapter, I aimed to develop an assay in which protein phosphorylation by cell cycle kinases can be investigated *in vitro* in whole cells. I also attempted to assess the specificity of this assay for the targeted residues as well as its sensitivity for dynamic changes to the added kinases. The assay involved phosphorylating substrates in fixed and permeabilized cells with a recombinant protein kinase. For a long time, fixation with Formaldehyde and permeabilization with methanol has been one of the standard protocols for IF studies, as it allowed antibodies to reach internal targets that would not be accessible for them otherwise[138]. As a result of this, a combination

of cell fixation and permeabilization, and FACS has been widely used to purify cells, for example of the different haematopoietic lineages, based on the expression of their intracellular markers[139]. It also formed the basis for the PRIMMUS method that was reported by our laboratory earlier[69]. Making biological interpretations from studies that involved fixation and permeabilization with these two reagents, however, has also been a source of concern for some[140]. The main issue that they raise is the artifacts that can be induced on protein structures. Formaldehyde for example is a cross-linker that induces di-methylation on Lysine residues. While this cross-linking will conserve the native structure of proteins in this assay, it can reduce the dynamic changes that would normally occur when these proteins are phosphorylated *in vivo*. Also, di-methylation by formaldehyde can also form on individual Lysines, which can interfere with substrates recognition by the protein kinases that I am adding to the cells. This modification, however, is not as likely to occur here as it requires the presence of a strong reductant like borohydride. Similarly, the use of methanol in this assay can be problematic. Incubation of cells with this permeabilizer causes some of their proteins to precipitate, leading to drastic changes in their native structures[141]. For this reason, other permeabilizers, such as Triton, have been utilised as alternatives in previous immunofluorescence studies[142]. When I permeabilized cells with detergents like Triton, Saponin or Digitonin, however, I observed reduced cleavage efficiency in the Tryptic digestion of fixed cells (data not shown). This could be because I prepared these peptides using the in-cell digestion protocol reported earlier by our group[124]. Digestion of proteins in-cells reduces the sample size required for generating datasets suitable for comprehensive analysis. This protocol, however, was optimised for cells fixed with formaldehyde and permeabilized with methanol. Swapping the latter with detergents might contribute to this decline in Trypsin digestion efficiency, possibly due to the lower efficiency of these detergents in permeabilizing cells when compared to methanol. The results presented here also demonstrated that residual phosphatase activity is retained in cells after fixation and permeabilization. This

shows that not all proteins are irreversibly precipitated in these cells. Additionally, titration of cells with Aurora B revealed phosphorylation of sites enriched with the consensus motif of this kinase. This demonstrates a high degree of specificity, at least for the sequences that this kinase would normally interact with *in vivo*. Furthermore, these experiments yielded an increase in the global phospho-proteome that correlated with the amount of Aurora B that was added to the cells. This suggests sensitivity to small changes in the stimulus that was induced by the active kinase.

Taken together, the use of fixed and permeabilized cells for *in vitro* phosphorylation studies has its pros and cons. The data that I discussed in this chapter suggest a degree of kinase consensus motif specificity. This presents the protocol as a suitable tool for understanding both the qualitative and quantitative determinant of kinase-substrate interactions in human cells. In the future, it will be interesting to compare the sites phosphorylated in this assay to those in active cell extracts.

Chapter 4:

Cyclin A2 promotes non-Proline directed phosphorylation by CDK1 and shifts its substrate specificity

4.1 Summary

The temporal ordering of DNA replication and mitosis is an important determinant for achieving faithful cell division. Ordered phosphorylation of cell cycle-related substrates by CDK is central to this process. In G2 and M phases of the cell cycle, CDK1 is activated by binding to Cyclin A2 and Cyclin B1. In this chapter, I aimed to understand how the Cyclin partner of CDK1 influences the ordering of substrate phosphorylation in fixed cells. I also investigated the impact of increased CDK1 activity on substrate choice. To do this, I used the phosphorylation assay that I presented in chapter 3 in combination with recombinant Cyclin A2- and Cyclin B1-CDK1 complexes. Results in this chapter demonstrate that CDK1 relies on two mechanisms to select its substrates: changing its preferred motif and progressively increasing its activity throughout cell division. Results here also reveal that CDK1, when in complex with Cyclin A2, can bypass the requirement for a +1 Proline and phosphorylate S/TXXK/R sites. This data adds a new dimension to the current models suggested for CDK1 phosphorylation of its substrates during cell division.

4.2 Introduction

Protein phosphorylation maintains the temporal order of cell cycle events. Master regulators of this post-translational modification during the cell cycle are members of the CDK family[72]. These are Serine and Threonine kinases that frequently phosphorylate residues in substrates when followed by a Proline amino acid. In addition to the +1 Proline, some phospho-acceptor sites have a basic amino acid in the position +3[97]. In human cells, over 20 proteins make up the CDK family, out of which, four are directly involved in phosphorylating the substrates that are critical for cell cycle progression (CDK1, CDK2, CDK4 and CDK6). This is in contrasts with both budding and fission yeasts, which only express the homologue of CDK1. The variability in the number of CDKs between upper and lower eukaryotes led some to investigate the necessity of having multiple CDKs in mammalian cells. Experiments

deleting CDKs in mouse embryos showed that CDK1 is the only essential CDK for the first embryonic cell division[143].

To gain their catalytic activity, CDK1/2/4/6 require binding to one of Cyclins A, B, D and E proteins. These four Cyclins are expressed periodically, meaning that the levels of each peak at a particular cell cycle phase before being degraded. Cyclin A and Cyclin B for example are expressed maximally in G2 and M phases, while Cyclin E peaks at G1/S phase. In contrast, expression changes of CDK1/2/4/6 across the cell cycle are relatively modest. In addition to their periodic expression, Cyclins also exhibit variable propensities in their binding to the four CDKs. For example, Cyclins A and E preferably form complexes with CDK2, while Cyclin D mostly forms a complex with CDK4 and CDK6[144]. This makes each of the four CDKs more specialised in the set of substrates that they target[76]. For example, CDK2 is more likely to target S phase substrates than CDK1, since it is activated by Cyclin E, which peaks during that phase. One complexity in this system, however, is that despite having four Cyclins to activate four CDKs, more than one Cyclin may show propensity to an individual CDK. For example, in mitotic cells, CDK1 exist in complexes with either Cyclin A or Cyclin B. The degree of specificity that these Cyclins provide a particular CDK with when selecting substrates for phosphorylation has always been a point of debate. Two models were suggested to answer this question with elegant studies supporting each. In one model, named the qualitative, Cyclin is a central element to the temporal ordering of substrates phosphorylation during the cell cycle, because it directs CDK to the right substrate. In contrast, in the second, quantitative model[84], this order in phosphorylating the cell cycle substrates is solely a result of the gradual increase in CDK activity occurring with cell cycle progression and Cyclin is only there to create this activity. In chapter 3, I optimised a method in which a recombinant kinase can be used to induce *in vitro* phosphorylation of substrates in fixed and permeabilized cells. In this chapter, I will use this assay to assess how each of the two models above contribute to the temporal ordering of substrates phosphorylation by

CDK1 through investigating the phospho-proteome induced by two recombinant protein complexes, Cyclin A2-CDK1 and Cyclin B1-CDK1.

4.3 Results

4.3.1 Cyclin A2/B1-CDK1 complexes can induce highly specific proteome-wide, concentration-dependent increase of protein phosphorylation in fixed cells

To investigate substrate phosphorylation by CDK1 proteome-wide, I applied the fixed cell kinase assay presented in chapter 3 with recombinant CDK1 kinase complexes. I performed the experiment in two conditions, replacing the Cyclin partner and treating the cells with either Cyclin A2-CDK1 or Cyclin B1-CDK1 to assess what impact would this have on CDK1 substrate choice. These two recombinant enzymes were generous gifts from the Endicott laboratory[93,145] in Newcastle University. Our interest in the somatic cells division led us to select these two complexes. On one hand, the functional redundancy of the three Cyclin B paralogues meant that any of them would be suitable for our biological question. On the other hand, human cells express more specialised paralogues of Cyclin A. In these, Cyclin A1 plays an essential role in meiotic divisions of germ line cells[146]. In contrast, Cyclin A2 is critical for G2/M transition, as it was demonstrated in cells acutely depleted of it with a double degron system[86,119].

I began this investigation with a relatively simple experiment in which I looked at the ability of these two complexes to phosphorylate sites located in one of the optimal CDK1 motifs, the SPXK (where x is any amino acid). IF of fixed cells that were phosphorylated with either Cyclin A2-CDK1 or Cyclin B1-CDK1 at 21°C with an antibody that targets the SPXK motif only when phosphorylated on the Serine residue revealed an increase in the signal intensity of this antibody following incubation with these complexes (Figure 4.1A). This demonstrates that these recombinant CDK1 complexes are active and can phosphorylate some CDK substrates

in fixed cells. It was not possible, however, to observe such increase in the SPXK phosphorylation signal when the experiment was performed at 37°C, in agreement with previous biochemical assays, where CDK1 complexes appeared to be unstable at temperatures higher than 30°C (J. Endicott, personal communication). Furthermore, there was no variability in the intensity of SPXK phosphorylation signal between Cyclin A2- and Cyclin B1-CDK1 treated cells, suggesting comparable catalytic activity for both complexes (Figure 4.1, compare magnified images).

Next, I wanted to evaluate the possibility of using these two complexes to study the phosphorylation dynamics of CDK1 in fixed cells. To do this, I titrated the two complexes and added them to fixed and permeabilized TK6 cells then prepared peptide digests from these samples for a label-free mass spectrometry-based phospho-proteomics experiment. Results unveiled a concentration dependent, proteome-wide increase in the number of sites that showed at least 5-fold increase in their phosphorylation intensity in the 4502 proteins identified in this experiment, when compared to a control sample only incubated with ATP (Figure 4.1B). Analysis of the amino acid sequence of these residues showed an enrichment of the TPXK motif compared to the rest of the phospho-proteome (Figure 4.1C). This data suggests that phosphorylation induced here is highly specific for CDK sites, since this is one of the motifs reported to be targeted by CDK1 *in vivo*. One thing that can be noticed when comparing the enrichment of Cyclin A2-CDK1 targets (Figure 4.1C, +Cyclin A2) with that of Cyclin B1 though, is the enrichment of the +3 Lysine, which is higher in the Cyclin A2 data. In contrast to this, Cyclin A2 targeted sites had lower enrichment of the +1 Proline compared to those of Cyclin B1. Together, this data demonstrates that both CDK1 complexes can phosphorylate fixed and permeabilized cells *in vitro* and suggest some variability in the sites targeted by them. However, since this dataset was generated from only a single, label-free experiment, it was important to investigate the reproducibility and impact of this potential variability using a more detailed, quantitative approach.

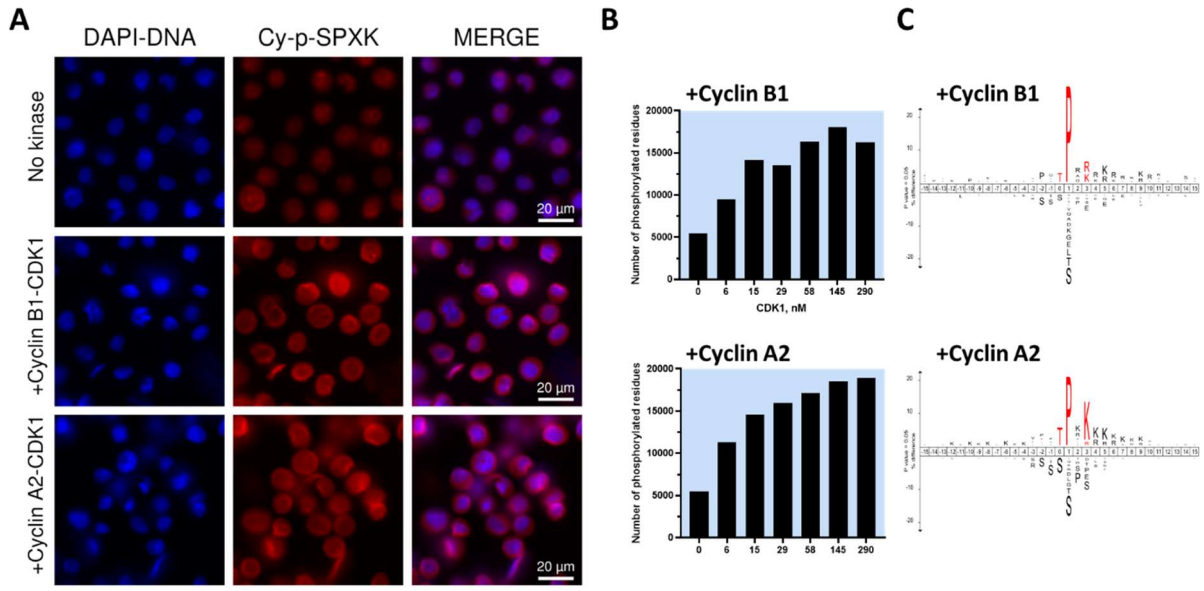

Figure 4.1: Recombinant Cyclin-CDK1 complexes can induce protein phosphorylation in fixed cells. TK6 cells from asynchronous cultures that were fixed with formaldehyde and permeabilized with methanol were incubated with recombinant CDK1 in complex with either Cyclin B1 or Cyclin A2 and IF microscopy was used to visualise the difference in the phosphorylation intensity of SPXK sites (Cy5) in comparison to a control sample that was not incubated with a recombinant kinase (No kinase). Scale bar: 100 µm. (B) A dilution series of CDK1 complexes were incubated with fixed cells as in (A) and the overall number of phosphorylated sites with increased phosphorylation intensity by fivefold or more compared to the No kinase sample in each condition was assessed (*y-axis*) using label-free mass spectrometry analysis. (C) Motif enrichment analysis of sites phosphorylated by 6 nM of CDK1 in complex with either Cyclin B1 (top panel) or Cyclin A2 (bottom panel).

4.3.2 Cyclin A2-CDK1 promotes the phosphorylation of non-Proline sites with a Lysine in the +3 position

Next, I performed a stimulus-response experiment where I titrated fixed cells with either Cyclin A2-CDK1 or Cyclin B1-CDK1 and prepared the samples for mass spectrometry analysis as it was described in section 3.2.4 of chapter 3. For fold

change calculations, I also prepared a control sample where cells were incubated with a kinase dead, $CDK1^{D146N}$ (D146N) that contains a single amino acid mutation in its DFG motif[93]. This will ensure that any changes detected in these samples are not resulting from the activity of a contaminant enzyme, since D146N was purified in a similar way to the active CDKs used here. In this experiment, I identified and quantified 27084 sites, 7438 of which showed at least 2-fold increase in one of the two samples treated with the maximum CDK1 concentrations when compared to D146N. A lower fold change cut off than that in Figure 4.1 was set here because the experimental samples were multiplexed prior to data acquisition. This made readings from the mass spectrometer more comparable. To segregate sites based on their phosphorylation propensity, I selected the 5113 residues that had no missing values in their phospho-proteomic data. To ensure that any differences observed are driven solely by the Cyclin partner and not through any potential variability between the endogenous activities of the two complexes, which were purified separately, I plotted the average fold change of all these 5113 sites induced by Cyclin B1-CDK1 and compared it to that of Cyclin A2-CDK1 (Figure 4.2A). This showed that the average increase in phosphorylation was higher in Cyclin A2-CDK1-treated cells, suggesting that recombinant Cyclin A2-CDK1 had higher activity. I then eliminated this activity difference between the two recombinant complexes by subtracting it from the fold changes of the Cyclin A2-CDK1 data (Figure 4.2A, bottom panel). Using this normalised data, I was curious to see the extent of phosphorylation that these complexes induced on Histone H1 in fixed cells, which has been extensively used as a model substrate that is equally phosphorylated by the different recombinant Cyclin-CDK1 complexes in the past[52,53,90]. Indeed, this analysis showed that both complexes phosphorylated two isoforms of Histone H1 (E and D) in the cells to the same extent, demonstrating the suitability of this substrate to be used for normalisation purposes, as having a different Cyclin partner had no impact on the extent of phosphorylation induced (Figure 4.2B).

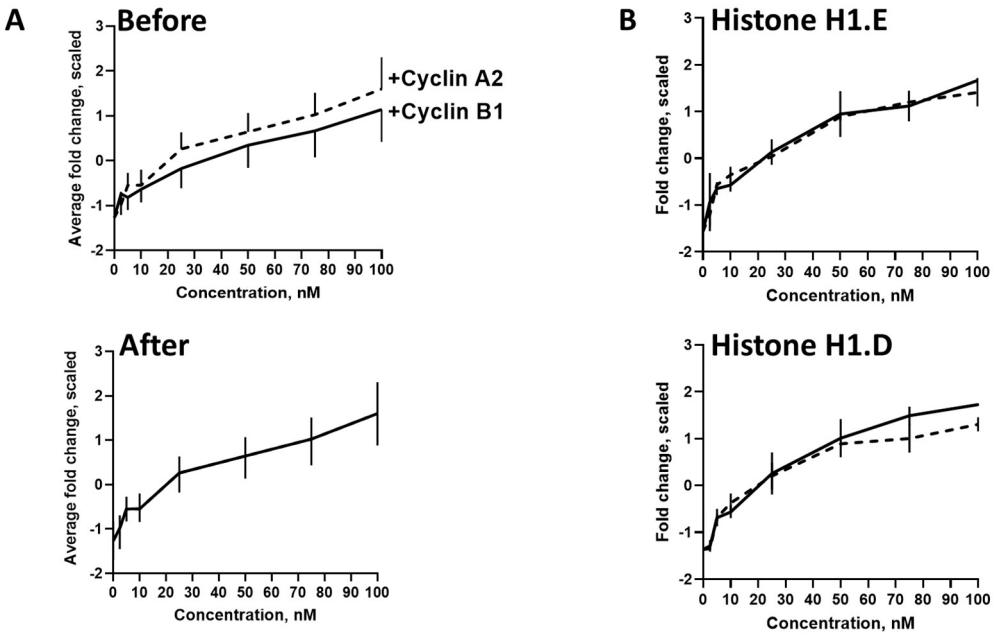

Figure 4.2: Normalising the variability in endogenous activity of the two recombinant Cyclin-CDK1 complexes used in the experiments described in this chapter. (A) Line plots showing the average fold change in phosphorylation of residues of fixed cells by either Cyclin A2-CDK1 (dotted line) or Cyclin B1-CDK1 (solid line) before (left) and after (right) normalisation. (B) The phosphorylation of two Histone H1 isoforms in fixed cells by the two complexes after normalisation in (A).

To assess how changing the Cyclin partner affects CDK1 phosphorylation of substrates, I plotted the normalised fold changes on a heat map and performed unsupervised hierarchal clustering to separate sites based on their phosphorylation patterns (Figure 4.3A). In this analysis, I noticed that in two of the clusters, clusters 1 and 5, sites were more efficiently phosphorylated by CDK1 when in complex with Cyclin A2 compared to a complex with Cyclin B1. The complete opposite can be observed in clusters 3 and 4 of the heat map, where sites preferred phosphorylation by Cyclin B1-CDK1. The differences between the two complexes, however, were more pronounced in clusters 1 and 3 (See fold change intensities on Figure 4.3A), therefore I focused on these for downstream analysis.

The impact of the Cyclin partner on CDK1 phosphorylation can be clearly seen when plotting the average fold change induced by Cyclin A2 to that by Cyclin B1 on sites within clusters 1 and 3 (Figure 4.3B). In contrast, the Cyclin partner had no impact on CDK1 phosphorylation of clusters 6 and 2 sites (Figure 4.3A). To understand the reason behind this selectivity, I performed motif enrichment analyses on sites in these clusters (Figure 4.3C and D). Results from these analyses unveiled that 64% of cluster 1 sites lacked the +1 Proline and had a basic residue in their +3 position. On the other hand, 74% of cluster 3 sites contained a +1 Proline and only 14% of them had the motif enriched in cluster 1. This data reveals phosphorylation of protein substrates by Cyclin A2-CDK1 on phospho-acceptor Serine or Threonine residues lacking the +1 Proline and enriched with +3 Lysine (S/TXXK/R; Figure 4.3C and D). These results suggest that Cyclin A2 may allow CDK1 to bypass the +1 Proline requirement when phosphorylating substrates. Similar results can be obtained if the analysis was performed on clusters 1 and 5 (57% S/TXXK/R; 19% +1 Proline), and 3 and 4 (8% S/TXXK/R; 82% +1 Proline) combined. No particular changes to the enrichment of Serine over Threonine were observed between the two clusters.

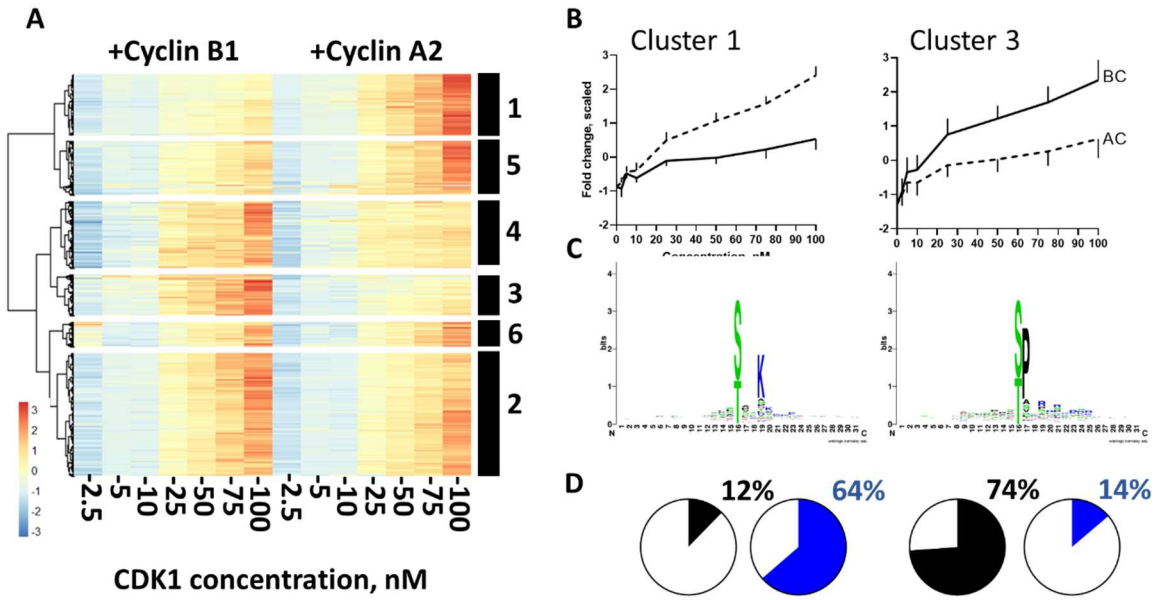

Figure 4.3: Cyclin A2 promotes the phosphorylation of non-canonical sites by CDK1. Fixed TK6 cells at the G2/M phases from elutriation fractions were incubated

with a series of concentrations of either Cyclin A2-CDK1 or Cyclin B1-CDK1 for 40 min. Proteins from these cells were digested with trypsin, labelled with TMT, fractionated, and analysed by LC-MS/MS+SPS-MS^3. (A) Representative heat map from one of the two biological replicates showing the fold change of the phosphorylation intensity at each Cyclin-CDK1 concentration versus that after incubation with D146N for each site (rows). The fold change values for individual sites at each concentration were scaled. Unsupervised hierarchal clustering was used to cluster the heat map into six clusters from which two (1 and 3) were taken for downstream analysis because they showed the highest contrast between the two Cyclin-CDK1 complexes (See methods). (B) The average scaled fold change plotted against the concentration of CDK1 either in complex with Cyclin A2 or Cyclin B1 for cluster 1 or cluster 3 from (A). Error bars represent the standard deviation of sites within the clusters. (C) Motif enrichment analysis using the online tool WebLogo of reproducible Cyclin A2-CDK1 sites (left) or Cyclin B1-CDK1 sites (right) from the two biological replicates. (D) Pie carts from the number of Proline directed sites (black) or S/TXXK/R sites (blue) in (C).

4.3.3 Cyclin A2-CDK1 dependent sites are characterised by highly dynamic phosphorylation

The data from the *in vitro* kinase assay presented in the earlier sections of this chapter have shown that a group of CDK1 sites lacking the +1 Proline and enriched with a +3 Lysine are more efficiently phosphorylated by this kinase when it was in complex with Cyclin A2 compared to Cyclin B1 (Section 4.2.2). The fact that these sites lacked the +1 Proline, which is highly conserved across eukaryotes as part of the optimal motif of CDK1 may suggest that they are weaker targets of this kinase. One way to investigate the likelihood that this, indeed, is the case is by assessing how quickly these sites are dephosphorylated when CDK1 activity is diminished. Recently, Holder and co-workers reported experiments in which they investigated the

dephosphorylation kinetics of sites in extracts from mitotic cells treated with the inhibitor of Mps1, Reversine (Mps1i)[147,148]. Inhibition of the kinase Mps1 will force these cells to exit mitosis causing progressive decline in the activity of CDK1 resulting from the degradation of Cyclin B1. We segregated the sites in this data based on the sequence motifs and compared their phosphorylation half-lives (Figure 4.4). This analysis showed that sites with the S/TXXK/R motif were the most rapidly dephosphorylated (median half-life of ~20 mins) upon mitotic exit (Figure 4.4B, red arrow). In contrast, sites within the Aurora motif ([KR]-[KR]-X-[ST]) were the slowest to dephosphorylate (median half-life ~50 min). These results suggest that non-Proline sites with +3 basic residues are more prone to dephosphorylation by the counteracting phosphatases and thus require much more CDK1 activity than those in the full CDK1 motif for phosphorylation. Thus, non-proline directed CDK1 sites are likely highly dynamic in cells and may require the presence of Cyclin A2 for their phosphorylation to be maintained.

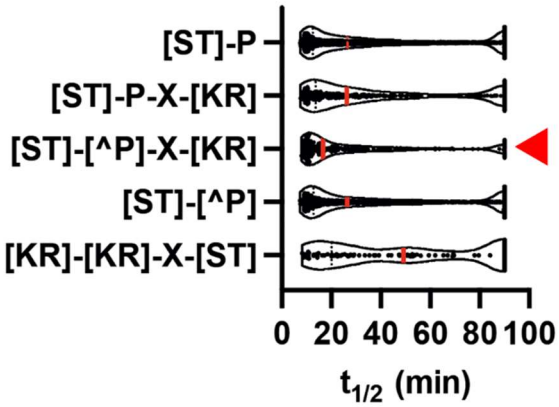

Figure 4.4: Rapidly reversible phosphorylation for sites matching the Cyclin A2-CDK1 targeted motif in mitotic cells. Violin plots showing the half-life of the phosphate group on either Proline-directed ([ST]-P or [ST]-P-X-[KR]), non-Proline directed ([ST]-[^P] or [ST]-[^P]-X-[KR]), or Aurora ([KR]-[KR]-X-[ST]) phosphorylated sites in these cells. Red lines showing the median half-life of phosphorylation on these sites. Red arrow represents sites within S/TXXK/R motif.

4.3.4 The Cyclin subunit shifts the substrate specificity of CDK1 in fixed cells

To study the impact of this consensus motif shifting on CDK1 interactions with its substrates, we performed GO analysis on substrate proteins. Proteins with sites exclusively from cluster 1 or cluster 3 were preferential substrates of Cyclin A2 and Cyclin B1, respectively. Results from the heat map in Figure 4.5 shows that the cellular functions and compartments targeted by Cyclin A2-CDK1 were completely different from those of Cyclin B1-CDK1, demonstrating a swap in substrate specificity coinciding with changing the Cyclin partner. Another striking finding is that the cells used here were dead and lacked active nuclear localisation/exclusion machineries. Such machineries were reported to be determinants of the subcellular compartment where CDK1 is targeted[87,88]. Both the enriched functions and locations of the substrates were consistent with the *in vivo* expression time of the Cyclin partner in the CDK1 complex by which they were phosphorylated. For example, Cyclin A2-CDK1 substrates were enriched in DNA replication factors. Similarly, Cyclin B1-CDK1 substrates were enriched in proteins localised to the mitotic spindle. Taken together, these results present the Cyclin partner as a determinant for substrate specificity of CDK1, potentially through shifting the motif that this enzyme targets.

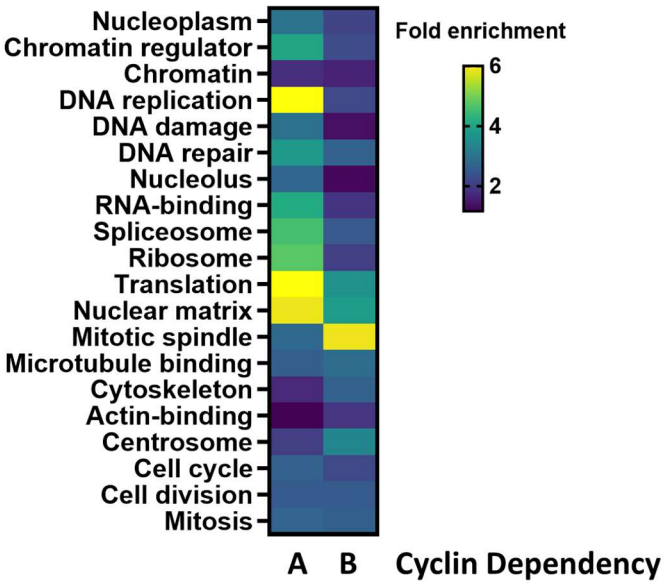

Figure 4.5: The Cyclin subunit shifts the substrate specificity of CDK1. Heat map showing the functional and cellular compartment annotations of proteins carrying the phosphorylated sites present only in cluster 1 (Cyclin A2 dependent) or cluster 3 (Cyclin B1 dependent) from Figure 4.3. The analysis was carried out using the online tool DAVID.

4.3.5 Quantitative changes in CDK1 activity also determines its substrate specificity

CDK kinase activity has been shown to be an important factor in maintaining temporal ordering of substrate phosphorylation in fission yeast cells. The fixed cell kinase assay I developed enables me to test this by titrating activity and measuring substrate specificity. To investigate how progressive increase in CDK1 activity would affect the phosphorylation of residues in fixed cells, I used the data presented in Figure 4.3A (left panel, pre-normalisation) for the Cyclin B1-CDK1 complex. One issue with using unscaled data is that the fold changes will be drastically variable among sites. This is partially because some of these sites have no phosphorylation intensity values in the control sample, whereas others exhibit some level of endogenous phosphorylation. When we consider sites with at least two-fold increase in phosphorylation against this control sample to be significant, their data become difficult to compare. Besides, because of the *in vitro* nature of this assay, most of the sites did not seem to reach saturation when phosphorylated by the two complexes. In fact, the *in vitro* phosphorylation of the SPXK motif induced by the two complexes seemed to be lower than that phosphorylated *in vivo* in STLC-arrested cells (Data not shown). To get around this issue, we decided to induce *in silico* saturation on Cyclin B1-CDK1 sites. But what should be the fold change cut off for determining this saturation? I used the data that will be discussed in chapter 6 to decide on that. I compared the average phosphorylation in cells that were arrested in mitosis using the drug STLC to those in G2 phase selected by centrifugal elutriation. The median fold change here was 6.5 increase in the mitotic cells. We used this to ‘cap’ the fold

change of sites phosphorylated *in vitro* by Cyclin B1-CDK1 in this chapter (Figure 4.6A).

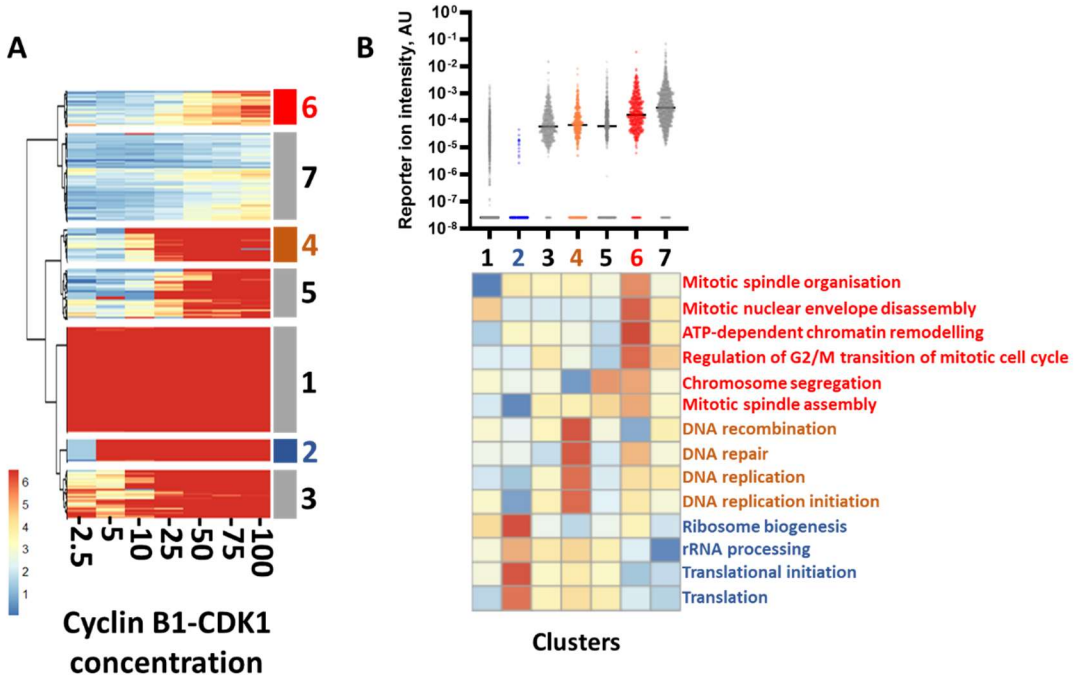

Figure 4.6: CDK1 activity affects the substrates specificity in fixed cells. (A) Data from Figure 3A were capped and their fold change against D146N was plotted on a heat map and clustered using the Ward algorithm. (B) The reporter ion intensities of sites in the D146N sample for the different clusters were used as a readout for their endogenous phosphorylation pre-fixation (top) and a heat map showing the scaled GO functional enrichment of sites in these clusters (bottom) calculated using the online tool DAVID.

Results in Figure 4.6A showed that sites can be clustered into 7 groups based on the minimum concentration of Cyclin B1-CDK1 required to reach that 'cap'. These results demonstrate that sites in the fixed cells used for this assay, which were mostly in G2 phase, may require different levels of CDK1 activity to reach saturation *in vivo*. To assess whether the endogenous phosphorylation of these sites led to these variable propensities, I used the intensity of the reporter ion channel corresponding to the

D146N sample as a readout to the extent of phosphorylation that occurred prior to cells fixation (Figure 4.6B, top panel). Strikingly, the activity required to reach *in silico* saturation showed some level of correlation with the endogenous phosphorylation of sites in the different clusters. I highlighted three clusters from the heat map (Figure 4.6A; clusters 2, 4, and 6) as examples to this. In cluster 2, the endogenous phosphorylation was extremely low, making sites require very small amount (activity) of Cyclin B1-CDK1 to reach the cap. In contrast, residues in cluster 6 had very high levels of endogenous phosphorylation, which meant that extremely high activity of Cyclin B1-CDK1 were required to reach the 6.5-fold increase for *in silico* saturation. In consistency with this pattern, cluster 4 sites, which showed intermediate levels of phosphorylation in the control sample, required intermediate levels of Cyclin B1-CDK1 for saturation. But why do we see this variability in the control sample? One possibility that may explain this would be the selectivity of protein phosphatases expressed in the cells at the time of fixation. Since the fixed cells used in this assay were mostly in G2, phosphatases like PP2A and PP1 are expected to be active in these cells. PP2A-B55 was shown to prefer dephosphorylating Threonine residues flanked by basic amino acids[64]. These results demonstrate that the propensity of CDK1 sites to protein phosphatases may determine the extent of kinase activity required for Cyclin B1-CDK1 to saturate sites in fixed G2 cells. To unveil the cell cycle phases at which sites of the 7 heat map clusters are functional, we performed GO analysis on them (Figure 4.6B, bottom panel). Strikingly, functional annotation showed that sites required the minimum activity to reach saturation, i.e., were most dephosphorylated endogenously, were enriched with translation-related functions, which usually occur in late G1 as cells are getting ready to enter their division cycle[3]. Sites in cluster 4 were on proteins involved in S phase functions like DNA replication and repair, and sites in cluster 6 with the highest phosphorylation levels in the control sample were predominantly on mitotic proteins. Taken together, these results suggest that the differential selectivity of protein phosphatases present in the cell is what creates the thresholds of activity

that CDK1 needs to surpass to drive cell cycle progression suggested in the qualitative model[84].

Next, I sought to compare the enrichment of amino acid sequences flanking phospho-acceptor sites of these clusters. Motif enrichment analyses of the heat map clusters revealed similar enrichment of the S/TXXK/R motif among these clusters, as these sites represented approximately 20-27% of the three clusters highlighted earlier (Figure 4.7A). In contrast to this, when the enrichment of the phospho-acceptor residue was investigated, the ratio of phosphorylated Serines to phosphorylated Theronines (S/T ratio) decreased with the increase in levels of Cyclin B1-CDK1 activity required for *in silico* saturation to be achieved (Figure 4.7B). In other words, the clusters that were mostly enriched with phospho-acceptor Threonine were the ones that were most dephosphorylated. This correlation between Threonine enrichment and dephosphorylation levels provides another evidence towards the argument that it was the differential targeting of sites by PP2A-B55 that caused the variability in endogenous phosphorylation of sites in these clusters (Figure 4.6B). In addition, it may suggest a negative correlation between the endogenous phosphorylation levels and the enrichment of Serines. To evaluate that, I used Cyclin B1-CDK1 to phosphorylate fixed G2 cells *in vitro* either with (+λ) or without (+Mock) pre-dephosphorylation with λ phosphatase (See the next chapter for more details) and compared the S/T between the two conditions (Figure 4.7C). Although the results did not show a decline that was statistically significant, there was a clear reduction in the enrichment of Serine when the residues were endogenously phosphorylated in both replicates of this experiment. These results suggest that Cyclin B1-CDK1 may prefer phosphorylating Serine amino acids to Threonines *in vivo* and removing this phosphorylation with a phosphatase frees sites for phosphorylation by recombinant Cyclin B1-CDK1.

The Cyclin A2-CDK1 data in Figure 4.3A were also analysed for CDK1 activity and similar patterns of phosphorylation, GO enrichments and S/T ratios were occurring

(data not shown). One difference, however, is that lower concentrations of Cyclin A2-CDK1 complex were required to phosphorylate substrates involved in DNA-replication. Besides, the Proline enrichment for the cluster in which residues from these proteins were grouped was lower than that in most of the other heatmap clusters. This may be explained by the higher activity of Cyclin A2-CDK1, which was not normalised for this analysis (Figure 4.2A), as well as the specificity induced by the Cyclin A2 for non-Proline sites that was discussed earlier (Figures 4.1 and 4.3).

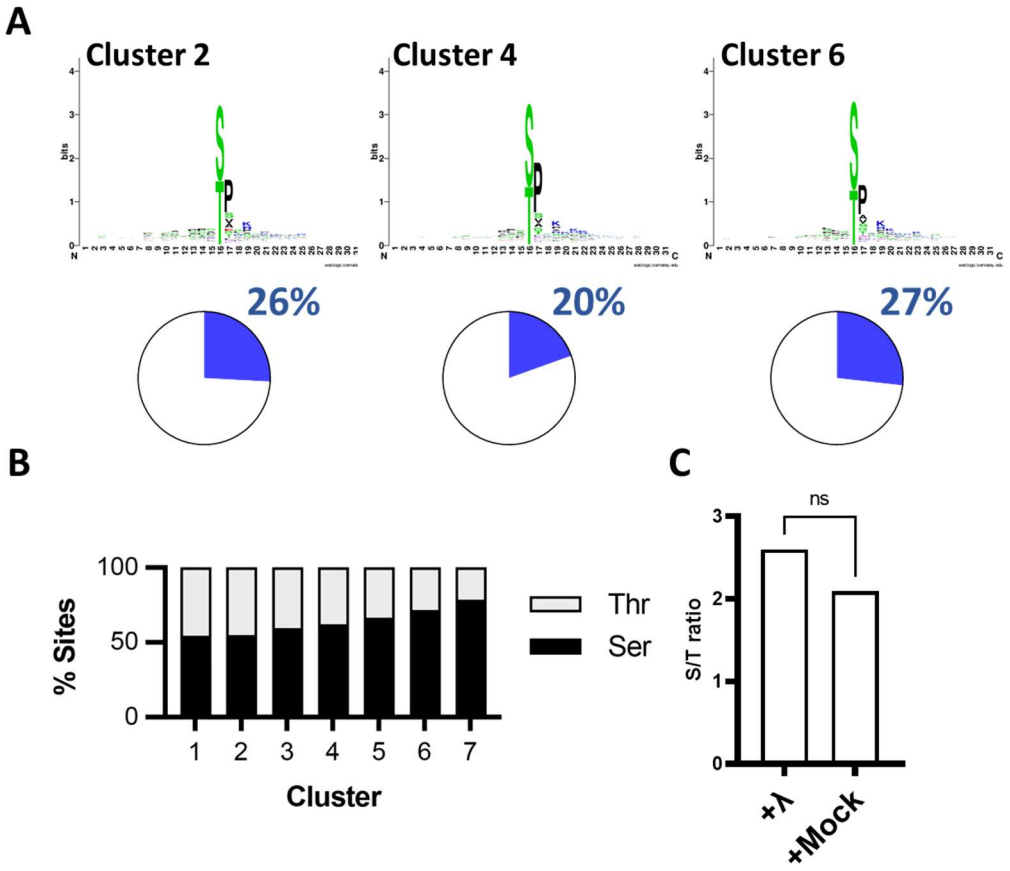

Figure 4.7: Motif enrichment analysis of sites showing variable quantitative differences to be phosphorylated by Cyclin B1-CDK1. (A) WebLogo[127] charts representing the enrichment of amino acids in the 15 sites flanking the phospho-acceptor residue (top) and pie charts illustrating the ratio of sites lacking the +1 Proline and carrying a basic residue in position +3 (bottom). (B) and (C) Bar plots representing the ratio of phosphorylated Serine (black) to phosphorylated Threonine (white) in the 7 clusters of Figure 4.6A (B) and of G2 and G2+λ cells (C).

4.4 Discussion

The temporal ordering of CDK1 phosphorylation is controlled by qualitative and quantitative aspects of CDK1 activity (see models described in section 4.2 and chapter 1). In this chapter, I aimed to understand how each aspect contributes to substrate specificity in a biochemically controlled, *in vitro* fixed cell kinase assay. The findings of this chapter suggest that CDK1 achieves its substrate specificity through two mechanisms. The first mechanism is by shifting its targeted consensus motif. The Cyclin partner appears to be critical element to that. In living cells, when the four members of the CDK family are present, CDK1 prefers forming a stable complex with either Cyclin A2 or Cyclin B1. It is evident from my results here that forming a complex with Cyclin A2 promotes the phosphorylation of S/TXXK/R sites. In contrast to this, CDK1 preferably targets sites within its canonical motif when in complex with Cyclin B1. These S/TXXK/R sites were reported in previous phospho-proteomic screens of mitotic cells[109]. They were also extensively thio-phosphorylated in cells expressing CDK1-as[134]. The GO analysis here suggests that these sites are present in abundance on proteins involved in the S phase events when Cyclin A2 would be highly expressed *in vivo*. Our data confirms that these are targets of CDK1 and reveals a requirement for Cyclin A2 to be the activating partner. By promoting these phosphorylations, Cyclin A2 may selectively initiate molecular events these protein substrates are involved in. How is the phosphorylation of S/TXXK/R sites regulated remains an open question. One possibility would be through a hydrophobic patch that is present in its structure[120]. Previous reports from experiments on the budding yeast Cyclin-CDK1 complexes suggested that this patch docks on certain sequence known as the Cy motifs[120]. These motifs were comprised of the sequence RXL (where X is any amino acid) and were predominantly within the same disordered region where the phospho-acceptor residue is located. Despite their abundance in the datasets, no particular enrichment of these sequences correlated with one Cyclin or

the other. This raises the possibility that other sequences specifically targeted by Cyclin A2 but not Cyclin B1 may exist. It will be interesting to investigate whether mutating the hydrophobic patch eliminate the differences in the substrate specificity of the two complexes observed here.

In the second mechanism, differential preferences for protein phosphatases determine the extent of CDK1 activity required to induce phosphorylation. Previous reports have shown that the catalytic activity of the fission yeast homologue of CDK1 increases during the cell cycle and that the level of this activity determines which substrate to be phosphorylated[70,84]. The results that I presented here agrees with that to some extent. When I titrated the fixed cells with CDK1, variable concentrations were required for saturation to be achieved among sites. The saturation here, however, was defined by the site reaching a 6.5-fold increase in its phosphorylation against the control sample. For some sites, this fold change could never be achieved (Figure 4.6A, cluster 7), but not because of the catalytic selectivity of CDK1 *per se*. Instead, it was the endogenous phosphorylation of these sites that caused this reduction. In other words, the extent of dephosphorylation of these sites caused this variability. Phospho-acceptor sites like those in cluster 1 were widely dephosphorylated and highly enriched with Threonines. This possibly made them better targets for protein phosphatases like PP2A-B55, which would be highly active in G2 cells prior to fixation and was reported to selectively target phosphorylated Threonines[64]. The opposite can be said for cluster 7, which had the lowest dephosphorylation among the heat map clusters and the least Threonine enrichment. Previous studies reported that in contrast to CDK1, the activity of protein phosphatases declines during the cell cycle[40]. Based on that, our analysis here suggests that it is the selectivity of protein phosphatases that may cause these activity thresholds required for CDK1 phosphorylation. It will be important to repeat this experiment in dephosphorylated cells in the future and assess whether this variability between sites occurs again.

In conclusion, this chapter presents a complex system in which both quantitative and qualitative differences in CDK1 complexes control the order of cell cycle related phosphorylation by this kinase in fixed cells.

Chapter 5:

Cks1 promotes proteome-wide multisite phosphorylation of non-canonical sites by CDK1

5.1 Summary

Cks1 is an essential protein and a subunit of Cyclin-CDK1 complexes. Through its phospho-adaptor pocket, this protein was shown to dock onto phosphorylated Threonine and promote CDK1 phosphorylation of low affinity sites *in vitro*. In this chapter, I aimed to understand the role of Cks1 in the global phosphorylation carried out by CDK1. To achieve that, I used active recombinant Cyclin B1-CDK1 proteins in complex with Cks1 to phosphorylate fixed and permeabilized cells *in vitro* and compared this phosphorylation with that induced by a binary complex lacking this subunit. Results showed that the presence of Cks1 allowed Cyclin B1-CDK1 to bypass the requirement of a +1 Proline in the targeted residues. This in turn, caused a significant increase the number of phosphorylated sites on the substrates. I also, for the first time, demonstrate here the possibility of carrying out sequential phosphatase followed by kinase reactions on protein substrates *in vitro*. Using these reactions, I was able to provide evidence that CDK1 is the main kinase priming the phosphorylation for Cks1 docking. This chapter reveals a global function for Cks1 as an enhancer of multisite phosphorylation of protein substrates by CDK1.

5.2 Introduction

In chapter 4, I investigated how the Cyclin subunit affects CDK1 phosphorylation of substrates and discussed how they may impact the temporal ordering of cell cycle events driven by this kinase. The Cyclin partners, however, are not the only proteins that exist in CDK1 complexes. A third 9 kDa subunit called Cks1 forms stable complexes with CDK1 (and CDK2)[110,149]. Relatively speaking, the role of this protein and its paralogue, Cks2, which shares 82% sequence homology with Cks1, in CDK1 mediated phosphorylation is less studied than that of Cyclins. Crystal structures of recombinant Cks proteins from human and budding yeast cells, however, revealed that the folding of both Cks1 and Cks2 create anion binding pockets in their structures[93]. Subsequent biochemical characterisation of recombinant budding yeast

Cks1 using dot blot arrays have shown that this pocket is involved in a strong preference for these proteins to bind to phosphorylated Threonine, suggesting that Cks1 may lead to the docking of CDK1 complexes on phosphorylated residues[94]. This was further confirmed by elegant studies on the budding yeast Cdk1 inhibitor Sic1, which demonstrated a role for this docking in phosphorylating a non-Proline site that was critical for cell cycle entry[98,99]. What this means is that through its phospho-binding pocket, Cks1 perhaps positions CDK1 near low affinity sites, promoting their phosphorylation. In addition, depletion of Cks1 and 2 in mammalian cells associated with a reduction in the multisite phosphorylation of component of the APC/C, causing mitotic arrest of cells that resulted from failure to establish a proper metaphase plate[100]. Despite these findings, a comprehensive analysis of how Cks1 presence impacts the global phospho-proteome of CDK1 and how could this contribute to the qualitative and quantitative models is still missing. It is also unclear why CDK1 requires a separate subunit to exert the effects that Cks1 promotes on the targeted substrate. In this chapter, I aimed to investigate the function of Cks1 in CDK1 phosphorylation of substrate proteins proteome-wide.

5.3 Results

5.3.1 Cks1 promotes widespread phosphorylation of non-proline directed sites *in vitro*

To study how Cks1 affects Cyclin B1-CDK1 phosphorylation of substrates, I titrated fixed and permeabilized TK6 cells with either a binary Cyclin B1-CDK1 or a ternary Cyclin B1-CDK1+Cks1 complexes and performed phosphorylation assays as described in chapter 4. The Cyclin B1-CDK1+/-Cks1 were a generous gift from the Endicott group in Newcastle University. Mass spectrometry analysis of peptide digests from these cells identified 24,139 phosphorylated residues, out of which, 3377 were showing at least a 2-fold increase in their phosphorylation intensity after adding 100 nM of one of the recombinant complexes (3623 in replicate 2). Because these

complexes were purified separately, variability in their endogenous activity may exist. To eliminate any potential artifact resulting from that, I normalised the data of the 3377 CDK1 sites here in the same way described in chapter 4.

Using this normalised data, I plotted the relative changes in phosphorylation levels against the D146N sample under the different concentrations on a heat map (Figure 5.1A). Results here unveiled differences in how these sites behave when the concentration of the added complex was increased. Unsupervised hierarchal clustering using the Ward algorithm revealed that the heat map residues can be clustered into 4 groups based on this variability. Out of these four groups, clusters 2 and 4 showed the highest contrast between the two CDK1 complexes. In cluster 2, the presence of Cks1 seemed to enhance the phosphorylation carried out by Cyclin B1-CDK1. In contrast, the phosphorylation of sites in cluster 4 was inhibited by Cks1. This can be clearly seen when averaging the data of the heat map for each cluster and comparing the data of the complex lacking Cks1 to that of Cyclin B1-CDK1+Cks1 (Figure 5.1B). To investigate whether differences in the amino acid composition is causing this variability, I performed motif enrichment analyses for the 15 amino acid regions flanking the phospho-acceptor residue on either side (Figure 5.1C). Results have shown very strong enrichment (in 75% of the sites) of a Proline residue in the +1 position in sites of cluster 4 (Figure 5.1D). This data is consistent with targeting of the consensus CDK1 motif (S/T-P). Unlike this and just like the sites targeted by Cyclin A2 discussed in chapter 4, most of cluster 2 sites (71%) here lacked this Proline residue and instead were enriched with a basic amino acid in position +3. When performing this analysis on cluster 1, in which sites were similarly phosphorylated by either complex, the enrichment mirrored that of cluster 4 (75% of sites with +1 Proline and 11% with no-Proline and were enriched with a +3 basic residue). These results demonstrate that the presence of Cks1 makes Cyclin B1-CDK1 better at phosphorylating non-consensus motifs. The enrichments of clusters 1 and 4 also suggest that the presence of a +1 Proline is not related to the inhibitory effect of Cks1 observed in cluster 4 (Figure 5.1C and D, bottom panel).

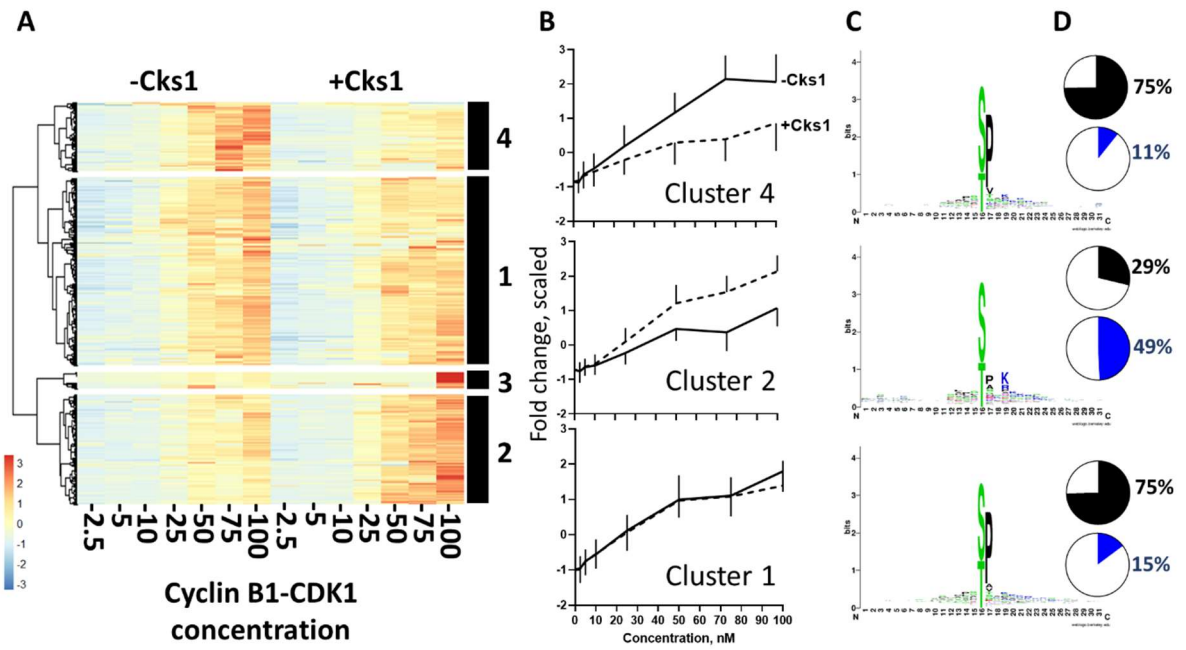

Figure 5.1: Cks1 promotes the phosphorylation of non-canonical sites by Cyclin B1-CDK1. (A) Heat map showing the phosphorylation intensity scaled fold change for sites (rows) in fixed TK6 cells incubated with Cyclin B1-CDK1 either with (+Cks1) or without (-Cks1) a Cks1 subunit in the complex calculated against a control sample treated with D146N. Hierarchal clustering was used to cluster the heat map into 4 sections. (B) Line charts showing the sites' average fold change pattern across the different concentrations in clusters 2 and 4 from (A), which were chosen for downstream analysis. Error bars represent the standard deviation. (C) Motif enrichment analyses for the reproducible sites from 2 replicates' sites using WebLogo. The amino acid in position 0 represents the phospho-acceptor residue. (D) Pie charts showing the ratio of Proline directed phosphorylation (black) and those with S/TXXK/R motif (blue) in the data of panel (C).

5.3.2 The presence of Cks1 dependent site on a substrate protein correlates with an increase in multisite phosphorylation for that substrate

The data that I presented in the previous section suggested that Cks1 enhances the phosphorylation of non-canonical sites by Cyclin B1-CDK1. How does this affect the

interaction of this complex with its protein substrates? To investigate this, we used the online tool DAVID to perform GO analysis on the proteins targeted by Cks1 (those with at least one phosphorylated residue from cluster 2, Cks1+) and compared the results to those with sites that were inhibited by Cks1 (proteins with at least one phosphorylated residue from cluster 4, Cks1-). Annotating the function and subcellular localisation of these proteins revealed that Cks1 enhances the targeting of components of the nuclear matrix and the mitotic spindle (Figure 5.2A). The most striking difference, however, can be seen in the enrichment of spliceosome subunits, which were preferentially phosphorylated by Cyclin B1-CDK1+Cks1. Aside from the spliceosome components, the addition of Cks1 does not seem to cause much of a difference in the substrate specificity of the Cyclin B1-CDK1 as the targeted cellular functions or compartments seem to be the same and the differences between the two complexes were only mild. Based on that, Cks1 does not seem to have a significant impact on the protein substrates targeted by Cyclin B1-CDK1.

Cks1 was shown to be an enhancer of multisite phosphorylation in previous studies on the budding yeast CDK1 substrate and inhibitor Sic1[98], and on components of the APC/C[100,105]. To assess the multisite phosphorylation status of the targeted substrates here, we plotted the number of phosphorylated residues on each protein from Figure 5.3A (Figure 5.2B). Results here revealed a median number of 2 phosphorylated sites on the Cks1+ proteins compared to only 1 in the Cks1- ones. This data demonstrates that the proteins with Cks1 dependent sites are significantly more likely to have additional phosphorylated residues (p<0.0001, student's t test). Because of the consistency of this data with that from the experiments on the budding yeast protein Sic1, it was important to look at the distance between the phosphorylated residues in the Cks1+ proteins, as this regulated phosphorylation of the Cks1-dependent site in that protein[99]. To simplify the analysis, we decided to segregate all the sites of the four heat map clusters in Figure 5.1A into either Proline or non-Proline based on the presence of this amino acid in their +1 position and to look for the enrichment of another site in their close vicinity. Results have shown

that overall, sites from both groups had nearby phosphorylated residues (Figure 5.2C). The Proline sites were more likely to have a secondary phosphorylated residue in 4 amino acids up- or downstream (Figure 5.2C, bottom panel). In contrast, the non-Proline sites had the strongest enrichment of a secondary site in positions +12 and -15 (Figure 5.2C, top panel).

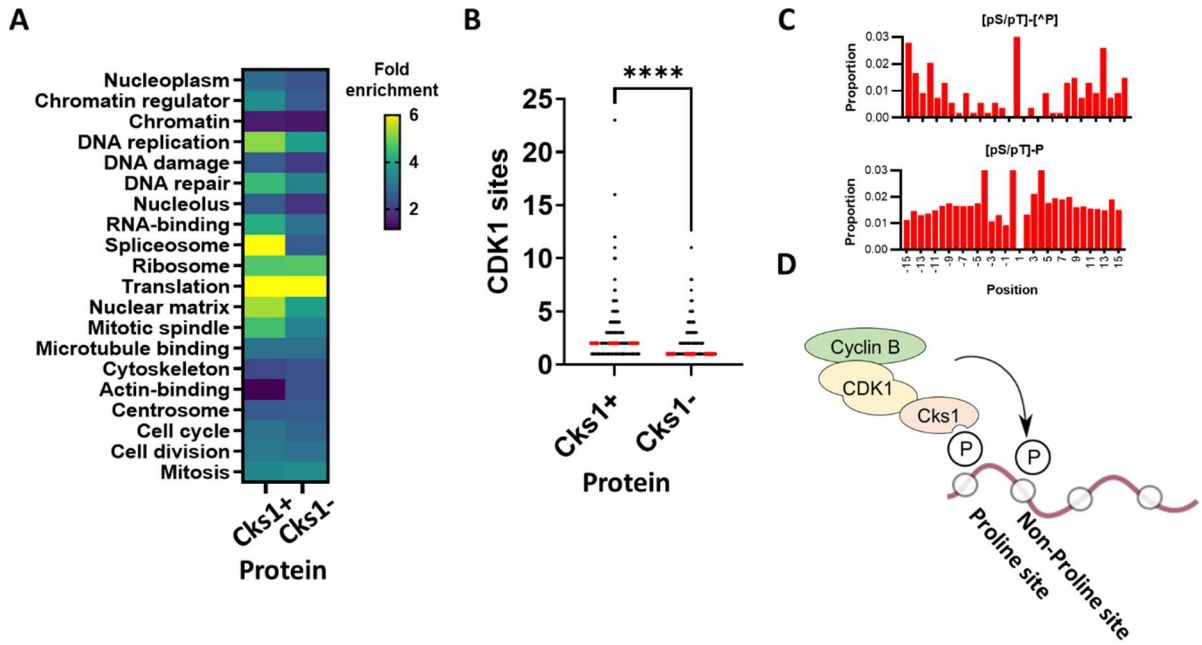

Figure 5.2: Cks1 promotes multisite phosphorylation of Cyclin B1-CDK1 substrates. (A) Heat map showing the GO functional and compartmental enrichments of either Cks1 dependent or independent proteins. Proteins with at least one site from cluster 2 were considered Cks1 dependent (Cks1+). Enrichment analysis was performed using the online tool DAVID. (B) Dot plot showing the number of sites phosphorylated (*y-axis*) in protein substrates (dots) targeted by Cyclin B1-CDK1 complexes presented in Figure 5.1 and panel (A). Red horizontal bars represent the median. ****$p<0.0001$, student's *t* test. (C) Proximity of either non-Proline (bottom) or Proline (top) phosphorylated sites to one another. Bars represent the frequency (*y-axis*) of having a phosphorylated residue in a particular position (*x-axis*) near the main site (central bar, location 0). (D) Model: Cyclin B1-CDK1 phosphorylates a

canonical site, which then serves as a docking residue for Cks1. This docking promotes the phosphorylation of nearby, non-canonical site by CDK1.

Another drastic difference is that the 6 amino acids flanking the phospho-acceptor residue, which was the region with the strongest enrichment in secondary phosphorylation in the Proline sites group, were completely depleted of that in the non-Proline group. Taken together, this data demonstrate that the presence of a Cks1 in Cyclin B1-CDK1 complexes promotes phosphorylation of sites lacking the +1 Proline and that this enhances the multisite phosphorylation of protein substrates carried out by this complex, which seemed to cluster in regions +12, -12 and -15 of the phospho-acceptor residues of the substrate proteins. Both these findings and the presence of a phosphate binding pocket in the structure of Cks1 suggest that this protein is involved in a priming phosphorylation event that promote the phosphorylation of the non-Proline sites by Cyclin B1-CDK1 revealed in this study (Figure 5.2D).

5.3.3 Cks1-dependent sites that require priming phosphorylation are primed by CDK1 itself

Because of the abundance of non-Proline sites in the dataset and because of the significant number of substrates with more than one phosphorylated residue among the targets of Cks1, the results that I presented so far in this chapter hints at the requirement for priming phosphorylation for Cyclin B1-CDK1+Cks1 to phosphorylate the residues that were specific to this complex. If that was the case, a question about the priming kinase in these experiments would arise. In the assays that I discussed in the previous sections, the priming phosphorylation may occur pre-fixation (by an endogenous kinase) or post-fixation (by the Cyclin B1-CDK1+Cks1 complex). To investigate either possibility, I sought to take advantage of our approach, which

would allow us to carry out sequential phosphatase then kinase reactions. To do that, I divided a sample of G2/M fixed and permeabilized TK6 cells into two groups: λ phosphatase treated (+λ) or mock treated (+Mock) (Figure 5.3A). Treatment with λ phosphatase will dephosphorylate phosphorylations from endogenous kinases. Western blotting with an antibody against phosphorylated sites in the SPXK motif revealed complete loss of the bands corresponding to this phosphorylation in the +λ group controls compared to those of the +Mock group (Figure 5.3B). Next, I used heat shock at 65°C to inhibit the phosphatase that was added to the cells then added the two Cyclin B1-CDK1+/-Cks1 complexes used in the previous sections to the cells of both groups. Results from the western blot show the phospho-SPXK bands reappearing on the blot in the lanes corresponding to latter conditions (Figure 5.3B). This demonstrates successful (re)phosphorylation of these cells. Data acquisition by mass spectrometry of peptide digests from these cells revealed 23911 phosphorylated residues, out of which 1013 sites were Cyclin B1-CDK1 phosphorylated, and their phosphorylation was particularly enhanced when Cks1 was present in the complex added to the +Mock group (Figure 5.3C, black arrow and Figure 5.3D). Also, motif enrichment analysis of these sites revealed that the majority of them (67%) lacked the +1 Proline (Figure 5.3E), consistent with our previous findings (Figure 5.1 and section 5.3.1).

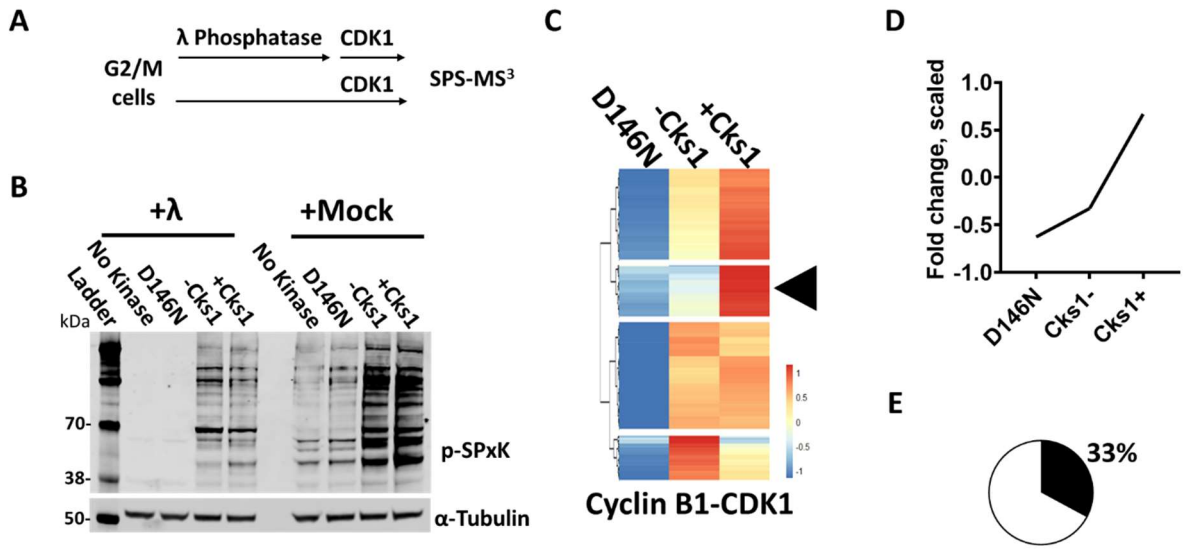

Figure 5.3: Cks1 mediated phosphorylation after pre-treatment with λ phosphatase. (A) Experimental design: Fixed TK6 cells at the G2/M phases of the cell cycle were phosphorylated by Cyclin B1-CDK1 complexes preceded by either λ phosphatase (+λ) or mock (+Mock) dephosphorylation. Proteins from both conditions were labelled with TMT, pooled, fractionated, and phosphorylation was assayed using LC-MS/MS+SPS-MS^3. (B) Western blot showing the phosphorylation of SPXK sites both in +λ (left) and in +Mock (right) samples. Number to the left represent readings from the molecular weight marker (ladder) in kilodalton (kDa). (C) Heat map showing the scaled fold change of phosphorylation intensity for sites in the +Mock samples calculated against the KD treated cells (left column). The black arrow points towards the Cks1 dependent cluster of that heatmap. (D) Average fold change pattern of the Cks1 dependent sites in (C). (E) Pie chart showing the ratio of sites with +1 Proline in (D).

The successful re-phosphorylation of these sites in the +λ group would demonstrate that Cyclin B1-CDK1 is the priming kinase for those of them that require priming phosphorylation. In contrast, failure to phosphorylate these sites would suggest a requirement for priming phosphorylation and that the priming kinase is not Cyclin B1-CDK1 (see model in Figure 5.4A). Results have shown that 86% of these sites can

be re-phosphorylated *in vitro*, suggesting that Cyclin B1-CDK1, at least under these experimental conditions, maybe the priming kinase for these phosphorylations (Figure 5.4B). In contrast to this, a small group of 140 sites was not re-phosphorylated in the +λ group, suggesting that they require priming by other kinases.

Taken together, these results demonstrate that by promoting the phosphorylation of non-Proline sites, the addition of a Cks1 protein to a Cyclin B1-CDK1 complex enhances the multisite phosphorylation of protein substrates and that the molecular mechanism underlying this could be through docking into a priming site that is very likely to be phosphorylated by Cyclin B1-CDK1 itself.

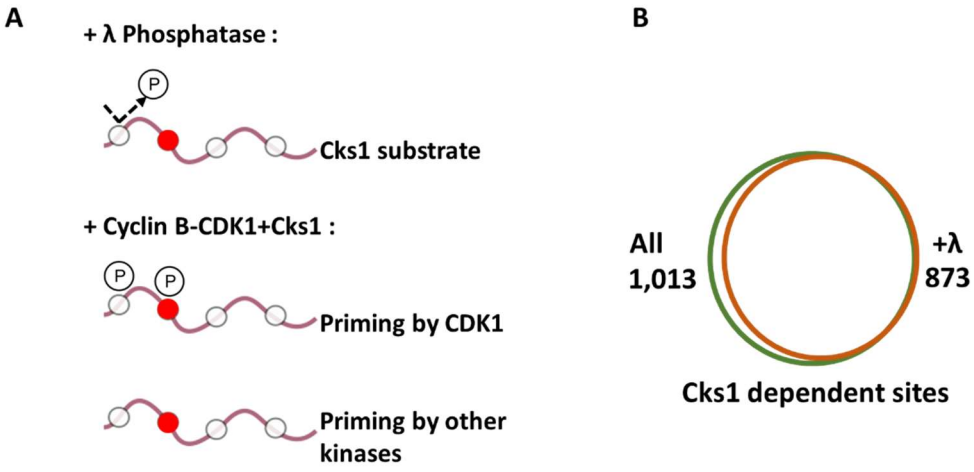

Figure 5.4: Cyclin B1-CDK1 primes protein substrates for Cks1 dependent phosphorylation *in vitro*. (A) Experimental design rationale: Pre-incubation with λ phosphatase cleaves the phosphate group from any priming site that is endogenously phosphorylated prior to fixation. The addition of Cyclin B1-CDK1+Cks1 will either re-phosphorylate the priming site promoting the phosphorylation of the Cks1 dependent site (red colour) again, or will fail to do so, preventing the addition of a phosphate group on the Cks1 dependent site. (B) Venn diagram representing the Cks1 dependent sites from Figure 5.3 (C-E, green). The orange circle represents the fraction of these sites that were re-phosphorylated after pre-treatment with λ phosphatase using the experiment described in (A).

5.3.4 An overlap between Cyclin A2 and Cyclin B1-Cks1 in phosphorylating S/TXXK/R motifs

Because both results of this chapter and those presented in chapter 4 unveiled an enrichment of non-Proline sites with a +3 basic residue in substrates of CDK1 when was either in complex with Cyclin A2, or Cyclin B1 together with Cks1, I wondered if there was an overlap in the sites targeted by these molecular elements. To assess this, I overlapped the Cyclin A2-CDK1 specific sites with those that were reproducibly enhanced by Cks1 in both replicates of the experiment discussed in Figures 5.1 and 5.2 of this chapter (Figure 5.5A).

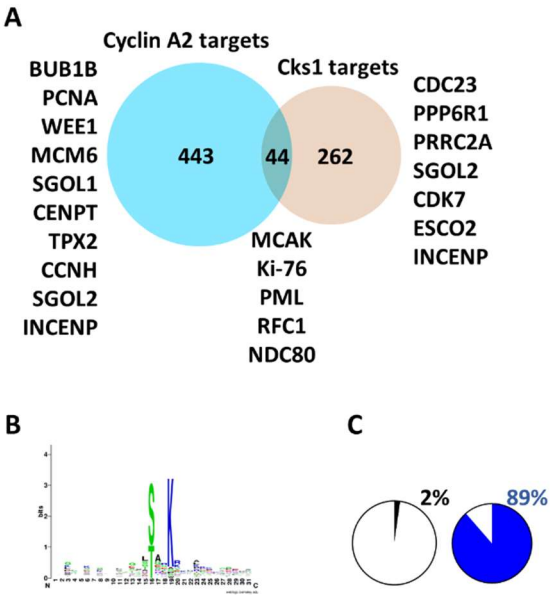

Figure 5.5: The overlap between Cyclin A2 and Cks1 targeted substrates. (A) Venn diagram showing the overlap between reproducible Cyclin A2 substrates in chapter 4 (blue circle) and those of Cks1 identified in Figure 1 of this chapter (orange circle). (B) Motif enrichment analysis for the 44 sites that appeared to be targeted by both Cyclin A2 and Cks1 in the four biological replicates of (A). (C) Pie charts representing the ratio of sites in (B) with Proline (Black) and those in the S/TXXK/R motif (blue).

Results showed that 44 of these reproducible sites were targeted by both protein complexes for phosphorylation. While this number seemed small considering the size

of datasets that these experiments produced, it can be an underrepresentation to the real numbers. This shrinkage may result from the separate acquisition of the four replicates' data on the mass spectrometer, which drastically compromises the reproducibility. Motif enrichment analysis of these 44 sites showed that only one site had a +1 Proline and that 43 were in the motif: S/TXXK/R (Figure 5.5B and C). Interestingly, this basic residue was Lysine in all these sites and no Arginine was detected in the +3 position of any of them. As discussed earlier, Cyclin A2 targeted CDK1 to proteins with functions in DNA replication such as MCM6 and PCNA[150], while Cyclin B1+Cks1 mediated phosphorylation on subunits of protein phosphatases and nuclear components. Interestingly, some mitotic proteins such as INCENP and Shugoshin were phosphorylated by both recombinant complexes, but that phosphorylation was on different sites. This suggests that these subunits add another layer of regulation to these substrates' phosphorylation by CDK1. In a similar manner, the two components of the CDK1 activating kinase (Cyclin H-CDK7) were phosphorylated by either one complex or the other (Figure 5.5A). Most of the 44 sites that were targeted by both complexes were located in proteins with known functions in cell division. These included Ki-6[151], RFC1[152] and TMPO[153]. Surprisingly, two of the phosphorylated residues were in disordered regions of microtubule binding proteins (NDC80[13] and MCAK[154]) and were in close vicinity to sites known to be phosphorylated by Aurora B in mitosis. Taken together, this data suggests that both Cyclin A2 and Cks1 may work together to regulate the phosphorylation of cell cycle substrates by CDK1.

To test whether Cyclin A2 and Cks1 can also promote phosphorylation of S/TXXK/R sites in natively folded proteins, I performed *in vitro* phosphorylation assays on three recombinant substrates from the lists described in Figure 5.5. These included PML-IV, and complexes that contained either NDC80 or Cyclin H-CDK7. The recombinant outer kinetochore protein NDC80 (described in detail in section 1.2.8 of chapter 1) is within a complex with NUF2 termed 'NDC80^{Broccoli}' from the group of Ian Cheeseman at the Massachusetts Institute of Technology[155]. Parts of the C-termini of the NDC80

and NUF2 subunits are truncated in this complex. The nuclear condensates protein PML-IV was a generous gift from Ronald Hay's group at University of Dundee. Like NDC80, PML-IV was on the list of proteins that had S/TXXK/R sites targeted by both Cyclin A2 and Cks1 described in Figure 5.5A. Recombinant Cyclin H and CDK7 are within a ternary complex with the regulatory subunit MAT1.

To assess the extent of phosphorylation that each of the Cyclin-CDK1 complexes induced on PML-IV, I performed SDS-PAGE on the reaction products. Phosphorylation was then visualised by staining bands with Pro-Q Diamond (Hereafter Pro-Q), a small molecule fluorophore phospho-sensor[156]. This stain specifically visualises protein bands when containing phosphate groups on them. Here, an increase in bands intensity following incubation with the three CDK1 complexes was evident, demonstrating successful phosphorylation by CDK1 (Figure 5.6A, lanes 7-10). Furthermore, incubation with Cyclin B1-CDK1+Cks1 induced a shift in the molecular weight of PML-IV, suggesting that Cks1 enhanced multisite phosphorylation of this protein (Figure 5.6A, lane 10 versus lane 9). Two CDK1-phosphorylated sites on PML-IV were detected by LC-MS/MS: Serine 518 (S518) and Threonine 473 (T473). While the amino acid sequence of S518 includes a +1 Proline, T473 is an S/TXXK/R site. Label-free quantitation of phosphorylation intensities showed that both Cyclin A2-CDK1 and Cyclin B1-CDK1+Cks1 were much more efficient than Cyclin B1-CDK1 in phosphorylating T473 (Figure 5.6B). In contrast, the three complexes induced comparable phosphorylation intensities on S518. The phosphorylation intensities of the Pro-Q-stained PML-IV bands induced by the three complexes were comparable despite the variability in T473 results (Figure 5.6A and B). This may be explained by the lower sensitivity of this technique when compared to LC-MS/MS. The results from assays on NDC80^{Broccoli} mirrored those of PML-IV. Cyclin A2 and Cks1 enhanced the phosphorylation of the non-Proline site Serine 76 (S76) by CDK1, while the three CDK1 complexes were able to phosphorylate the canonical site Threonine 31 (T31) to the same extent (Figure 5.6C). The enhanced phosphorylation of non-Proline sites here is unlikely to be an artifact of variable catalytic activity for CDK1 in the three

complexes. This is because Pro-Q staining of MAT1 bands was higher in the Cyclin A2-CDK1 treated samples, whereas Cks1 induced stronger staining on PML-IV (Figure 5.6A). Interestingly, while CDK7 non-Proline Threonine 25 (T25) appeared to be a specific target for Cyclin B1-CDK1+Cks1 in the assays on fixed cells, its phosphorylation by CDK1 followed similar trend to that of PML-IV and NDC80^{Broccoli} non-Proline sites (Figure 5.6B). Taken together, these results are in agreement with the data from fixed cells presenting both Cyclin A2 and Cks1 as promoters of CDK1 phosphorylation of S/TXXK/R sites, and Cks1 as an enhancer of multisite phosphorylation of substrates by CDK1.

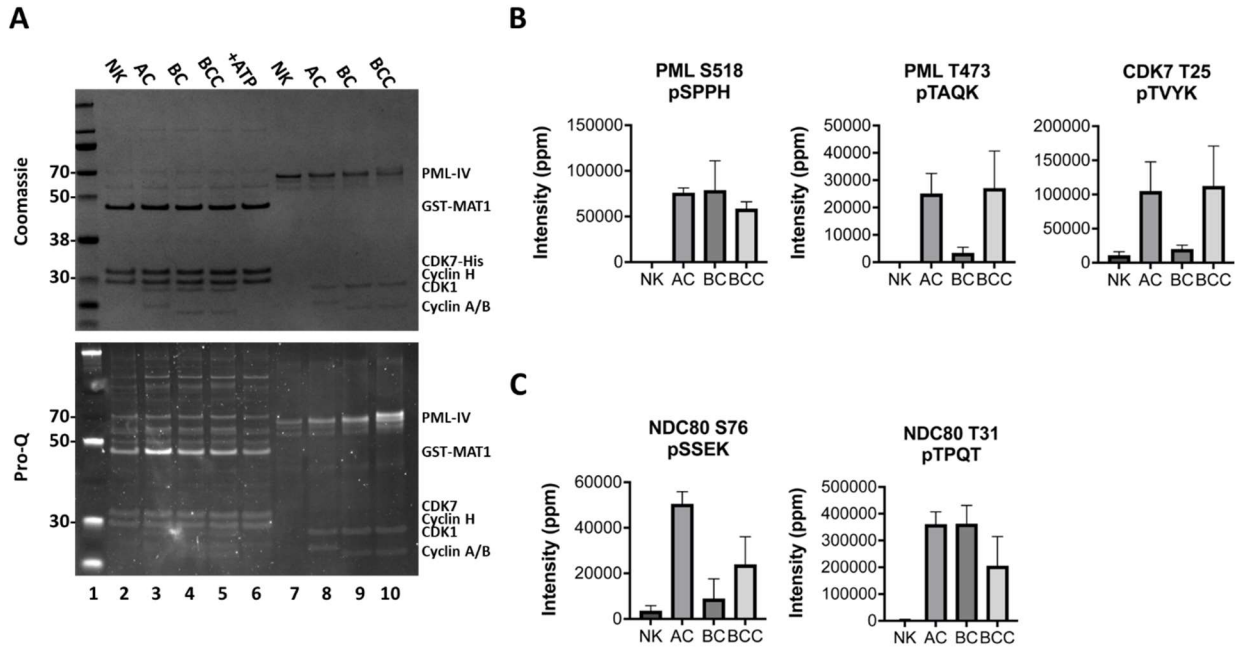

Figure 5.6: Cyclin A and Cks1 promote CDK1 phosphorylation of S/TXXK/R sites in recombinant substrates. Recombinant PML-IV, NDC80^{Broccoli} and Cyclin H-CDK7-MAT1 were phosphorylated *in vitro* by one of the three CDK1 complexes used in this study. Reactions were performed at 1:3 kinase to substrate ratio for NDC80^{Broccoli} and at 1:5 ratio for the other substrates. (A) Products from reactions involving Cyclin H-CDK7-MAT1 (Lanes 1-6) or PML-IV (Lanes 7-10) were visualised by SDS-PAGE followed by staining with either Instant Blue or ProQ Diamond. (B) and (C) Bar plots representing the phosphorylation intensity in parts per million (ppm) of the residues

indicated on the plots as acquired by label-free LC-MS/MS. The amino acid sequence downstream these residues is indicated underneath the phosphorylated site on top of each plot. Error bars represent the standard deviation of two biological replicates.

5.4 Discussion

In this chapter, I attempted to use the *in vitro* assay that was developed and discussed in chapter 3 to study how the addition of a Cks1 subunit to CDK1 may affect the phosphorylation of protein substrates by Cyclin B1-CDK1. The results here present Cks1 as a global enhancer of multisite phosphorylation of protein substrates by Cyclin B1-CDK1, as substrates contained a median number of 2 phosphorylated residues when the complex had this subunit. This is consistent with previous reports where the depletion of this protein led to a decline in the number of sites phosphorylated on the APC3 subunit of the APC/C, resulting in failure to degrade Cyclin A2 and a mitotic arrest[100,105]. The underlying mechanism for this can be through promoting the phosphorylation of sites lacking the +1 Proline in their sequence motifs as the targeting of these sites by Cyclin B1-CDK1 was also enhanced in the presence of Cks1 (see Figure 5.1). This data is in agreement with previous reports where Cks1 promoted the phosphorylation of a non-Proline site in Sic1 by the budding yeast Cdk1[98]. Previous studies also highlighted the importance of phosphorylating cell cycle substrates, such as Wee1 and CDC25C, on multiple sites for creating rapid (ultrasensitive) switch like responses[52,53]. These are particularly important for gathering sufficient CDK1 activity before initiating major cell cycle events like mitotic entry and segregation of chromosomes, as they help filtering small increases in this activity prematurely induced through external stimuli[157]. This is an important factor for maintaining the timely occurrence of cell cycle events.

The fact that Cks1 bears a phosphate binding pocket in its structure, as well as the proximity of the phosphorylated residues that were specifically targeted in its presence reported here, suggested that these multisite phosphorylations may

involve Cks1 docking on nearby phosphorylated residues. The docking of Cks1 on such residues was shown to be critical for shielding a phospho-degron on a Cdc6 protein phosphorylated on multiple sites by CDK1 in budding yeast[101]. My attempts to identify what the priming kinase might be, through using sequential phosphatase then CDK1 reactions, revealed that the main priming kinase for these phosphorylations was CDK1 (see Figures 5.3 and 5.4). Data here also suggested that the phosphorylation of a small fraction of these sites may require Cks1 docking on residues phosphorylated by other kinases. This may also agree with previous reports where Cks1 was shown to dock on a residue that was phosphorylated by the budding yeast kinase Fus3[158].

Because of the similarity between the sequences targeted by CDK1 in the presence of Cyclin A2 and those of Cks1, I investigated the possibility that these sites overlap with one another. This analysis demonstrated that a group of sites were preferentially phosphorylated by both complexes over a binary Cyclin B1-CDK1, suggesting the possibility of a 'hand out' model similar to that revealed in earlier studies investigating the phospho-proteomes of different Cyclin-CDK complexes in human cells[91]. In this scenario, the 'hand out' may occur after Cyclin A2 degradation in early prometaphase when the phosphorylation of sites on kinetochore components, such as NDC80, may need to be maintained[13]. The data here also showed that almost all these overlapping sites had no +1 Proline and, instead, had a Lysine residue in the +3 position. It is important to mention that in the case of Cyclin A2, the +3 basic residue was mostly Lysine, and the enrichment was stronger (64%) when compared to Cks1 sites, which were enriched with both Lysine and Arginine and only 49% of them had this residue in position +3.

Another intriguing finding is that the phosphorylation of some substrates was enhanced by both Cyclin A2 and Cks1 but on different sites. This may represent another layer of regulation similar to that reported on MCM4, where the level of phosphorylation coincides with the loading this protein during S phase[159]. Overall,

the results of this chapter identify global roles for Cks1 in CDK1 phosphorylation of substrate proteins. In the future, it will be important to follow up on these results and to investigate whether the phosphorylation of these sites occur *in vivo* and if it is also enhanced by Cyclin A2 and Cks1.

Finally, because all these conclusions were based on data generated by phosphorylating fixed and permeabilized cells, it is possible that the enhanced efficiency of Cyclin A2-CDK1 and Cyclin B1-CDK1+Cks1 in phosphorylating S/TXXK/R sites was an artifact of the cell fixation protocol. Therefore, it was important to demonstrate the reproducibility of these conclusions on natively folded proteins. Both PML-IV and the tail of NDC80 contained CDK1-phosphorylated Proline and non-Proline sites that appeared in the assays with fixed cells. I used recombinant PML-IV that carried the full-length sequence of the endogenous counterpart and recombinant NDC80^{Broccoli} complex that retained the tail domain. Both the full length and biophysical data from SEC-multiangle light scattering (SEC-MALS; Ronald Hay through personal communications), ensured that the folding of the recombinant PML-IV is comparable to that in cells. Results from assays on both complexes were consistent with those presented both in this chapter and in chapter 4 in that Cyclin A2 and Cks1 promoted CDK1 phosphorylation of S/TXXK/R sites and that Cks1 enhanced the multisite phosphorylation of PML-IV by CDK1. It will be important to understand how hyperphosphorylation of PML-IV impacts its function in forming PML bodies in the future. Similar experiments were carried out on recombinant Cyclin H-CDK7-MAT1. Phosphorylation of the S/TXXK/R site T25 of recombinant CDK7 was equally enhanced by Cyclin A2 and Cks1. In contrast, no phosphorylation for this site was detected by Cyclin A2-CDK1 in fixed cells. This inconsistency may be resulting from failure to detect the phosphorylation of this site during data acquisition by LC-MS/MS.

Chapter 6:

Evidence for non-canonical CDK1 phosphorylation *in vivo*

6.1 Summary

Protein kinases and their counteracting phosphatases are core elements to cells division. Together, they establish a balanced system that allows rapid transitions between the different phases of this process. CDK1 is a main regulator in this system. By associating with a Cyclin partner and a phospho-adaptor Cks1, it can drive the phosphorylation of hundreds of sites on protein substrates in the cell. In the previous chapters, I have developed an *in vitro* assay through which I was able to establish roles for Cyclin A2 and Cks1 in promoting the phosphorylation of non-canonical sites by CDK1. In this chapter, I aimed to investigate the biological relevance of these findings. To do that, I identified the sites with high phosphorylation dynamics across the cell cycle. I then matched these sites with our *in vitro* data. Results have shown that phosphorylation of many of the non-canonical sites was cell cycle regulated and overlapped mainly with that on residues targeted by Cyclin A2 or Cks1. I also attempted to identify the *bona fide* targets of CDK1 in cells expressing CDK1-as and investigate the impact of Cyclin A2 depletion on them. Finally, I identified a site on the N-terminal tail of the outer kinetochore protein NDC80 as a model substrate to study the role of S/TXXK/R sites in the cell cycle. I also used cell biology approaches to create a cell-based assay for future investigations on NDC80. In brief, this chapter suggests functional significance for the non-canonical targets of CDK1 during the cell cycle.

6.2 Introduction

An essential element for cell survival is the maintenance of a faithful division. One way to achieve this is through the temporal ordering of processes required for the completeness of this division. For example, DNA replication needs to proceed the segregation of chromosomes. As it was discussed in chapter 1, critical for initiating cell cycle events in the right order is the temporal order of cellular proteins' phosphorylation by CDKs[39] and their dephosphorylation by PP2A and PP1[40]. Based on

that, one can expect the phosphorylation of functional sites to show more drastic changes during the cell cycle while that of non-functional sites to be steadier. This makes it possible, by looking at the dynamics of the phospho-proteome, to identify which sites are functional for cell division. But how is this balance between kinases and phosphatases achieved? While the system is very complex, a basic concept to that is the extent of activity that these enzymes exert toward a particular site. As it was discussed in chapter 1, this activity is regulated through the expression levels of the enzymes, their activating partners, like the Cyclins in the case of CDK1, their folding status, and the feedback loops that exist between them.

Because the catalytic activity of kinases is so important, the cellular system evolved to eliminate any disturbances to it. Protein kinases share a central domain with approximately 290 amino acids composition[160]. Despite variations between kinase families, certain features are shared between the catalytic sites of these enzymes. For examples, all kinases contain a DFG motif that is important for the transfer of the gamma phosphate of the ATP molecule to the bound substrate. Another example is the Glycine-rich loop, which is important for holding the substrate in the catalytic site. A few years ago, pioneer studies on CDK1 identified a Phenylalanine that acts as a 'gatekeeper' to the ATP binding site of this kinase[161]. Because of its size, Phenylalanine restricts the access of this region to the ATP molecule that is synthesised in the cell. Biochemical studies on mutant CDK1 where this Phenylalanine was swapped with Glycine created a system by which one can specifically label CDK1 substrates using exogenous molecules that are chemically analogous to ATP[134]. This CDK1-as can be a great tool to study the role of CDK1 in maintaining the balance of the phospho-proteome *in vivo*.

A perfect example of a system where the balance between the mitotic activities of kinases and phosphatase is a functional determinant is the kinetochore[11,22,162]. As it was discussed in chapter 1, this is a site where spindle microtubules form stable attachments to the chromosomes at the centromere (See chapter 1 and ref.[12]). The

phosphorylation status of some of the components in the Kinetochore not only determines the strength of these attachments, but also the progression of cells through mitosis. One example of this is the phosphorylation of the N-terminal tail of the protein NDC80[13]. This is heterooligomer of four subunits: NUF2, SPC24, SPC25 and NDC80/Hec1 (NDC80). The interaction between the N-terminal tail of NDC80 and microtubules is electrostatic in nature. The N-terminal tail has several positively charged residues, which interacts with negatively charged residues (Glutamates) on microtubules (See chapter 1). Phosphorylation of the N-terminal tail of NDC80 by several enzymes, such as the Auroras and CDK1, disturbs that interaction by reducing the positive charge of the tail[13,115]. In addition, NDC80 mediates the recruitment of the mitotic kinase Mps1 and the Ska complex that are both important for creating a stable faithful attachment with the spindle poles[116,163,164]. Just like the binding to microtubules, both processes are regulated by phosphorylation of residues on NDC80.

In the previous chapters, I presented and discussed how the catalytic activity of CDK1 and its Cyclin partners as well as Cks1 affect its global phosphorylation of substrates *in vitro*. In this chapter, I will present results from experiment in which I combined different biochemical approaches, including a CDK1-as system, to investigate how many of these *in vitro* sites are phosphorylated *in vivo* and whether their phosphorylation is regulated throughout the cell cycle. Finally, I will present early preparations for future cell biology experiments where the functional significance of the phosphorylation of an S/TXXK/R site on NDC80 by CDK1 can be investigated.

6.3 Results

6.3.1 Cyclin-CDK1 phosphorylated sites *in vitro* overlap with *in vivo* cell cycle regulated sites

In order to assess how many of the sites that were phosphorylated during the *in vitro* assay designed in chapter 3 are phosphorylated endogenously and to establish an idea about the dynamics of their phosphorylation, I designed an experiment that combined both *in vitro* assays with cell cycle phase fractionation and mass spectrometry (Figure 6.1A). In this experiment, I used elutriation to separate fixed TK6 cells from asynchronous culture into either G1 or G2/M cells. I incubated these cells with either active Cyclin-CDK1 complexes or the kinase dead D146N. In parallel, I used the Eg5 inhibitor STLC to arrest cells in prometaphase before fixation. I then multiplexed these samples into one set of TMTpro to minimise technical variation that may arise from separate data acquisition on the mass spectrometer. Results identified 23911 phosphorylated sites in this experiment. Next and as a readout to their dynamics, I sought to identify how many of these sites are regulated during the cell cycle. For this purpose, I used the controls data of G1 and G2/M samples, which were incubated with D146N as well as those from the M phase cells arrested with STLC. Sites in these cells should represent the endogenous phosphorylation during these cell cycle phases, since the D146N is catalytically inactive. To identify the dynamic sites, I calculated the fold change in phosphorylation between the G2/M cells and the G1, and also that of M phase cells versus G2/M. Based on these results, sites that showed 2-fold or more phosphorylation in G2/M cells compared to G1 were considered to be interphase regulated. Similarly, those with at least twice as much phosphorylation in M phase compared to G2/M were M phase regulated. This analysis unveiled 5102 sites with cell cycle phase associated changes in their phosphorylation. The criteria are summarised schematically in Figure 6.1B.

How many of the sites that we phosphorylate *in vitro* overlap with these? To answer this question, I used the data from G1 cells phosphorylated by either Cyclin A2- or

Cyclin B1-CDK1 complexes, and those of G2/M cells phosphorylated by Cyclin B1-CDK1+/-Cks1 multiplexed with this experiment to investigate that. CDK1 sites in each case were, as described in the previous chapters, defined as those with at least 2-fold or more phosphorylation against their control samples. Results from this analysis revealed 3912 *in vitro* sites being cell cycle regulated (Figure 6.1C). This number represents 56% of all the *in vitro* phosphorylations by these Cyclin-CDK1 complexes, demonstrating that the majority of these sites are phosphorylated in TK6 cells endogenously, and that this phosphorylation changes with cell cycle progression. These results suggest functional significance to these residues during the cell cycle.

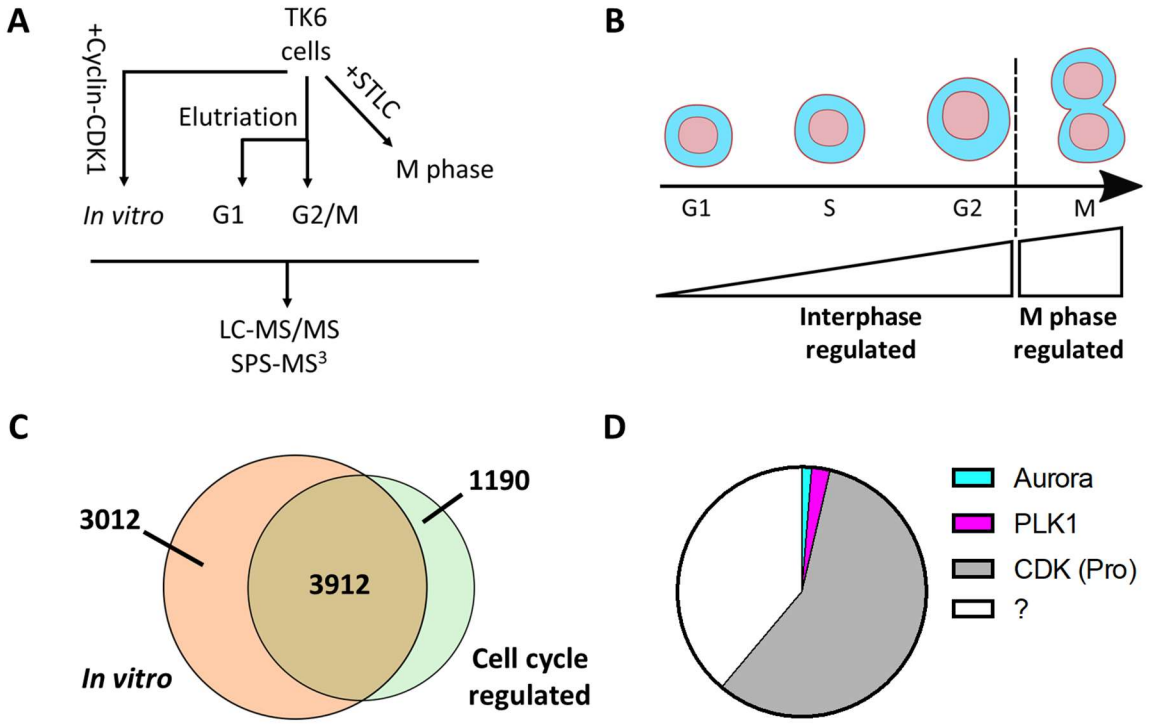

Figure 6.1: Identification of the *in vivo* cell cycle regulated sites that were also phosphorylated by CDK1 *in vitro*. (A) Schematic describing the experimental design: TK6 cells from asynchronous culture were separated into either G1 or G2/M using centrifugal elutriation or arrested in M phase using STLC. Some of the G1 cells were phosphorylated with 100 nM of Cyclin A2/B1-CDK1 (WT/D146N) complexes *in vitro*. Similarly, some of the G2/M cells were phosphorylated by Cyclin B1-CDK1+/-Cks1 or by D146N. Peptides digests from all these samples were pooled into one set of

TMTpro and data were acquired using the LC-MS/MS+SPS-MS^3 method. (B) Schematic description to the identification of cell cycle regulated sites: Any site showing at least two-fold increase in the G2/M cells when compared to G1 is considered interphase regulated. Similarly, sites showing at least 2-fold more phosphorylation in mitotic cells compared to the elutriated G2/M are considered mitotic regulated sites. (C) Venn diagram representing the sites that were phosphorylated *in vitro* by the three complexes (pink) and their overlap with sites regulated *in vivo* (green). (D) Pie chart representing the mitotic regulated sites and their upstream kinases, which were identified either through *in vitro* (CDK1) phosphorylation or based on their sequence motifs (PLK1 and Aurora).

Although many studies investigated the phospho-proteome of M phase cells in the past, there is always the missing piece of the puzzle about the driving kinase behind these phosphorylations[109]. While sequence motifs can be used to guess that, many sites are not located within defined motifs. Similarly, many kinases do not have known sequences that they prefer targeting. I sought to use the data above to investigate whether any of the two Cyclin B1-CDK1+/-Cks1 complexes are behind this segment of the phospho-proteome, which is termed the 'dark phospho-proteome'. Cyclin A2-CDK1 complexes data were not considered in this analysis because the endogenous Cyclin A2 is degraded after prolonged treatment with STLC[118]. Results have shown that 69% of sites in the 'dark phospho-proteome' are indeed phosphorylated by Cyclin B1-CDK1 complexes (Figure 6.1D). This was not surprising to us since CDK1 is known to be the main regulator of protein phosphorylation in mitotic cells. Careful investigation to the amino acid sequences of these sites revealed that many residues in this 'dark phospho-proteome' are located within the S/TXXK/R motif. This raises the possibility of a Cks1-enhancement for their phosphorylation.

6.3.2 Mitotic regulated CDK1 sites that are enhanced by Cks1 showed non-Proline enrichment in their motifs

To elaborate on the last point of section 6.3.1, I decided to look in more details at the *in vitro* phosphorylation dynamics by the different CDK1 complexes of the cell cycle regulated residues that they overlapped with in the experiment above (Figure 6.1A-C). I began by seeking to identify the Cks1-specific sites in mitotic cells. I looked at these specifically in mitotic cells because the only complex that we used in this study with a Cks1 subunit is the Cyclin B1-CDK1, which is expressed predominantly during this phase *in vivo*. Data analysis from the previous section identified 4198 mitotic regulated sites. Out of these sites, the two Cyclin B1-CDK1 complexes (with or without Cks1) phosphorylated 3117. To identify those that were enhanced by Cks1, I plotted the phosphorylation intensities of the 3117 sites on a heat map and compared how Cyclin B1-CDK1 phosphorylated them *in vitro* in comparison with Cyclin B1-CDK1+Cks1 (Figure 6.2A). Results unveiled similar phosphorylation patterns to those observed in chapter 5, as the phosphorylation of some mitotic regulated sites was enhanced by the presence of Cks1 (Figure 6.2A, cluster 3) while being inhibited by this subunit for others. Does Cks1 still facilitate the phosphorylation of non-Proline sites after applying the cell cycle regulation filter? To evaluate that, I performed motif enrichment analysis using the online tool IceLogo. This tool allows looking at finer details in variations between groups, since the enrichment is performed comparatively between two datasets[128]. This is particularly important here as all heat map clusters were enriched with phospho-acceptor residues having +1 Proline in their sequences. Results demonstrated stronger enrichment of +1 Proline in all heat map sites compared to sites in cluster 3 (Figure 6.2B, bottom panel, position 17). In contrast, cluster 3 residues were enriched with +3 Lysine compared to the rest of the heat map (Figure 6.2B, top panel, position 19). This data demonstrates that mitotic regulated sites preferably phosphorylated by Cyclin B1-CDK1+Cks1 *in vitro* are enriched with the S/TXXK/R motif in their amino acid sequences.

As it was mentioned earlier, the data generated and presented in this chapter identify CDK1 as the upstream kinase for many of the mitotic 'dark' phospho-proteome residues and that these include sites lacking the +1 Proline in their sequence motifs (Figure 6.1D). I wanted to assess whether Cks1 might be a promoting factor for the phosphorylation of these non-Proline sites, especially that it previously appeared to do so (chapter 5) and that its depletion was reported to reduce the number of sites phosphorylated on the APC3 component of the APC/C in mitotic cells, including some non-Proline residues[105]. Results in Figure 6.2C show that CDK1 phosphorylated the majority of the mitotic regulated phospho-proteome (Figure 6.2C, black segment) and those of cluster 3 represented 12.8% of that phospho-proteome. Closer examination of the sequences for the 529 sites of cluster 3 demonstrates that the Cks1-enhanced phosphorylation of non-Proline sites accounts for 7.3% of the entire mitotic regulated phospho-proteome (Figure 6.2C, orange segment, exploded slice). Taken together, these results demonstrate that non-Proline directed phosphorylation by CDK1 that is promoted by Cks1 occurs *in vivo* and in a cell cycle regulated manner.

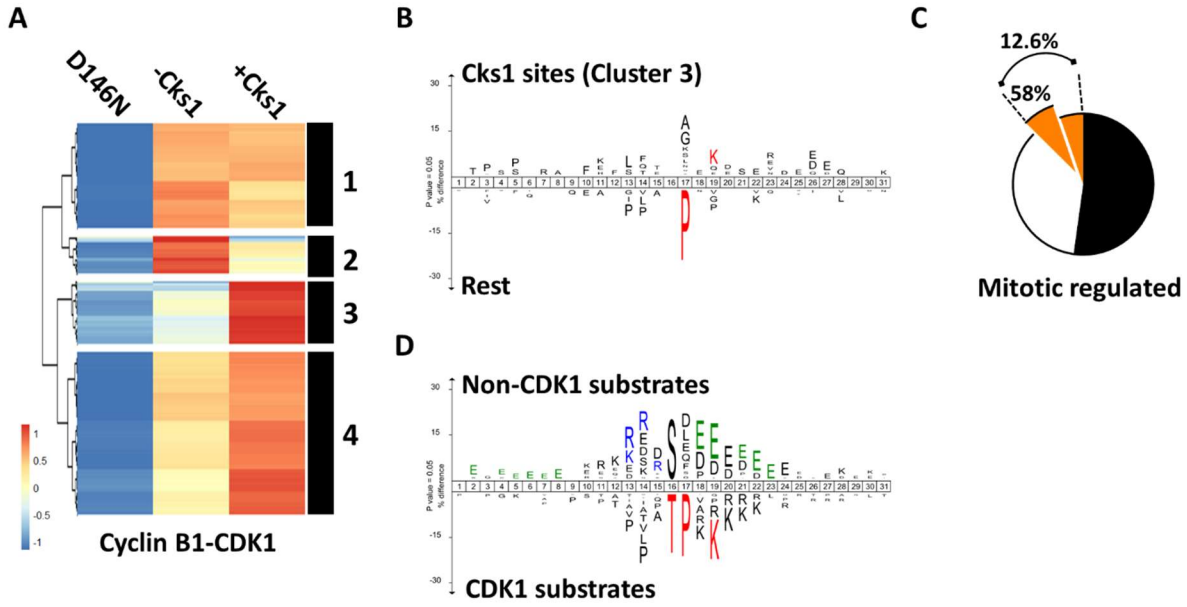

Figure 6.2: Cks1-enhanced mitotic sites. (A) Heat map showing the sites phosphorylated by Cyclin B1-CDK1+/-Cks1 in G2/M cells that were also identified as

mitotic regulated sites in Figure 6.1. Cluster 3 here, represents the sites with phosphorylation enhanced in the presence of Cks1. (B) Motif enrichment analysis of sites from cluster 3 (top) in comparison with the rest (bottom) of heat map sites presented in panel (A). (C) Pie chart representing the mitotic regulated sites and those of which that were phosphorylated by Cyclin B1-CDK1+/-Cks1 *in vitro* (black and orange segments). Orange segment represents the Cyclin B1-CDK1 sites that were in cluster 3 of panel (A). Exploded slice represents non-Proline sites within this group. (D) Motif enrichment analysis showing the amino acid sequence enrichment of mitotic regulated sites that were not overlapping with sites phosphorylated *in vitro* by Cyclin B1-CDK1+/-Cks1 in G2/M cells (top) in comparison to those that were phosphorylated by these complexes (bottom).

Examination of data in Figure 6.2C also shows that a large fraction of the mitotic regulated sites is not phosphorylated by CDK1 (Figure 6.2C, white segment). Could these be targeted by other kinases? To answer this question, I performed comparative motif enrichment analysis with IceLogo between these sites and those that were CDK1 phosphorylated (Figure 6.2D). Results showed that while the CDK1 sites were enriched with +1 Proline and +3 Lysine in their sequences (Figure 6.2D, bottom panel, positions 17 and 19), the rest of the mitotic regulated sites were enriched with sequences that are associated with other kinases (Figure 6.2D, top panel, blue and green symbols). For example, positions -2 and -3 for many sites were enriched with Arginine residues, which are associated with the mitotic kinases of the Aurora family. Similarly, the +/-15 amino acid regions flanking many of these phospho-acceptor residues were enriched with acidic amino acids, particularly Glutamates, reflecting a relaxed PLK motif. These results suggest that CDK1 phosphorylation of sites in fixed cells is selective to those with sequences that it normally targets *in vivo* as it failed to do so for sites located within consensus motifs targeted by other kinases, demonstrating potential biological relevance for this data.

6.3.3 Cyclin A2-CDK1 sites that are interphase regulated are enriched with S/TXXK/R motif

As it was mentioned earlier, Cyclin A2 is degraded after long prometaphase arrest, which makes it difficult to try overlapping mitotic regulated sites with those phosphorylated by this complex *in vitro*, despite the reported significance for these phosphorylations in destabilising spindle attachments to chromosomes during early mitosis[77]. For this reason, I sought to assess the overlap with the sites regulated during interphase identified in Figure 6.1. In consistency with the data presented in chapter 4, plotting the interphase regulated sites that overlapped with the *in vitro* phosphorylations of the two binary Cyclin-CDK1 complexes on a heat map revealed selectivity for these complexes in targeting cellular residues (Figure 6.3A). In this heat map, the phosphorylation of two groups of sites (clusters 1 and 4) by CDK1 seemed to be enhanced by the presence of a Cyclin A2 subunit. To investigate if the basis of this selectivity mirrors that appeared in earlier *in vitro* titration experiment, I performed motif enrichment analysis on these sites using IceLogo (Figure 6.3B). Results revealed that in comparison to the rest of the heat map sites, clusters 1 and 4 were enriched with S/TXXK/R sequences. This demonstrates that interphase regulated sites that are preferably targeted by Cyclin A2-CDK1 are also enriched with this motif, suggesting that the selectivity for this protein complex that I present here arises from its ability to better phosphorylate these residues compared to the Cyclin B1-CDK1. I also noticed that the enrichment of the +3 Lysine was stronger than that in the Cks1 dataset of section 6.3.2. Additionally, the enrichment of Arginine in that position was stronger in the rest of the heat map compared to these two clusters, which was not the case in the Cks1 results (compare the bottom motif of Figure 6.3B and Figure 6.2B). Both points are consistent with the observed enrichment of a +3 Arginine in the Cks1-enhanced sites when compared to those of Cyclin A2 in chapters 4 and 5, respectively (See discussion).

Finally, just like with Cks1 in section 6.3.2, I wanted to unveil the ratio of interphase regulated sites that were phosphorylated by Cyclin A2-CDK1 complex. Results in Figure 6.3C showed that 8% of these sites were phosphorylated by this complex *in vitro*. Furthermore, 41% of these sites were located within the S/TXXK/R motif (Figure 6.3C, exploded slice). It is difficult to eliminate the possibility that the *in vivo* phosphorylation of these sites is carried out by the Cyclin A2-CDK2 complex, since both CDK1 and 2 can be redundant when present with the right activity, and that both can form complexes with Cyclin A2 in baseline cellular conditions[93]. Having said that, the results that I present here still suggest that at least, these sites may have required the presence of Cyclin A2 when phosphorylated by the endogenous CDKs.

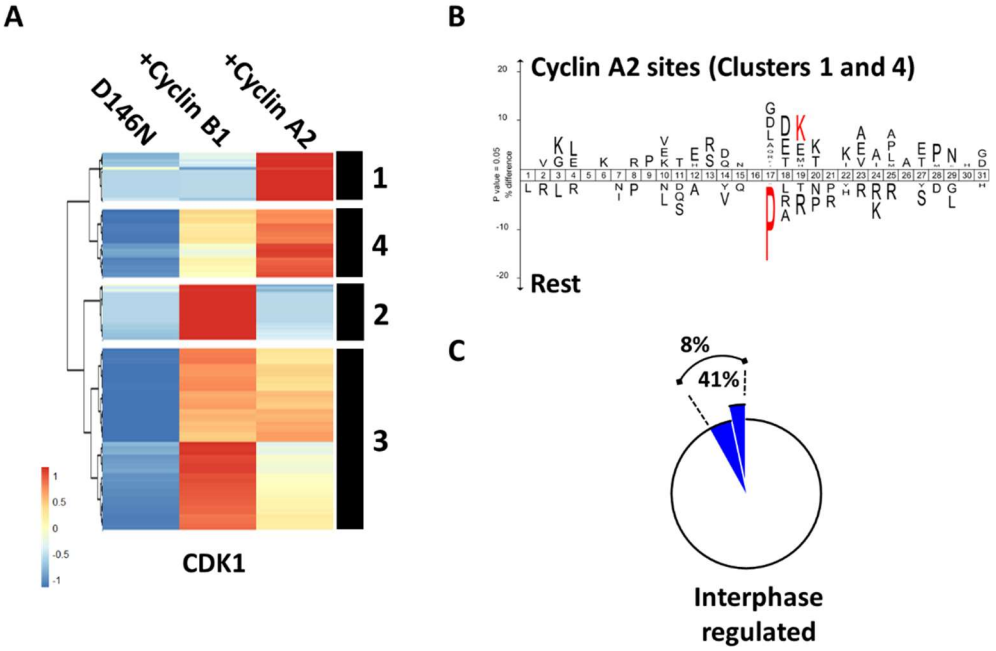

Figure 6.3: Interphase regulated phosphorylation is targeted by Cyclin A2- and Cyclin B1-CDK1 *in vitro*. (A) Heat map showing the sites that were phosphorylated *in vitro* by Cyclin A2/B1-CDK1 (WT/D146N) complexes in G1 cells and overlapped with interphase regulated sites from Figure 6.1. Clusters 1 and 4 represent the sites that were Cyclin A2 specific. (B) Motif enrichment analysis of sites from clusters 1 and 4 (top panel) compared to sites in the rest of the heat map (bottom panel) of panel (A). (C) Pie chart representing all interphase regulated sites and the ratio of Cyclin A2-

CDK1 specific sites (blue) within these. Exploded slice represents the sites that are located within the S/TXXK/R motif.

6.3.4 Depletion of Cyclin A2 reduces thio-phosphorylation of sites in G2 cells expressing CDK1-as

So far, I have presented data from fixed cells that were phosphorylated *in vitro* by recombinant CDK1 complexes and demonstrated that this kinase can phosphorylate sites located outside its canonical motif when in complex with either Cyclin A2 or Cks1. I also presented evidence that these non-canonical sites are phosphorylated endogenously, and that their phosphorylation is highly dynamic across the cell cycle. It was also reported previously that CDK1 can thio-phosphorylate substrates in murine embryonic stem cells expressing CDK1-as in the presence of a bulky-ATP-S molecule[134]. However, it is unclear if these non-canonical phosphorylations are regulated by Cyclin A2 or Cks1 as suggested by my *in vitro* data. For these reasons, I attempted to assess the phosphorylation of these non-canonical CDK1 sites in the absence of Cyclin A2. I chose to deplete Cyclin A2 rather than Cks1 because it is highly dynamic and can be removed with siRNA within 16 hours. Cks1, on the other hand, is much more stable and requires over 6 days to be depleted in HeLa cells. In addition, Cks2, the paralogue of Cks1, needs to be removed, too, for cells show the mitotic arrest phenotype reported earlier, as the two proteins show functional redundancy[92]. To label the *bona fide* substrates of CDK1 *in vivo*, I followed a previously published protocol[134], where cells expressing CDK1-as are used in combination with a bulky-ATP-S, to thio-phosphorylate CDK1 substrates. To investigate how Cyclin A2 depletion affects thio-phosphorylation of residues lacking the +1 Proline, I used siRNA to target the expression of the Cyclin A2 gene (*CCNA2*) in HeLa cells expressing the CDK1-as. These cells were a generous gift from the Earnshaw group at the University of Edinburgh and were used in previous reports both from their laboratory[111,135] and by others[165]. For control cells, I incubated these

cells with siRNA molecule carrying a scrambled sequence that should not possess interference to the expression of any gene in these cells. Analysing the cell cycle populations of both cultures by flow cytometry revealed an enrichment of cells expressing low levels of H3pS10, suggesting an arrest in late G2[135] (Figure 6.4A). This is consistent with the phenotype of cells depleted of Cyclin A2, which fail to enter mitosis in the absence of a Wee1 inhibitor[86]. The results in Figure 6.4A (bottom panel) raise two problems: One is that in both cultures, most cells are not in the cell cycle phases that CDK1-as is mostly active and functional at, which are G2 and M. Two is that there are more G2 cells in the culture depleted of Cyclin A2, making it hard to compare any results these cultures would generate. To minimise these issues, I used the molecule NM, which is an ATP analogue that selectively inhibits CDK1-as, to reversibly arrest cells in G2 phase (Figure 6.4A, compare top and bottom panels). To induce thio-phosphorylation of substrates, I detached these cells and placed them in a reaction buffer containing the Bulky-ATP-S molecule, which in the presence of digitonin, can penetrate the cell membrane and be used by the CDK1-as. Results from western blotting with a ThioP antibody unveiled weaker thio-phosphorylation of residues in the absence of Cyclin A2 (Figure 6.4B). Also, when HeLa cells expressing WT CDK1 (CDK1-wt), no staining for ThioP could be observed on that. These results demonstrate that cellular proteins were selectively thio-phosphorylated by CDK1-as and the levels of this were reduced when Cyclin A2 was depleted. The blot also shows a decline in the levels of CDK1-as as well as those of Cyclin B1, suggesting that the presence of Cyclin A2 is critical for their expression.

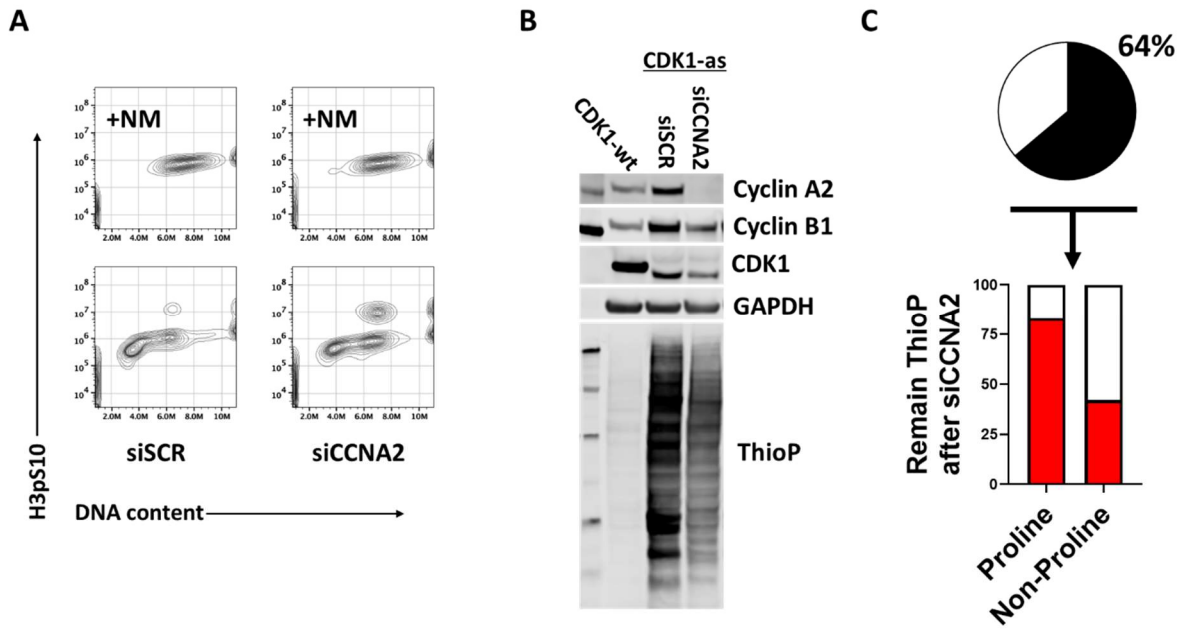

Figure 6.4: CDK1 fails to thio-phosphorylate non-Proline sites in the absence of Cyclin A2 *in vivo*. (A) Contour plots from flow cytometry analysis showing the cell cycle populations of HeLa cells with CDK1-as assayed based on their DNA content (*x-axis*) and H3pS10 (*y-axis*) after treatment either with siCCNA2 or siSCR. Top panel represents the populations after G2 arrest with NM (+NM) and bottom panel represents the distribution before that. (B) Western blotting of cell lysates with antibodies against the protein labelled on the plot after thio-phosphorylation assays. (C) Pie chart representing residues from mass spectrometry-based thio-phospho-proteomic analysis of the lysates from panel (B) of either Proline (Black) or non-Proline (white) sites on the top panel and bar plots representing Proline and non-Proline residues that are thio-phosphorylated (red) after Cyclin A2 depletion at the bottom.

To investigate the impact of Cyclin A2 depletion on the thio-phosphorylation of non-Proline sites, I prepared peptide digests from the lysates presented in Figure 6.4B and used mass spectrometry for global thio-phospho-proteomic analysis. Results revealed only 90 thio-phosphorylated residues in these cells, 64% of which had a +1 Proline (Figure 6.4C, top panel). Despite of their low number, the ratio of Proline to

non-Proline residues in this dataset is very consistent with that reported earlier from the murine embryonic stem cells that expressed the CDK1-as mutant[134]. When I compared the thio-phosphorylation intensity of both categories in the absence of Cyclin A2, I noticed that more than twice as much non-Proline sites showed at least 2-fold reduction in their thio-phosphorylation as the Proline sites (Figure 6.4C, bottom panel). While it is very difficult to eliminate the possibility that this reduction is caused by the decline in the levels of CDK1, Cyclin B1 or even failure of cells to enter M phase, it pinpoints the importance of Cyclin A2 for the *in vivo* phosphorylation of sites outside the canonical sequence by CDK1 one way or another.

6.3.5 NDC80-GFP mutants to investigate the importance of S76 phosphorylation

The results that I have presented pointed out that CDK1 in the presence of Cyclin A2 or Cks1 can phosphorylate highly dynamic sites lacking the +1 Proline of the CDK consensus motif, and many of which carry a +3 basic residue (mostly Lysine). The fact that these sites showed cell cycle regulation suggests that they are functional. It remains unclear if these non-Proline directed CDK1 phosphorylations have cellular functions. To investigate that, we needed to identify a model substrate through which we can study the importance of non-Proline directed phosphorylation by CDK1 for cell division. In preliminary experiments, I depleted both Cks1 and 2 and noticed that the absence of these proteins causes a decline in proliferation and a mitotic arrest (data not shown). Both results are consistent with previous reports from the Pines laboratory[100]. Also, in consistency with their findings, these mitotic cells showed a phenotype in which cells failed to establish a proper metaphase plate. One possibility for this is the presence of erroneous kinetochore-microtubule attachments. In my phospho-proteomic dataset, I noticed that one of the sites that appeared to be a target of both Cyclin A2 and Cks1 discussed in chapter 5 was on the protein NDC80. The location of this Serine in the 76th position of the amino acid

sequence makes it part of the N-terminal tail of NDC80 and places it in close vicinity to the toe domain. Therefore, S76 site may be involved in several functions, such as the binding to microtubules and the interaction with Mps1[163,164,166,167]. Our recently published report demonstrated that NDC80 can be phosphorylated by CDK1 on the canonical site T31[115]. Before attempting to express mutants of NDC80 in cells, I decided to IP either interphase or mitotic lysates that were thio-phosphorylated as described in Figure 6.4B with NDC80 antibody in order to investigate whether CDK1-as can directly thio-phosphorylate NDC80 in cells and whether this is specifically mitotic, as our previous report was based on using CDK1 inhibitors approach to look at the phosphorylation levels of T31. Western blotting with ThioP of NDC80 pulled down from these lysates demonstrated that this protein is thio-phosphorylated by CDK1-as specifically in mitotic cells (Figure 6.5A). Because NDC80 exists in two pools, soluble and kinetochore localised, I sought to investigate the thio-phosphorylation of the kinetochore localised pool, as this is the fraction that would be binding to spindle microtubules in mitotic cells. To selectively look at that, I used an antibody against the inner kinetochore protein CENP-C[11] to IP lysates from thio-phosphorylated interphase and mitotic cells. Results also showed that the kinetochore localised pool of NDC80 is thio-phosphorylated by CDK1-as and that this thio-phosphorylation was predominantly in mitotic cells (Figure 6.5B). To investigate whether S76 is also a mitotic site, HeLa cells expressing NDC80-FLAG were arrested in mitosis with STLC and IP with anti-FLAG antibody was performed after treatment with either CDK1 (+RO) or Mps1 (+AZ) inhibitor (Figure 6.5B). Treatment with any of the two inhibitors will drive cells out of mitosis due to a decline in CDK1 activity. For control, cells were treated only with DMSO (+Mock), which means that this sample will remain in prometaphase. The phosphorylation of sites in these samples, which were generated by the Compton laboratory at Dartmouth College, was then assayed using mass spectrometry. Results in Figure 6.5C demonstrate that S76 was phosphorylated in mitotic cells and that this phosphorylation is lost upon treatment with either inhibitor. This data is consistent with our *in vitro* results where the phosphorylation

of S76 was specifically mitotic. Similar findings were also observed for both T31 and T49 (Figure 6.5C).

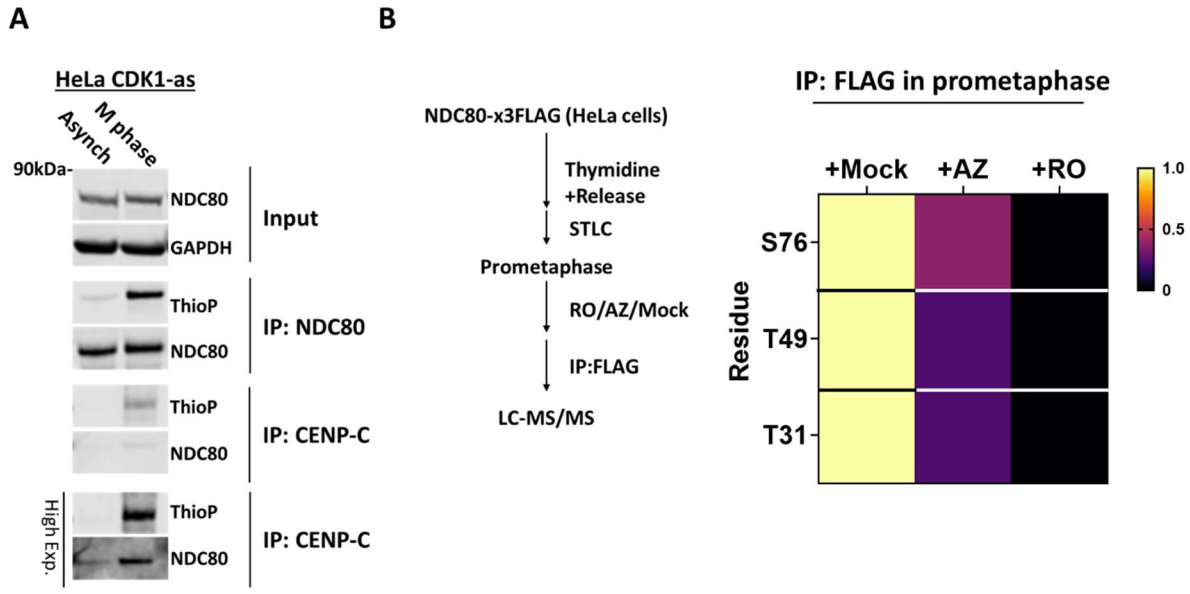

Figure 6.5: Phosphorylation of NDC80 by CDK1 *in vivo*. (A) Western blot from IP of lysates from thio-phosphorylated HeLa CDK1-as cells with either NDC80 or CENP-C antibodies. (B) Dephosphorylation kinetics of CDK1 sites in cells existing mitosis. Schematic description to the experiment (left) and mass spectrometry-based quantitation for the phosphorylation of sites that appeared in the *in vitro* dataset of CDK1 (right).

After establishing that NDC80 S76 is a mitotic target of CDK1 *in vivo*, we decided to go ahead and generate cell lines expressing mutant NDC80 that would allow future investigations into how phosphorylation of S76 would impact progression through mitosis. For this purpose, I used HeLa cells cloned with FRT locus. In the presence of a Flp Recombinase enzyme, we can selectively insert DNA sequences into this locus. To allow visualisation of spindle-kinetochore attachments in these cells, I first transfected the cells with a plasmid carrying mCherry-β-Tubulin sequence. This plasmid was a generous gift from the research group of Aaron Straight in Stanford

University. I then used FACS to sort single cells stably expressing mCherry into 96 wells (Figure 6.6A). To investigate both the localisation and the brightness of this mCherry signal, I arrested subclones of these and imaged them, first while in prometaphase with the Eg5 inhibitor Monastrol, and then in metaphase after a release into medium supplemented with the proteasomal inhibitor MG132 (Figure 6.6B). Based on the results, I selected the three brightest clones that successfully released into metaphase and pooled them for making the NDC80 mutants. To generate these mutants, I transfected the mCherry-Tubulin HeLa FRT cells with a plasmid of carrying siRNA resistant NDC80-GFP sequences, which in combination with a Flp Recombinase construct should be inserted into the FRT locus of these cells. Both original plasmids were prepared by the Saurin and the DeLuca laboratories at the Universities of Dundee and Colorado, respectively. Prior to co-transfection with Flp Recombinase, I performed site-directed mutagenesis on the NDC80-GFP plasmids to generate mutants where either S76 was mutated into a phospho-mimicking Aspartate or a non-phosphorylatable Alanine. Also, I generated some mutants in a background where the 9 Aurora sites[13] were mutated (9A/D) as well as in combination with mutant T31 (T31A/D) to investigate the synergy and redundancy of these sites. The Serine site next to S76 (S77) was also mutated in some clones (S76/77) to eliminate any potential redundancy in the phosphorylation of the two sites.

Insertion of these constructs into the FRT loci of cells allow conditional expression of NDC80-GFP as these regions is located downstream a repressed promotor sequence. Addition of Dox targets the repressor, allowing the expression of NDC80-GFP to be initiated (Figure 6.6C). Western blotting analysis with NDC80 antibody confirms the presence of a band bearing extra 27 kDa, which corresponds to the molecular weight of NDC80-GFP, after 16 hours of culture with growth medium supplemented with Dox (Figure 6.6D). By this I was able to establish a system that one can exploit in the future to investigate how the phosphorylation of the S/TXXK/R site S76 by CDK1 co-

operate with the other residues of the NDC80 tail to allow HeLa mCherry-Tubulin cells to establish proper metaphase plates.

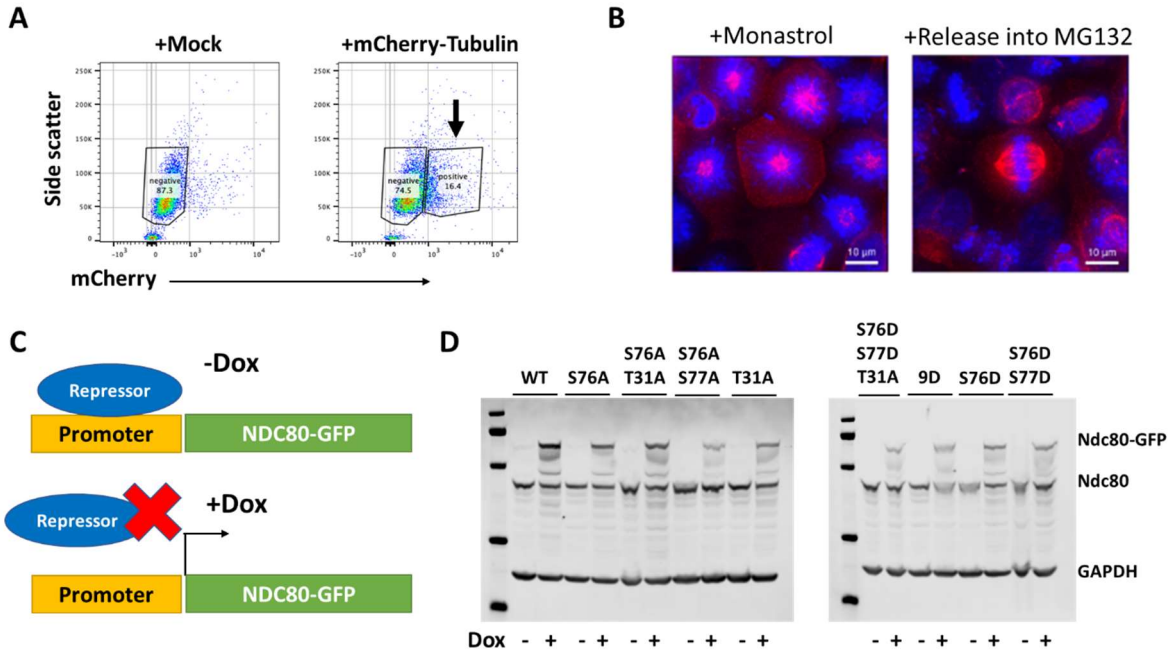

Figure 6.6: HeLa cells with mCherry-Tubulin and mutants of NDC80-GFP with conditional expression. (A) Density plots showing the mCherry fluorescence of cells after transfection with a plasmid carrying mCherry-Tubulin (+mCherry-Tubulin) in comparison to those with Mock transfection (+Mock). (B) IF images of cells from (A) arrested in prometaphase with Monastrol (+Monastrol) in the left panel and after a release into MG132 supplemented medium (+Release into MG132) in the right panel. (C) Schematic describing the expression of NDC80-GFP mutants transfected into the FRT locus of HeLa cells from panels (A) and (B) both in the presence (+) or absence (-) of Dox. (D) Western blotting of HeLa cells lysates from (C) with anti-NDC80 and GAPDH antibodies.

6.4 Discussion

In this chapter, I attempted to extend the characterisation of the non-Proline directed phosphorylation by CDK1 that I presented in the previous two chapters.

Since both kinases and phosphatases create a balanced phospho-proteome that allows cells to initiate and terminate their division events through dynamic phosphorylation and dephosphorylation of sites, I used these *in vivo* oscillations in phosphorylation as a readout to the functionality of CDK1 non-Proline sites. To our surprise, more than half of the sites that CDK1 phosphorylated *in vitro* have cell cycle regulated phosphorylation *in vivo*. Furthermore, the cell cycle regulated sites that lacked the +1 Proline were also preferably targeted by Cyclin A2 and Cks1 and similar sequence patterns to those observed *in vitro* could be seen. For example, a +3 Arginine was enriched within the sequences of Cks1 targets but not in those of Cyclin A2 (Figure 6.7). Consistent with the qualitative model, these results confirmed our speculations that by allowing CDK1 to switch its preferred consensus motif, the Cyclin partners control the temporal ordering of substrate's phosphorylation by CDK1 in dividing cells[143]. One advantage of this system is the difference in the dynamics of Cyclins and CDKs, as the former are extremely dynamic while the latter are relatively stable[72]. One limitation to the current data is that only one CDK1 concentration was used to induce *in vitro* phosphorylation, which meant that we could not resolve settler differences in substrate specificity between the three different complexes. Another issue is that we used Cyclin A2/B1-CDK1 complexes driven phosphorylations to investigate the overlap with interphase regulated sites. These are not the *bona fide* complexes that exist *in vivo* during that stage of the cell cycle. Although one would not expect much impact for this, since both CDK1 and 2 were shown to be redundant[83], it will be interesting to repeat these assays with CDK2 and observe differences in the phosphorylation patterns.

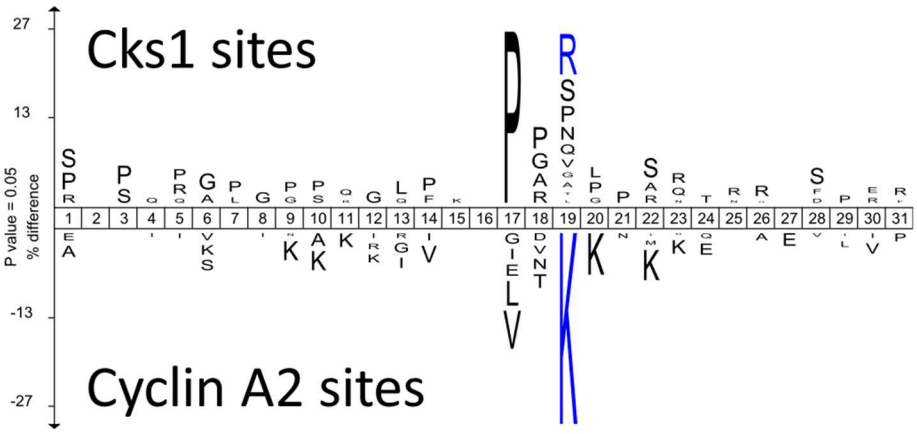

Figure 6.7: Variable enrichment for the +3 basic residue between targets of Cyclin A2-CDK1 and Cyclin B1-CDK1+Cks1. IceLogo chart showing the motif enrichment of Cks1 specific sites from chapter 5 (top, Cks1 sites) in comparison with Cyclin A2-CDK1 sites in chapter 4 (bottom, Cyclin A2 sites).

Another thing that I attempted in this chapter was to identify the real targets of CDK1 *in vivo* and assess how Cyclin A2 depletion would affect their phosphorylation. I used a previously published system where CDK1-as and a Bulky-ATP-S are combined to thio-phosphorylate residues in living cells[161]. Unlike the case with previous studies where hundreds of thio-phosphorylated sites were identified, our experiments did not generate a dataset with a sensitivity that would allow us to make biological conclusions. In addition to this, depletion of Cyclin A2 prevented cells from releasing into M phase, which was expected based on the data previously reported on cells depleted of this protein[86]. I tried avoiding this by shortening the thio-phosphorylation reaction time during the assay. Albeit with that, some of the control cells appeared to be entering mitosis, which made it difficult to eliminate the contribution of this to the differences observed between this sample and the Cyclin A2 depleted cells. CDK1 levels were also decreased after Cyclin A2 depletion, which may reflect a role for the latter in maintaining the stability of CDK1. This may also have contributed to the variations between the two datasets. Despite these technical challenges, when looking at the overall results it was evident that third of the thio-

phosphorylated sites by CDK1-as were lacking the +1 Proline, which was consistent with the data that were reported previously using this system[134]. All of these issues, which reflect the complexities of using such system, stress the importance of the *in vitro* assay that I presented and discussed in chapter 1 for this sort of investigations.

Finally, I wanted to identify a model substrate and to establish a cellular system based on it that can be used to investigate the importance of non-Proline CDK1 targets for cell division. The amino acid sequence, the dynamics of *in vivo* phosphorylation and the reproducibility, not only in our datasets, but also in previous reports, as well as the established function in microtubules binding, identified S76 of NDC80 as a potential candidate for this[77,118]. I generated several mutants with inducible expression of NDC80-GFP, as constant expression of this protein at high levels was associated with cellular toxicity (data not shown). The siRNA resistant sequences of these mutants should allow one to deplete the endogenous WT NDC80 and express the desired mutant. The GFP tag, along with the mCherry of tubulin that the HeLa cells express, will allow investigating how S76 mutagenesis affects the spatio-temporal distribution of NDC80 *in vivo*. Aspartate mutants of S76 and T31 in combination with 9A will show whether CDK1 phosphorylation of NDC80 can compensate in the absence of that by the Auroras. Finally, we also generated an antibody against phosphorylated S76, which in combination with the T31A mutant, allows one to investigate the dependency of S76 on T31 for its phosphorylation and may potentially identify T31 as a priming site. In the future, it will be crucial to use this cellular system to try answering all these questions.

Chapter 7:

Conclusion

7.1 Conclusion

A significant number of cell cycle proteins are regulated by CDK1. Through the addition of a phosphate group, this kinase can modify the activity of its substrates in several ways, allowing cells to progress through their division process. Both the complexity of the cell cycle, which includes several events that need to occur in a particular order, and the involvement of CDK1 in regulating all these events, raised a question about how this kinase can select the right substrate for phosphorylation at the right time of this process. Previous attempts to answer this question suggested qualitative[143] and quantitative[84] models to explain the selectivity of CDK1. Based on what I presented in chapter 1, one can see two issues with these attempts. The first was that most of these experiments were carried out in yeast cells, which have a relatively simpler genome than that of humans, expressing only one CDK[70,75]. The second was that these investigations focused on looking at the interactions of CDK1 with proteins rather than sites, which can be too simplistic to explain how the cell cycle system works[90]. Take the *Xenopus laevis* (*X. laevis*) MCM4 as an example of the last point. Here, variable multisite phosphorylation levels correlate with the DNA loading status of this protein during the cell cycle. So, in phases like metaphase, when DNA replication must not occur, MCM4 is hyperphosphorylated on multiple sites some of which by the *X. laevis* homologue of Cyclin B-CDK1[159]. The DNA loading of MCM4 can also be inhibited experimentally through complete dephosphorylation with a phosphatase. What this shows really, is that both high and no phosphorylation of this protein coincide with or lead to the same outcome. In contrast to both, intermediate phosphorylation levels of MCM4 in S phase cells coincide with its loading on their DNA.

The availability of tools that would allow investigating the phosphorylation of a substrate with such resolution was a limiting factor, as most of these investigations utilised radio-active phosphate incorporation or western blotting with phospho-antibodies for this purpose. Recent advances in mass spectrometry-based phospho-

proteomics can overcome these resolution issues. My first aim in this project was to develop a simplified system that can benefit from these advances, and through which I could investigate the contribution of each of the qualitative and quantitative models in CDK1 phosphorylation of the human proteome. To achieve this, I fixed and permeabilized human cell lines, and optimised an *in vitro* assay in which they were used as substrates for recombinant protein kinases. The advantage here is that I could investigate the phosphorylation of thousands of proteins without having to purify any of them. Also, the presence of these proteins within their native vicinities in the cell meant that protein-protein interactions are maintained. The locations of sites that would normally be buried *in vivo* due to these interactions will be retained in fixed cells, but not in soluble recombinant proteins, or cellular extracts. The disadvantage in using fixed and permeabilized cells, however, is that the permeabilization approach that I chose can affect the native structures of cellular proteins. Having said that, the experiment that I presented in chapter 3, which demonstrated the presence of residual phosphatase activity in these cells, suggests that some cellular proteins may have refolded when the methanol was washed off. Also, the enrichments of both the Aurora and CDK consensus motifs when cells were treated with their corresponding kinase reflect high degree of specificity for kinase consensus motifs in their interactions with cellular substrates (see chapters 3 and 4). Finally, a conserved feature about CDK sites is that they tend to cluster together in disordered domains in the substrates[168]. The lack of structural features in these regions means that they perhaps will not be affected by the methanol permeabilization to the same extent as the structured ones. The disturbance of the structured domains, however, may still impact the interactions that involve docking onto these regions. And last, the reproducibility of my data in the assays presented in chapter 5, where recombinant PML-IV, NDC80 and CDK7 were used as CDK1 substrates is a demonstration that key conclusions drawn from phosphorylating fixed and permeabilized cells were not artifacts of the sample preparation protocol.

Based on both the degree of specificity that I observed in this assay and the sensitivity to kinase stimulus, which was evident from the titration experiments with Aurora B (Figure 3.1, chapter 3), I used fixed and permeabilized cells for the second aim of this project. Here, I investigated how the presence of each of Cyclin A, B and Cks1 affect CDK1 substrate choice.

7.1.1 Conditional consensus motif switching for CDK1

To investigate the qualitative model of CDK phosphorylation ordering, I performed the assay described in chapter 3 with recombinant CDK1 complexes in two conditions, swapping the Cyclin partner between them. The Cyclin switching occurs in cells due to periodic expression of A and B, with A peaking in G2 and B in M. Less is known about Cks1. Therefore, to understand what contribution Cks1 has to CDK1 ordering of substrate phosphorylation, I also compared the phosphorylation induced by Cyclin B1-CDK1 in the presence and absence of this subunit. What all these experiments uncovered was a role for Cyclin A2 and Cks1 in promoting CDK1 phosphorylation of non-Proline sites, many of which were enriched with a +3 Lysine. This S/TXXK/R motif is widely phosphorylated in mitotic cells[109], when CDK1 would be reaching the peak of its cell cycle-related activity[169]. The fact that CDK1 can phosphorylate these sites did not come as a surprise, however. This is perhaps because third of its reported *in vivo* targets were lacking that Proline residue[134]. Similarly, and albeit on a single substrate, and in budding yeasts, Cks1 was also shown in the past to enhance the phosphorylation of a non-Proline site by Cdk1[98]. What was surprising here though, was the ability of Cyclin A2 to promote such phosphorylations. The significance here is not only in the novelty, but also in the combination of this non-canonical phosphorylation with the dynamics of Cyclin A2, which may explain why CDK1 would benefit from having type A2 as a partner and not a B1. The cellular levels of Cyclin A2 begin to rise during S phase when it forms a stable complex with CDK2. These levels then continue to elevate, reaching a peak in

G2 and M phases, where a complex with Cyclin A2-CDK1 promotes mitotic entry mediated by Wee1 degradation[86]. Perhaps the most interesting point though, is in early prometaphase, when cells express both Cyclin A2 and Cyclin B1 to comparable levels. Here, Kabeche and Compton showed a necessity for Cyclin A2 to destabilise kinetochore-microtubule interactions[77]. Both this and the high dynamics of S/TXXK/R sites that I presented in chapter 4, which were reported by Holder et al.[148], demonstrate that Cyclin A2 allows CDK1 to initiate highly dynamic events during both G2 and M phases by promoting these non-canonical phosphorylations. Based on this, it is fair to say that by expressing Cyclin A2 in S phase then degrading it in prometaphase, cells can direct CDK1 to phosphorylate selected targets on substrates involved in the events occurring during that period (Figure 7.1).

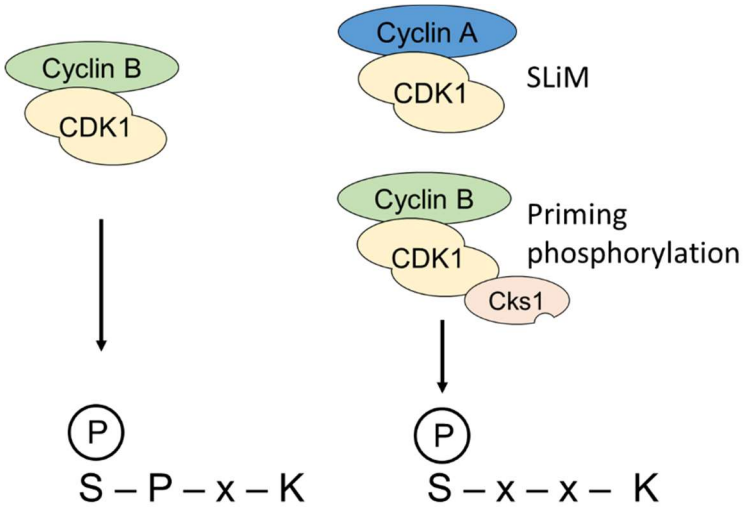

Figure 7.1: CDK1 can phosphorylate non-canonical sites in the presence of either Cyclin A2 or Cks1 in its complexes.

The role that Cks1 plays in all of this is still puzzling. Repeating the kinase assay with a complex that carries both Cyclin A2 and Cks1 may allow one to assess any possible synergy between the two subunits in promoting the phosphorylation of S/TXXK/R sites. Besides, even though the levels of Cks1 are relatively stable across the cell cycle, it is unclear whether this subunit associates with CDK complexes to

stoichiometric levels in all the cell cycle phases. It will be interesting to investigate this point with methods such as Proximity Ligation Assay (PLA)[170]-based microscopy in the future.

7.1.2 The global roles of Cyclins and Cks1 are consistent with those on individual substrates

The impact that Cyclins and Cks1 have on the interaction with the substrate as a whole has been investigated historically. For Cyclin, the qualitative model considers this subunit the determinant for the substrate selectivity of CDK1[171]. In my results, we noticed that swapping this subunit indeed, leads to a shift in the proteins targeted by this kinase. In addition, the consistency between the targeted cellular compartments and functions, and the cell cycle phase at which their targeting Cyclin would be expressed *in vivo*, was very intriguing. What was remarkable here though, was this occurring in dead cells like those used in the assay. One of the mechanisms that viable cells use to control the activity of CDK1, which was explained in chapter 1, was through associating this kinase with subunits that would impact its subcellular localisations[87]. The *in vivo* Cyclin-CDK complexes that mirrors those used in the assays here are affected by this control mechanism. Cyclin B1 for example, contains a nuclear exclusion signal that ensures timely phosphorylation of its nuclear targets in mitotic cells. In contrast, there is no evidence that Cyclin A has such a signal[172]. *In vitro*, both complexes that I used were truncated and lacked such sequence[93]. This completely eliminates any contribution from this control mechanism to the selectivity of CDK1 observed here. What this means is that these distinct subcellular localisations may have occurred by other means. One of these could be through the hydrophobic patch that exist on Cyclin A2. Through this, the budding yeast homolog was shown to dock onto RXL motifs on substrates, which in turn, facilitates their phosphorylation by CDK1[120]. Despite of its frequency in my dataset, no enrichment for this motif associated with one Cyclin over the other. It is possible however, that

docking onto these sequences is not conserved to human cells and that other docking sequences are targeted instead. It will be important to identify such motifs in the future.

The evidence in the literature shows a clear link between the presence of Cks1 and the multisite phosphorylation of substrates by both the human and the budding yeast CDK1[90,100,105]. However, since these findings were based on experiments carried out on individual substrates, it was important to investigate how global this role of Cks1 is. In chapter 5, I noticed a consistency with the literature in that significantly higher number of phosphorylated residues were present on the substrates that the Cyclin B1-CDK1+Cks1 complex targeted. In contrast, the impact of Cks1 on the substrate specificity was minimal. For many cell cycle phase transitions, like G2/M for example, cellular proteins need to be phosphorylated on multiple sites by CDK1. In the example above, these will be the phosphatase CDC25C[52] and the kinase Wee1[53]. The enhancement of multisite phosphorylation by Cks1 may reflect a role for this subunit in promoting these transitions. The phenotype that both we and others observed in cells depleted of the Cks proteins, however, suggests that it is mostly the mitotic events that require this subunit[100]. It is possible though, that this depletion also affected the kinetics of mitotic entry, which is something that both investigations did not take into account. This is especially true when knowing that the proliferation of these cells was drastically reduced (data not shown).

The mechanism by which Cks1 induces multisite phosphorylations on substrates is thought to be through its phospho-binding pocket. The docking of this phospho-adaptor protein on phosphorylated sites was shown to bring Cdk1 near less optimal sites on Sic1[173]. Both my findings here and those of others suggest that CDK1 is not necessarily the priming kinase for docking events like these. In budding yeasts for example, the MAP kinase Fus3 phosphorylates a site on Sic1[158]. The docking of Cks1 on this site then prevents the degradation of Sic1 and ensures a timely cell cycle entry. Docking of Cks1 on sites phosphorylated by other kinases does not seem to be

limited to Sic1 or even budding yeasts. In my dataset, sequential dephosphorylation with a λ phosphatase then phosphorylation by Cyclin B1-CDK1+Cks1, unveiled 140 sites that may require priming phosphorylation by other kinases. This, along with the evidence in chapter 6 that many Cks1 sites were cell cycle regulated, puts this subunit at the interface between the distinct regulatory mechanisms that cells use to regulate different protein kinases. It might be that through this, Cks1 contributes the most to the ordered phosphorylation of cell cycle related proteins. It is still important to identify the priming sites and the kinases that drive their phosphorylation to understand this better.

7.1.3 Qualitative and quantitative determinants promoting the temporal ordering of substrates phosphorylation by CDK1

From the sections above, it seems that it is the Cyclin specificity that creates this temporal ordering of cell cycle events. However, just like these proteins, the activity of CDK1 is very dynamic during division[84,174] (Figure 7.2). This makes it a potential factor for determining whether a substrate is to be phosphorylated or not. One of the complications of studying how manipulating CDK1 activity may impact the progression of the cell cycle is in all the layers of regulation that cellular enzymes exert on each other, such as feedback loops between kinases and phosphatases. Using dead cells as substrates though, eliminates these layers, making it possible to investigate the contribution of the second, quantitative model to this process. In consistency with previous reports[74,175], titration of cells with CDK1 activity in chapter 4 also uncovered a level of control through that. Here, cells establish activity thresholds that need to be surpassed for cell cycle events to be initiated. The distinct activity thresholds for these events make it possible, through the linear increase in CDK activity, to initiate these events in the order that the cell desires. For example, the phosphorylation of proteins related to early cell cycle processes, such as ribosomal synthesis and DNA replication, required lower CDK1 activity. In contrast,

later processes, like the segregation of chromosomes, were only targeted in the presence of a higher one. When looking at the endogenous phosphorylation of these sites, it was clear that it was the extent of this that determined how likely a site will be phosphorylated in the fixed cells. *In vivo*, this would translate into the amount of activity that protein phosphatases are exerting on that site. The crosstalk between these two counteracting forces is possibly what creates the CDK activity-mediated substrate specificity that I discuss here. It will be interesting to investigate whether this specificity will still exist if cells used in the assay were dephosphorylated in advance.

So, where does this leave us? Is it qualitative or quantitative? The results that all the experiments presented here show, is that it is a combination of both, and that assuming that it is one model and not the other would be too simplistic of an explanation to how the cell cycle works. The mechanisms by which sites are targeted in these models differ, however. In the quantitative model, the threshold of activity required to phosphorylate a particular site seems to be a result of differential selectivity of protein phosphatases for CDK1 targets. On the other hand, the Cyclins target CDKs by two means. One, through docking into amino acid sequences or phosphate groups depending on the Cyclin type. Two, and this is what this study adds to the field, is through switching the CDK consensus motif from the canonical Proline one, to the S/TXXK/R (Figure 7.2). The contribution of Cks1 has yet to be established, however, the data here suggest that it is possibly through incorporating the activity of other cellular enzymes into this system.

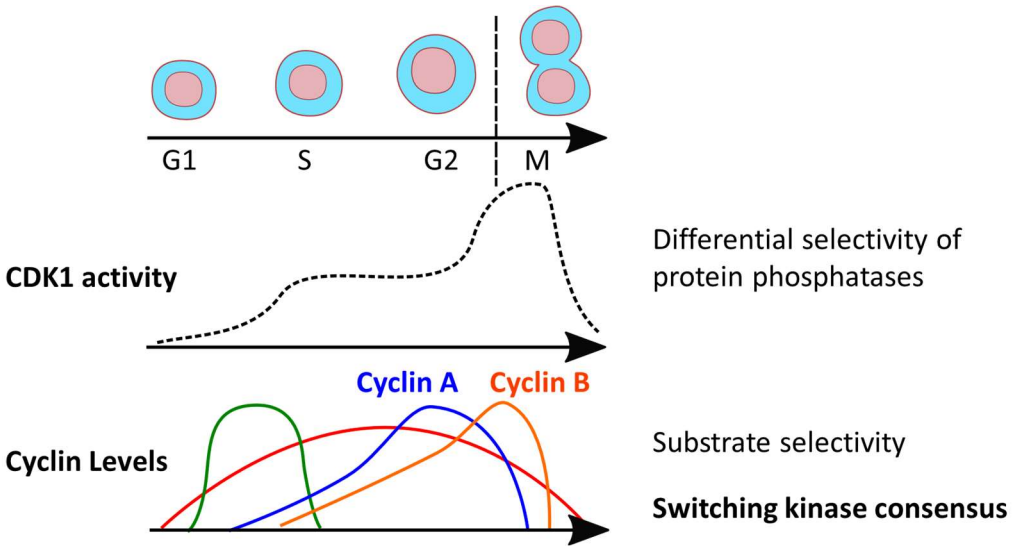

Figure 7.2: CDK1 activity and non-catalytic partners contribute to its substrate choice.

7.2 Future plans

One of the main conclusions of this study was that under certain conditions, CDK1 can switch its consensus motif and phosphorylate non-Proline sites. The observation that phosphorylation of these non-canonical sites is regulated throughout the cell cycle suggests functional significance. What is missing here, however, is comprehensive understanding of the roles that they play in the cell cycle events. The dataset was rich in phosphorylated residues of several proteins with known cell cycle functions. These included Ki-67, MCAK, RFC1, Cyclin H-CDK7, INCENP and Shugoshin. Along with these, was the S/TXXK/R S76 residue of the outer kinetochore protein, NDC80, which was discussed in chapter 6. Beside the fact that phosphorylation of this site was cell cycle regulated, it was also targeted by both Cyclin A2 and Cks1. By studying mitotic cells, one can compare the phosphorylation dynamics of this site in the presence and absence of Cyclin A2, which is degraded at some point during that phase. It is possible that a 'handout' model resembling that suggested for the cell Cyclin-CDK complexes earlier also exist between Cyclin A2 and Cks1[91]. Beside this, it is important to investigate what phenotypes do mutants of this site generate and

why are they occurring, especially that NDC80 is involved in many protein-protein interactions at the kinetochore[11]. For example, were these phenotypes caused by tighter microtubule attachments? A lack of the Ska-mediated crosslinking? Furthermore, we have raised a sheep antibody against phosphorylated S76. Using this, in combination with the anti- phospho-T31 antibody that we reported earlier[115], we can assess the dependency of priming phosphorylation. It will also be necessary to use these antibodies to compare the phosphorylation of their targets in the 9A mutant NDC80 with that in the WT, as this will reveal if such relationship exist between the CDK1 sites and those of the Aurora, especially that a combination of these is also present near the non-Proline site of MCAK. By answering all these questions, it will be possible to uncover how the function of a particular substrate is modulated during the cell cycle through a crosstalk between its residues.

Appendix

Scientific publications

Cyclin A and Cks1 promote kinase consensus switching to non-proline directed CDK1 phosphorylation

Authors: **Aymen al-Rawi**, Edward Kay, Svitlana Korolchuk, Jane Endicott, Tony Ly

Journal: Cell Reports, 2023

DOI: https://doi.org/10.1016/j.celrep.2023.112139

Contribution: Conceptualisation, performing most of the experiments and the data analysis, and writing the final manuscript (Described in chapters 4-6).

Low Cell Number Proteomic Analysis Using In-Cell Protease Digests Reveals a Robust Signature for Cell Cycle State Classification

Authors: Van Kelly, **Aymen al-Rawi**, David Lewis, Georg Kustatscher, Tony Ly

Journal: Molecular Cell Proteomics, 2022

DOI: https://doi.org/10.1016/j.mcpro.2021.100169

Contribution: data validation using cell biology techniques and western blotting (described in chapter 3).

Small changes in phospho-occupancy at the kinetochore-microtubule interface drive mitotic fidelity

Authors: Thomas J Kucharski, Rufus Hards, Sarah E Vandal, Maria Alba Abad, A. Arockia Jeyaprakash, Edward Kaye, **Aymen Al-Rawi**, Tony Ly, Kristina M Godek, Scott A Gerber, Duane A Compton

Journal: The Journal of Cell Biology, 2022

DOI: https://doi.org/10.1083/jcb.202107107

Contribution: Purification of recombinant proteins, design of the *in vitro* assay, supervision of Edward Kay and manuscript draft editing (described in chapters 3, 6 and 7).

Abbreviations

MCM: minichromsome maintenance

SAC: Spindle assembly checkpoint

LADs: Lamina-associated domains

RB: retinoblastoma

PLK1: Polo-like kinase

CPC: chromosome passenger complex

INCENP: inner centromere protein

PP2A: protein phosphatase 2 A

CDK: Cyclin-dependent kinase

CDK1-as: analogue-sensitive CDK1

WT: wild type

Cks: Cyclin-dependent kinase subunit

T48: Threonine 48

T33: Threonine 33

T31: Threonine 31

S76: Serine 76

S518: Serine 518

T473: Threonine 473

S25: Serine 25

FTMS: Fourier transformation mass spectrometry

m/z: mass-to-charge ratio

FACS: Fluorescent antibody-activated sorting

RPMI: Roswell Park Memorial Institute

FBS: foetal bovine serum

DPBS: Dulbecco's phosphate-buffered saline

FRT: Flip Recombinase target

DMEM: Dulbecco's modified Eagle medium

siRNA: short interfering-RNA

GFP: green fluorescent protein

PCR: Polymerase chain reaction

E. coli: Escherichia coli

LB: Luria-Bertani

DMSO: di-methyl sulphoxide

Dox: doxycycline

CEB: cells extraction buffer

TCEP: tris carboxyethyl phosphine

PAGE: poly-acrylamide gel electrophoresis

TBS: tri-buffered saline

MBS-F: MES-buffered saline with 0.1% Tween

STLC: S-trityl L-Cysteine

DTT: dithiothreitol

BSA: bovine serum Albumin

ATP: adenosine triphosphate

TEAB: triethyl ammonium bicarbonate

TMT: tandem mass tag

TFA: trifluoroacetic acid

HPLC: high performance liquid chromatography

SCR: scrambled sequence

NM: 1nm-PP1

PNBM: p-nitro benzyl mesylate

BCA: bicinchoninic acid

ThioP: thio-phospho-ester

IP: immunoprecipitation

SPS: synchronous precursor selection

GO: gene ontology

IF: immunofluorescence

pNPP: p-nitro phenyl phosphate

Ti-IMAC: titanium-immobilised affinity chromatography

D146N: $CDK1^{D146N}$

MPSi: inhibitor of Mps1

λ: protein phosphatase lambda

+Mock: no treatment

X. Laevis: Xenopus Laevis

NDC80: NDC80/Hec1 subunit of the NDC80 complex

CCNA2: Cyclin A2 gene

CDK1-wt: wild type CDK1

RO: RO3306

AZ: AZ3146

PLA: Proximity Ligation Assay

SEC-MALS: Size exclusion chromatography -multiangle light scattering

Bibliography

1 Pollard, T. D., Earnshaw, W. C., Lippincott-Schwartz, J. & Johnson, G. T. *Cell Biology: Third edition*. 697 - 819 (Elsevier Inc., 2016/11/30).

2 Bertoli, C., Skotheim, J. M. & de Bruin, R. A. Control of cell cycle transcription during G1 and S phases. *Nature reviews. Molecular cell biology* **14**, 518-528, doi:10.1038/nrm3629 (2013).

3 Bernstein, K. A., Bleichert, F., Bean, J. M., Cross, F. R. & Baserga, S. J. Ribosome biogenesis is sensed at the Start cell cycle checkpoint. *Mol Biol Cell* **18**, 953-964, doi:10.1091/mbc.e06-06-0512 (2007).

4 Fragkos, M., Ganier, O., Coulombe, P. & Méchali, M. DNA replication origin activation in space and time. *Nature Reviews Molecular Cell Biology* **16**, 360-374, doi:10.1038/nrm4002 (2015).

5 Mukherjee, P., Cao, T. V., Winter, S. L. & Alexandrow, M. G. Mammalian MCM loading in late-G(1) coincides with Rb hyperphosphorylation and the transition to post-transcriptional control of progression into S-phase. *PloS one* **4**, e5462, doi:10.1371/journal.pone.0005462 (2009).

6 Johnson, A. & Skotheim, J. M. Start and the restriction point. *Current opinion in cell biology* **25**, 717-723, doi:10.1016/j.ceb.2013.07.010 (2013).

7 Moiseeva, T. N. & Bakkenist, C. J. Regulation of the initiation of DNA replication in human cells. *DNA repair* **72**, 99-106, doi:10.1016/j.dnarep.2018.09.003 (2018).

8 Morgan, D. O. N. S. P. The cell cycle : principles of control. (2007).

9 Bettencourt-Dias, M. & Glover, D. M. Centrosome biogenesis and function: centrosomics brings new understanding. *Nature Reviews Molecular Cell Biology* **8**, 451-463, doi:10.1038/nrm2180 (2007).

10 Conduit, P. T., Wainman, A. & Raff, J. W. Centrosome function and assembly in animal cells. *Nature Reviews Molecular Cell Biology* **16**, 611-624, doi:10.1038/nrm4062 (2015).

11 Musacchio, A. & Desai, A. A Molecular View of Kinetochore Assembly and Function. *Biology* **6**, doi:10.3390/biology6010005 (2017).

12 Fukagawa, T. & Earnshaw, William C. The Centromere: Chromatin Foundation for the Kinetochore Machinery. *Developmental Cell* **30**, 496-508, doi:https://doi.org/10.1016/j.devcel.2014.08.016 (2014).

13 Wimbish, R. T. & DeLuca, J. G. Hec1/Ndc80 Tail Domain Function at the Kinetochore-Microtubule Interface. *Frontiers in cell and developmental biology* **8**, 43, doi:10.3389/fcell.2020.00043 (2020).

14 Dey, G. & Baum, B. Nuclear envelope remodelling during mitosis. *Current opinion in cell biology* **70**, 67-74, doi:10.1016/j.ceb.2020.12.004 (2021).

15 Pollard, T. D. & O'Shaughnessy, B. Molecular Mechanism of Cytokinesis. *Annual Review of Biochemistry* **88**, 661-689, doi:10.1146/annurev-biochem-062917-012530 (2019).
16 Pennycook, B. R. & Barr, A. R. Restriction point regulation at the crossroads between quiescence and cell proliferation. *FEBS Letters* **594**, 2046-2060, doi:https://doi.org/10.1002/1873-3468.13867 (2020).
17 Levine, M. S. & Holland, A. J. The impact of mitotic errors on cell proliferation and tumorigenesis. *Genes & development* **32**, 620-638, doi:10.1101/gad.314351.118 (2018).
18 Herr, P. *et al.* Cell Cycle Profiling Reveals Protein Oscillation, Phosphorylation, and Localization Dynamics. *Mol Cell Proteomics* **19**, 608-623, doi:10.1074/mcp.RA120.001938 (2020).
19 Barnum, K. J. & O'Connell, M. J. Cell cycle regulation by checkpoints. *Methods in molecular biology (Clifton, N.J.)* **1170**, 29-40, doi:10.1007/978-1-4939-0888-2_2 (2014).
20 Wang, J. Y. J. & Ki, S. W. in *Encyclopedia of Cancer (Second Edition)* (ed Joseph R. Bertino) 425-431 (Academic Press, 2002).
21 O'Connell, M. J., Walworth, N. C. & Carr, A. M. The G2-phase DNA-damage checkpoint. *Trends in Cell Biology* **10**, 296-303, doi:https://doi.org/10.1016/S0962-8924(00)01773-6 (2000).
22 Musacchio, A. The Molecular Biology of Spindle Assembly Checkpoint Signaling Dynamics. *Current Biology* **25**, R1002-R1018, doi:https://doi.org/10.1016/j.cub.2015.08.051 (2015).
23 Visconti, R., Della Monica, R. & Grieco, D. Cell cycle checkpoint in cancer: a therapeutically targetable double-edged sword. *Journal of Experimental & Clinical Cancer Research* **35**, 153, doi:10.1186/s13046-016-0433-9 (2016).
24 Otto, T. & Sicinski, P. Cell cycle proteins as promising targets in cancer therapy. *Nature reviews. Cancer* **17**, 93-115, doi:10.1038/nrc.2016.138 (2017).
25 Zhang, X. H., Hsiang, J. & Rosen, S. T. Flavopiridol (Alvocidib), a Cyclin-dependent Kinases (CDKs) Inhibitor, Found Synergy Effects with Niclosamide in Cutaneous T-cell Lymphoma. *Journal of clinical haematology* **2**, 48-61, doi:10.33696/haematology.2.028 (2021).
26 Yamashita, K. *et al.* Okadaic acid, a potent inhibitor of type 1 and type 2A protein phosphatases, activates cdc2/H1 kinase and transiently induces a premature mitosis-like state in BHK21 cells. *EMBO J* **9**, 4331-4338, doi:10.1002/j.1460-2075.1990.tb07882.x (1990).
27 Hunt, T., Luca, F. C. & Ruderman, J. V. The requirements for protein synthesis and degradation, and the control of destruction of cyclins A and B in the meiotic and mitotic cell cycles of the clam embryo. *Journal of Cell Biology* **116**, 707-724, doi:10.1083/jcb.116.3.707 (1992).
28 Potapova, T. A. *et al.* The reversibility of mitotic exit in vertebrate cells. *Nature* **440**, 954-958, doi:10.1038/nature04652 (2006).

29 Seok, S. H. Structural Insights into Protein Regulation by Phosphorylation and Substrate Recognition of Protein Kinases/Phosphatases. *Life (Basel, Switzerland)* **11**, doi:10.3390/life11090957 (2021).
30 Manning, G., Whyte, D. B., Martinez, R., Hunter, T. & Sudarsanam, S. The protein kinase complement of the human genome. *Science* **298**, 1912-1934, doi:10.1126/science.1075762 (2002).
31 Ardito, F., Giuliani, M., Perrone, D., Troiano, G. & Lo Muzio, L. The crucial role of protein phosphorylation in cell signaling and its use as targeted therapy (Review). *International journal of molecular medicine* **40**, 271-280, doi:10.3892/ijmm.2017.3036 (2017).
32 Rubin, S. M., Sage, J. & Skotheim, J. M. Integrating Old and New Paradigms of G1/S Control. *Molecular Cell* **80**, 183-192, doi:https://doi.org/10.1016/j.molcel.2020.08.020 (2020).
33 Larasati & Duncker, B. P. Mechanisms Governing DDK Regulation of the Initiation of DNA Replication. *Genes* **8**, doi:10.3390/genes8010003 (2016).
34 Colicino, E. G. & Hehnly, H. Regulating a key mitotic regulator, polo-like kinase 1 (PLK1). *Cytoskeleton (Hoboken, N.J.)* **75**, 481-494, doi:10.1002/cm.21504 (2018).
35 Saurin, A. T., Van Der Waal, M. S., Medema, R. H., Lens, S. M. A. & Kops, G. J. P. L. Aurora B potentiates Mps1 activation to ensure rapid checkpoint establishment at the onset of mitosis. *Nature Communications* **2**, doi:10.1038/ncomms1319 (2011).
36 von Schubert, C. *et al.* Plk1 and Mps1 Cooperatively Regulate the Spindle Assembly Checkpoint in Human Cells. *Cell Reports*, doi:10.1016/j.celrep.2015.06.007 (2015).
37 Alfieri, C. *et al.* Molecular basis of APC/C regulation by the spindle assembly checkpoint. *Nature* **536**, 431-436, doi:10.1038/nature19083 (2016).
38 Gelens, L., Qian, J., Bollen, M. & Saurin, A. T. The Importance of Kinase–Phosphatase Integration: Lessons from Mitosis. *Trends in Cell Biology* **28**, 6-21, doi:https://doi.org/10.1016/j.tcb.2017.09.005 (2018).
39 Saurin, A. T. Kinase and Phosphatase Cross-Talk at the Kinetochore. *Frontiers in cell and developmental biology*, doi:10.3389/fcell.2018.00062 (2018).
40 Krasinska, L. *et al.* Protein Phosphatase 2A Controls the Order and Dynamics of Cell-Cycle Transitions. *Molecular Cell* **44**, 437-450, doi:https://doi.org/10.1016/j.molcel.2011.10.007 (2011).
41 Bollen, M., Peti, W., Ragusa, M. J. & Beullens, M. The extended PP1 toolkit: designed to create specificity. *Trends in biochemical sciences* **35**, 450-458, doi:10.1016/j.tibs.2010.03.002 (2010).
42 Xu, Y. *et al.* Structure of the protein phosphatase 2A holoenzyme. *Cell* **127**, 1239-1251, doi:10.1016/j.cell.2006.11.033 (2006).
43 Holder, J., Poser, E. & Barr, F. A. Getting out of mitosis: spatial and temporal control of mitotic exit and cytokinesis by PP1 and PP2A. *FEBS Letters* **593**, 2908-2924, doi:https://doi.org/10.1002/1873-3468.13595 (2019).

44 Espert, A. *et al.* PP2A-B56 opposes Mps1 phosphorylation of Knl1 and thereby promotes spindle assembly checkpoint silencing. *Journal of Cell Biology* **206**, 833-842, doi:10.1083/jcb.201406109 (2014).
45 Dohadwala, M. *et al.* Phosphorylation and inactivation of protein phosphatase 1 by cyclin-dependent kinases. *Proceedings of the National Academy of Sciences of the United States of America* **91**, 6408-6412, doi:10.1073/pnas.91.14.6408 (1994).
46 Wu, J. Q. *et al.* PP1-mediated dephosphorylation of phosphoproteins at mitotic exit is controlled by inhibitor-1 and PP1 phosphorylation. *Nat Cell Biol* **11**, 644-651, doi:10.1038/ncb1871 (2009).
47 Gharbi-Ayachi, A. *et al.* The substrate of Greatwall kinase, Arpp19, controls mitosis by inhibiting protein phosphatase 2A. *Science* **330**, 1673-1677, doi:10.1126/science.1197048 (2010).
48 Ma, S. *et al.* Greatwall dephosphorylation and inactivation upon mitotic exit is triggered by PP1. *Journal of cell science* **129**, 1329-1339, doi:10.1242/jcs.178855 (2016).
49 Kamenz, J. & Ferrell, J. E. The Temporal Ordering of Cell-Cycle Phosphorylation. *Molecular Cell* **65**, 371-373, doi:10.1016/j.molcel.2017.01.025 (2017).
50 Verdugo, A., Vinod, P. K., Tyson, J. J. & Novak, B. Molecular mechanisms creating bistable switches at cell cycle transitions. *Open Biology* **3**, 120179, doi:10.1098/rsob.120179.
51 Forester, C. M., Maddox, J., Louis, J. V., Goris, J. & Virshup, D. M. Control of mitotic exit by PP2A regulation of Cdc25C and Cdk1. *Proceedings of the National Academy of Sciences of the United States of America* **104**, 19867-19872, doi:10.1073/pnas.0709879104 (2007).
52 Trunnell, N. B., Poon, A. C., Kim, S. Y. & Ferrell, J. E., Jr. Ultrasensitivity in the Regulation of Cdc25C by Cdk1. *Molecular cell* **41**, 263-274, doi:10.1016/j.molcel.2011.01.012 (2011).
53 Kim, S. Y. & Ferrell, J. E. Substrate Competition as a Source of Ultrasensitivity in the Inactivation of Wee1. *Cell* **128**, 1133-1145, doi:https://doi.org/10.1016/j.cell.2007.01.039 (2007).
54 Ferrell, J. E., Jr. Feedback loops and reciprocal regulation: recurring motifs in the systems biology of the cell cycle. *Current opinion in cell biology* **25**, 676-686, doi:10.1016/j.ceb.2013.07.007 (2013).
55 Watanabe, N. *et al.* M-phase kinases induce phospho-dependent ubiquitination of somatic Wee1 by SCFβ-TrCP. *Proceedings of the National Academy of Sciences* **101**, 4419-4424, doi:10.1073/pnas.0307700101 (2004).
56 He, J. *et al.* Insights into degron recognition by APC/C coactivators from the structure of an Acm1-Cdh1 complex. *Mol Cell* **50**, 649-660, doi:10.1016/j.molcel.2013.04.024 (2013).
57 Ferreira, M. F., Santocanale, C., Drury, L. S. & Diffley, J. F. Dbf4p, an essential S phase-promoting factor, is targeted for degradation by the anaphase-

promoting complex. *Mol Cell Biol* **20**, 242-248, doi:10.1128/mcb.20.1.242-248.2000 (2000).

58 Johnson, L. N., Noble, M. E. M. & Owen, D. J. Active and Inactive Protein Kinases: Structural Basis for Regulation. *Cell* **85**, 149-158, doi:https://doi.org/10.1016/S0092-8674(00)81092-2 (1996).

59 Kim, H. J., Kwon, H. R., Bae, C. D., Park, J. & Hong, K. U. Specific primary sequence requirements for Aurora B kinase-mediated phosphorylation and subcellular localization of TMAP during mitosis. *Cell Cycle*, doi:10.4161/cc.9.10.11753 (2010).

60 Kettenbach, A. N. *et al.* Quantitative phosphoproteomics identifies substrates and functional modules of Aurora and Polo-like kinase activities in mitotic cells. *Science Signaling*, doi:10.1126/scisignal.2001497 (2011).

61 Cheeseman, I. M. *et al.* Phospho-regulation of kinetochore-microtubule attachments by the Aurora kinase Ipl1p. *Cell* **111**, 163-172, doi:10.1016/s0092-8674(02)00973-x (2002).

62 Nakajima, H., Toyoshima-Morimoto, F., Taniguchi, E. & Nishida, E. Identification of a Consensus Motif for Plk (Polo-like Kinase) Phosphorylation Reveals Myt1 as a Plk1 Substrate*. *Journal of Biological Chemistry* **278**, 25277-25280, doi:https://doi.org/10.1074/jbc.C300126200 (2003).

63 Hendrickx, A. *et al.* Docking Motif-Guided Mapping of the Interactome of Protein Phosphatase-1. *Chemistry & Biology* **16**, 365-371, doi:https://doi.org/10.1016/j.chembiol.2009.02.012 (2009).

64 Cundell, M. J. *et al.* A PP2A-B55 recognition signal controls substrate dephosphorylation kinetics during mitotic exit. *J Cell Biol* **214**, 539-554, doi:10.1083/jcb.201606033 (2016).

65 Ruchaud, S., Carmena, M. & Earnshaw, W. C. in *Cell* (2007).

66 Carmena, M., Ruchaud, S. & Earnshaw, W. C. Making the Auroras glow: regulation of Aurora A and B kinase function by interacting proteins. *Current opinion in cell biology* **21**, 796-805, doi:https://doi.org/10.1016/j.ceb.2009.09.008 (2009).

67 Ruchaud, S., Carmena, M. & Earnshaw, W. C. in *Nature Reviews Molecular Cell Biology* (2007).

68 Wang, F. *et al.* Histone H3 Thr-3 phosphorylation by Haspin positions Aurora B at centromeres in mitosis. *Science* **330**, 231-235, doi:10.1126/science.1189435 (2010).

69 Ly, T. *et al.* Proteomic analysis of cell cycle progression in asynchronous cultures, including mitotic subphases, using PRIMMUS. *Elife*, doi:10.7554/eLife.27574 (2017).

70 Coudreuse, D. & Nurse, P. Driving the cell cycle with a minimal CDK control network. *Nature* **468**, 1074-1080, doi:10.1038/nature09543 (2010).

71 Łukasik, P., Załuski, M. & Gutowska, I. Cyclin-Dependent Kinases (CDK) and Their Role in Diseases Development-Review. *International journal of molecular sciences* **22**, doi:10.3390/ijms22062935 (2021).

72 Morgan, D. O. CYCLIN-DEPENDENT KINASES: Engines, Clocks, and Microprocessors. *Annual Review of Cell and Developmental Biology*, doi:10.1146/annurev.cellbio.13.1.261 (1997).
73 Hu, B., Mitra, J., van den Heuvel, S. & Enders, G. H. S and G2 phase roles for Cdk2 revealed by inducible expression of a dominant-negative mutant in human cells. *Mol Cell Biol* **21**, 2755-2766, doi:10.1128/mcb.21.8.2755-2766.2001 (2001).
74 Swaffer, M. P., Jones, A. W., Flynn, H. R., Snijders, A. P. & Nurse, P. CDK Substrate Phosphorylation and Ordering the Cell Cycle. *Cell* **167**, 1750-1761.e1716, doi:10.1016/j.cell.2016.11.034 (2016).
75 Fisher, D. L. & Nurse, P. A single fission yeast mitotic cyclin B p34cdc2 kinase promotes both S-phase and mitosis in the absence of G1 cyclins. *EMBO J* **15**, 850-860 (1996).
76 Minshull, J., Blow, J. J. & Hunt, T. Translation of cyclin mRNA is necessary for extracts of activated Xenopus eggs to enter mitosis. *Cell*, doi:10.1016/0092-8674(89)90628-4 (1989).
77 Kabeche, L. & Compton, D. A. Cyclin A regulates kinetochore microtubules to promote faithful chromosome segregation. *Nature*, doi:10.1038/nature12507 (2013).
78 Timofeev, O., Cizmecioglu, O., Settele, F., Kempf, T. & Hoffmann, I. Cdc25 phosphatases are required for timely assembly of CDK1-cyclin B at the G2/M transition. *The Journal of biological chemistry* **285**, 16978-16990, doi:10.1074/jbc.M109.096552 (2010).
79 Cerqueira, A. *et al.* Genetic characterization of the role of the Cip/Kip family of proteins as cyclin-dependent kinase inhibitors and assembly factors. *Mol Cell Biol* **34**, 1452-1459, doi:10.1128/mcb.01163-13 (2014).
80 Jeffrey, P. D., Tong, L. & Pavletich, N. P. Structural basis of inhibition of CDK-cyclin complexes by INK4 inhibitors. *Genes & development* **14**, 3115-3125, doi:10.1101/gad.851100 (2000).
81 Besson, A., Dowdy, S. F. & Roberts, J. M. CDK Inhibitors: Cell Cycle Regulators and Beyond. *Developmental Cell* **14**, 159-169, doi:https://doi.org/10.1016/j.devcel.2008.01.013 (2008).
82 Santamaría, D. *et al.* Cdk1 is sufficient to drive the mammalian cell cycle. *Nature*, doi:10.1038/nature06046 (2007).
83 Lau, H. W. *et al.* Quantitative differences between cyclin-dependent kinases underlie the unique functions of CDK1 in human cells. *Cell Reports* **37**, 109808, doi:10.1016/J.CELREP.2021.109808 (2021).
84 Stern, B. & Nurse, P. A quantitative model for the cdc2 control of S phase and mitosis in fission yeast. *Trends in Genetics* **12**, 345-350, doi:https://doi.org/10.1016/S0168-9525(96)80016-3 (1996).
85 Geng, Y. *et al.* Kinase-Independent Function of Cyclin E. *Molecular Cell*, doi:10.1016/j.molcel.2006.11.029 (2007).

86 Hégarat, N. *et al.* Cyclin A triggers Mitosis either via the Greatwall kinase pathway or Cyclin B. *EMBO J*, doi:10.15252/embj.2020104419 (2020).
87 Moore, J. D., Kornbluth, S. & Hunt, T. Identification of the nuclear localization signal in Xenopus cyclin E and analysis of its role in replication and mitosis. *Mol Biol Cell*, doi:10.1091/mbc.E02-07-0449 (2002).
88 Toyoshima, F., Moriguchi, T., Wada, A., Fukuda, M. & Nishida, E. Nuclear export of cyclin B1 and its possible role in the DNA damage-induced G2 checkpoint. *EMBO Journal*, doi:10.1093/emboj/17.10.2728 (1998).
89 Bloom, J. & Cross, F. R. in *Nature Reviews Molecular Cell Biology* (2007).
90 Loog, M. & Morgan, D. O. Cyclin specificity in the phosphorylation of cyclin-dependent kinase substrates. *Nature* **434**, 104-108, doi:10.1038/nature03329 (2005).
91 Pagliuca, F. W. *et al.* Quantitative Proteomics Reveals the Basis for the Biochemical Specificity of the Cell-Cycle Machinery. *Molecular Cell*, doi:10.1016/j.molcel.2011.05.031 (2011).
92 Martinsson-Ahlzén, H.-S. *et al.* Cyclin-Dependent Kinase-Associated Proteins Cks1 and Cks2 Are Essential during Early Embryogenesis and for Cell Cycle Progression in Somatic Cells. *Molecular and Cellular Biology*, doi:10.1128/mcb.01833-07 (2008).
93 Brown, N. R. *et al.* CDK1 structures reveal conserved and unique features of the essential cell cycle CDK. *Nature Communications*, doi:10.1038/ncomms7769 (2015).
94 McGrath, D. A. *et al.* Cks confers specificity to phosphorylation-dependent CDK signaling pathways. *Nat Struct Mol Biol* **20**, 1407-1414, doi:10.1038/nsmb.2707 (2013).
95 Sitry, D. *et al.* Three different binding sites of Cks1 are required for p27-ubiquitin ligation. *Journal of Biological Chemistry*, doi:10.1074/jbc.M205254200 (2002).
96 Liberal, V. *et al.* Cyclin-dependent kinase subunit (Cks) 1 or Cks2 overexpression overrides the DNA damage response barrier triggered by activated oncoproteins. *Proceedings of the National Academy of Sciences of the United States of America* **109**, 2754-2759, doi:10.1073/pnas.1102434108 (2012).
97 Adams, P. D. *et al.* Identification of a cyclin-cdk2 recognition motif present in substrates and p21-like cyclin-dependent kinase inhibitors. *Molecular and Cellular Biology*, doi:10.1128/mcb.16.12.6623 (1996).
98 Köivomägi, M. *et al.* Cascades of multisite phosphorylation control Sic1 destruction at the onset of S phase. *Nature*, doi:10.1038/nature10560 (2011).
99 Kõivomägi, M. *et al.* Multisite phosphorylation networks as signal processors for Cdk1. *Nat Struct Mol Biol* **20**, 1415-1424, doi:10.1038/nsmb.2706 (2013).
100 Wolthuis, R. *et al.* Cdc20 and Cks Direct the Spindle Checkpoint-Independent Destruction of Cyclin A. *Molecular Cell* **30**, 290-302, doi:https://doi.org/10.1016/j.molcel.2008.02.027 (2008).

101 Örd, M., Venta, R., Möll, K., Valk, E. & Loog, M. Cyclin-Specific Docking Mechanisms Reveal the Complexity of M-CDK Function in the Cell Cycle. *Molecular Cell* **75**, 76-89.e73, doi:10.1016/j.molcel.2019.04.026 (2019).
102 Yu, J. *et al.* Structural basis of human separase regulation by securin and CDK1–cyclin B1. *Nature* **596**, 138-142, doi:10.1038/s41586-021-03764-0 (2021).
103 Yu, V. P. C. C., Baskerville, C., Grünenfelder, B. & Reed, S. I. A Kinase-Independent Function of Cks1 and Cdk1 in Regulation of Transcription. *Molecular Cell* **17**, 145-151, doi:https://doi.org/10.1016/j.molcel.2004.11.020 (2005).
104 Ng, H. H., Dole, S. & Struhl, K. The Rtf1 component of the Paf1 transcriptional elongation complex is required for ubiquitination of histone H2B. *The Journal of biological chemistry* **278**, 33625-33628, doi:10.1074/jbc.C300270200 (2003).
105 Zhang, S., Tischer, T. & Barford, D. Cyclin A2 degradation during the spindle assembly checkpoint requires multiple binding modes to the APC/C. *Nature Communications* **10**, 3863, doi:10.1038/s41467-019-11833-2 (2019).
106 Olsen, J. V. *et al.* Quantitative Phosphoproteomics Reveals Widespread Full Phosphorylation Site Occupancy During Mitosis -- Olsen et al. 3 (104): ra3 -- Science Signaling (Supplemental). *Science signaling* (2010).
107 Hu, Q. *et al.* The Orbitrap: a new mass spectrometer. *Journal of mass spectrometry : JMS* **40**, 430-443, doi:10.1002/jms.856 (2005).
108 Scigelova, M., Hornshaw, M., Giannakopulos, A. & Makarov, A. Fourier transform mass spectrometry. *Mol Cell Proteomics* **10**, M111.009431, doi:10.1074/mcp.M111.009431 (2011).
109 Dephoure, N. *et al.* A quantitative atlas of mitotic phosphorylation. *Proceedings of the National Academy of Sciences of the United States of America*, doi:10.1073/pnas.0805139105 (2008).
110 Pines, J. Cell cycle: Reaching for a role for the Cks proteins. *Current Biology*, doi:10.1016/S0960-9822(96)00741-5 (1996).
111 Samejima, I. *et al.* Mapping the invisible chromatin transactions of prophase chromosome remodeling. *Molecular Cell* **82**, 696-708.e694, doi:https://doi.org/10.1016/j.molcel.2021.12.039 (2022).
112 Caldas, G. V. & DeLuca, J. G. KNL1: bringing order to the kinetochore. *Chromosoma* **123**, 169-181, doi:10.1007/s00412-013-0446-5 (2014).
113 Petrovic, A. *et al.* Structure of the MIS12 Complex and Molecular Basis of Its Interaction with CENP-C at Human Kinetochores. *Cell* **167**, 1028-1040.e1015, doi:10.1016/j.cell.2016.10.005 (2016).
114 Huis in 't Veld, P. J. *et al.* Molecular basis of outer kinetochore assembly on CENP-T. *Elife* **5**, e21007, doi:10.7554/eLife.21007 (2016).
115 Kucharski, T. J. *et al.* Small changes in phospho-occupancy at the kinetochore-microtubule interface drive mitotic fidelity. *J Cell Biol* **221**, doi:10.1083/jcb.202107107 (2022).

116 Huis in 't Veld, P. J., Volkov, V. A., Stender, I. D., Musacchio, A. & Dogterom, M. Molecular determinants of the Ska-Ndc80 interaction and their influence on microtubule tracking and force-coupling. *Elife* **8**, e49539, doi:10.7554/eLife.49539 (2019).
117 Nilsson, J. Mps1-Ndc80: one interaction to rule them all. *Oncotarget* **6**, 16822-16823, doi:10.18632/oncotarget.4837 (2015).
118 Dumitru, A. M. G., Rusin, S. F., Clark, A. E. M., Kettenbach, A. N. & Compton, D. A. Cyclin A/Cdk1 modulates Plk1 activity in prometaphase to regulate kinetochore-microtubule attachment stability. *Elife* **6**, 1-23, doi:10.7554/eLife.29303 (2017).
119 Gong, D. *et al.* Cyclin A2 Regulates Nuclear-Envelope Breakdown and the Nuclear Accumulation of Cyclin B1. *Current Biology*, doi:10.1016/j.cub.2006.11.066 (2007).
120 Mok, J. *et al.* Deciphering protein kinase specificity through large-scale analysis of yeast phosphorylation site motifs.
121 Skopek, T. R., Liber, H. L., Penman, B. W. & Thilly, W. G. Isolation of a human lymphoblastoid line heterozygous at the thymidine kinase locus: possibility for a rapid human cell mutation assay. *Biochemical and biophysical research communications* **84**, 411-416, doi:10.1016/0006-291x(78)90185-7 (1978).
122 Rata, S. *et al.* Two Interlinked Bistable Switches Govern Mitotic Control in Mammalian Cells. *Current biology : CB* **28**, 3824-3832.e3826, doi:10.1016/j.cub.2018.09.059 (2018).
123 Tighe, A., Staples, O. & Taylor, S. Mps1 kinase activity restrains anaphase during an unperturbed mitosis and targets Mad2 to kinetochores. *J Cell Biol* **181**, 893-901, doi:10.1083/jcb.200712028 (2008).
124 Kelly, V., al-Rawi, A., Lewis, D., Kustatscher, G. & Ly, T. Low Cell Number Proteomic Analysis Using In-Cell Protease Digests Reveals a Robust Signature for Cell Cycle State Classification. *Molecular & Cellular Proteomics* **21**, doi:10.1016/j.mcpro.2021.100169 (2022).
125 McAlister, G. C. *et al.* MultiNotch MS3 enables accurate, sensitive, and multiplexed detection of differential expression across cancer cell line proteomes. *Anal Chem* **86**, 7150-7158, doi:10.1021/ac502040v (2014).
126 Cox, J. & Mann, M. MaxQuant enables high peptide identification rates, individualized p.p.b.-range mass accuracies and proteome-wide protein quantification. *Nature Biotechnology* **26**, 1367-1372, doi:10.1038/nbt.1511 (2008).
127 Crooks, G. E., Hon, G., Chandonia, J.-M. & Brenner, S. E. WebLogo: a sequence logo generator. *Genome Res* **14**, 1188-1190, doi:10.1101/gr.849004 (2004).
128 Colaert, N., Helsens, K., Martens, L., Vandekerckhove, J. & Gevaert, K. Improved visualization of protein consensus sequences by iceLogo. *Nature Methods* **6**, 786-787, doi:10.1038/nmeth1109-786 (2009).
129 Kong, A. T., Leprevost, F. V., Avtonomov, D. M., Mellacheruvu, D. & Nesvizhskii, A. I. MSFragger: ultrafast and comprehensive peptide

identification in mass spectrometry-based proteomics. *Nat Methods* **14**, 513-520, doi:10.1038/nmeth.4256 (2017).

130 Wang, F. *et al.* Histone H3 Thr-3 phosphorylation by haspin positions Aurora B at centromeres in mitosis. *Science* **330**, 231-235, doi:10.1126/science.1189435 (2010).

131 Ly, T. *et al.* A proteomic chronology of gene expression through the cell cycle in human myeloid leukemia cells. *Elife* **3**, e01630-e01630, doi:10.7554/eLife.01630 (2014).

132 Lorge, E. *et al.* Standardized cell sources and recommendations for good cell culture practices in genotoxicity testing. *Mutation Research/Genetic Toxicology and Environmental Mutagenesis* **809**, 1-15, doi:https://doi.org/10.1016/j.mrgentox.2016.08.001 (2016).

133 Hendzel, M. J. *et al.* Mitosis-specific phosphorylation of histone H3 initiates primarily within pericentromeric heterochromatin during G2 and spreads in an ordered fashion coincident with mitotic chromosome condensation. *Chromosoma* **106**, 348-360, doi:10.1007/s004120050256 (1997).

134 Michowski, W. *et al.* Cdk1 Controls Global Epigenetic Landscape in Embryonic Stem Cells. *Molecular Cell*, doi:10.1016/j.molcel.2020.03.010 (2020).

135 Ruppert, J. G. *et al.* HP1α targets the chromosomal passenger complex for activation at heterochromatin before mitotic entry. *EMBO J* **37**, e97677, doi:10.15252/embj.201797677 (2018).

136 Yi, Q. *et al.* Aurora B kinase activity-dependent and -independent functions of the chromosomal passenger complex in regulating sister chromatid cohesion. *The Journal of biological chemistry* **294**, 2021-2035, doi:10.1074/jbc.RA118.005978 (2019).

137 Kim, H. J., Kwon, H. R., Bae, C. D., Park, J. & Hong, K. U. Specific primary sequence requirements for Aurora B kinase-mediated phosphorylation and subcellular localization of TMAP during mitosis. *Cell Cycle* **9**, 2027-2036, doi:10.4161/cc.9.10.11753 (2010).

138 Berod, A., Hartman, B. K. & Pujol, J. F. Importance of fixation in immunohistochemistry: use of formaldehyde solutions at variable pH for the localization of tyrosine hydroxylase. *The journal of histochemistry and cytochemistry : official journal of the Histochemistry Society* **29**, 844-850, doi:10.1177/29.7.6167611 (1981).

139 Vadakke-Madathil, S., Limaye, L. S., Kale, V. P. & Chaudhry, H. W. Flow Cytometry and Cell Sorting Using Hematopoietic Progenitor Cells. *Methods in molecular biology (Clifton, N.J.)* **2029**, 235-246, doi:10.1007/978-1-4939-9631-5_18 (2019).

140 Li, Y. *et al.* The effects of chemical fixation on the cellular nanostructure. *Experimental cell research* **358**, 253-259, doi:10.1016/j.yexcr.2017.06.022 (2017).

141 Yamazaki, K., Iwura, T., Ishikawa, R. & Ozaki, Y. Methanol-induced tertiary and secondary structure changes of granulocyte-colony stimulating factor. *Journal of biochemistry* **140**, 49-56, doi:10.1093/jb/mvj133 (2006).
142 Im, K., Mareninov, S., Diaz, M. F. P. & Yong, W. H. An Introduction to Performing Immunofluorescence Staining. *Methods in molecular biology (Clifton, N.J.)* **1897**, 299-311, doi:10.1007/978-1-4939-8935-5_26 (2019).
143 Örd, M. & Loog, M. How the cell cycle clock ticks. *Mol Biol Cell* **30**, 169-172, doi:10.1091/mbc.E18-05-0272 (2019).
144 Ding, L. *et al.* The Roles of Cyclin-Dependent Kinases in Cell-Cycle Progression and Therapeutic Strategies in Human Breast Cancer. *International journal of molecular sciences* **21**, doi:10.3390/ijms21061960 (2020).
145 Brown, N. R. *et al.* The crystal structure of cyclin A. *Structure* **3**, 1235-1247, doi:https://doi.org/10.1016/S0969-2126(01)00259-3 (1995).
146 Liu, D. *et al.* Cyclin A1 is required for meiosis in the male mouse.
147 Hayward, D. *et al.* CDK1-CCNB1 creates a spindle checkpoint-permissive state by enabling MPS1 kinetochore localization. *J Cell Biol* **218**, 1182-1199, doi:10.1083/jcb.201808014 (2019).
148 Holder, J., Mohammed, S. & Barr, F. A. Ordered dephosphorylation initiated by the selective proteolysis of cyclin B drives mitotic exit. *Elife*, doi:10.7554/ELIFE.59885 (2020).
149 Khattar, V. & Thottassery, J. V. Cks1: Structure, Emerging Roles and Implications in Multiple Cancers. *Journal of cancer therapy* **4**, 1341-1354, doi:10.4236/jct.2013.48159 (2013).
150 Siddiqui, K., On, K. F. & Diffley, J. F. Regulating DNA replication in eukarya. *Cold Spring Harbor perspectives in biology* **5**, doi:10.1101/cshperspect.a012930 (2013).
151 Cuylen, S. *et al.* Ki-67 acts as a biological surfactant to disperse mitotic chromosomes. *Nature*, doi:10.1038/nature18610 (2016).
152 Shiomi, Y. *et al.* Two different replication factor C proteins, Ctf18 and RFC1, separately control PCNA-CRL4Cdt2-mediated Cdt1 proteolysis during S phase and following UV irradiation. *Mol Cell Biol* **32**, 2279-2288, doi:10.1128/mcb.06506-11 (2012).
153 Zhang, L. *et al.* Depletion of thymopoietin inhibits proliferation and induces cell cycle arrest/apoptosis in glioblastoma cells. *World Journal of Surgical Oncology* **14**, 267, doi:10.1186/s12957-016-1018-y (2016).
154 McHugh, T. *et al.* The depolymerase activity of MCAK shows a graded response to Aurora B kinase phosphorylation through allosteric regulation. *Journal of cell science* **132**, doi:10.1242/jcs.228353 (2019).
155 Schmidt, Jens C. *et al.* The Kinetochore-Bound Ska1 Complex Tracks Depolymerizing Microtubules and Binds to Curved Protofilaments. *Developmental Cell* **23**, 968-980, doi:https://doi.org/10.1016/j.devcel.2012.09.012 (2012).

156 Martin, K. *et al.* Quantitative analysis of protein phosphorylation status and protein kinase activity on microarrays using a novel fluorescent phosphorylation sensor dye. *Proteomics* **3**, 1244-1255, doi:10.1002/pmic.200300445 (2003).
157 Ferrell, J. E., Jr. Building a cellular switch: more lessons from a good egg. *BioEssays : news and reviews in molecular, cellular and developmental biology* **21**, 866-870, doi:10.1002/(sici)1521-1878(199910)21:10<866::Aid-bies9>3.0.Co;2-1 (1999).
158 Venta, R. *et al.* A processive phosphorylation circuit with multiple kinase inputs and mutually diversional routes controls G1/S decision. *Nature Communications* **11**, 1836, doi:10.1038/s41467-020-15685-z (2020).
159 Pereverzeva, I., Whitmire, E., Khan, B. & Coué, M. Distinct Phosphoisoforms of the XenopusMcm4 Protein Regulate the Function of the Mcm Complex. *Molecular and Cellular Biology* **20**, 3667-3676, doi:10.1128/MCB.20.10.3667-3676.2000 (2000).
160 Chen, C. *et al.* Identification of a Major Determinant for Serine-Threonine Kinase Phosphoacceptor Specificity. *Molecular Cell* **53**, 140-147, doi:10.1016/j.molcel.2013.11.013 (2014).
161 Bishop, A. C. *et al.* A chemical switch for inhibitor-sensitive alleles of any protein kinase. *Nature* **407**, 395-401, doi:10.1038/35030148 (2000).
162 Singh, P. *et al.* BUB1 and CENP-U, Primed by CDK1, Are the Main PLK1 Kinetochore Receptors in Mitosis. *Molecular Cell* **81**, 67-87.e69, doi:https://doi.org/10.1016/j.molcel.2020.10.040 (2021).
163 Cheerambathur, D. K. *et al.* Dephosphorylation of the Ndc80 Tail Stabilizes Kinetochore-Microtubule Attachments via the Ska Complex. *Developmental Cell* **41**, 424-437.e424, doi:https://doi.org/10.1016/j.devcel.2017.04.013 (2017).
164 Abad, M. A. *et al.* Structural basis for microtubule recognition by the human kinetochore Ska complex. *Nature communications* **5**, 2964, doi:10.1038/ncomms3964 (2014).
165 Hochegger, H. *et al.* An essential role for Cdk1 in S phase control is revealed via chemical genetics in vertebrate cells. *Journal of Cell Biology* **178**, 257-268, doi:10.1083/jcb.200702034 (2007).
166 Redli, P. M., Gasic, I., Meraldi, P., Nigg, E. A. & Santamaria, A. The Ska complex promotes Aurora B activity to ensure chromosome biorientation. *Journal of Cell Biology*, doi:10.1083/jcb.201603019 (2016).
167 Welburn, J. P. I. *et al.* The Human Kinetochore Ska1 Complex Facilitates Microtubule Depolymerization-Coupled Motility. *Developmental Cell* **16**, 374-385, doi:10.1016/J.DEVCEL.2009.01.011 (2009).
168 Holt, L. J. *et al.* Global analysis of cdk1 substrate phosphorylation sites provides insiqhts into evolution. *Science*, doi:10.1126/science.1172867 (2009).
169 Gavet, O. & Pines, J. Progressive Activation of CyclinB1-Cdk1 Coordinates Entry to Mitosis. *Developmental Cell*, doi:10.1016/j.devcel.2010.02.013 (2010).

170 Söderberg, O. *et al.* Direct observation of individual endogenous protein complexes in situ by proximity ligation. *Nature Methods* **3**, 995-1000, doi:10.1038/nmeth947 (2006).
171 Örd, M. *et al.* Multisite phosphorylation code of CDK. *Nat Struct Mol Biol* **26**, 649-658, doi:10.1038/s41594-019-0256-4 (2019).
172 Toyoshima, F., Moriguchi, T., Wada, A., Fukuda, M. & Nishida, E. Nuclear export of cyclin B1 and its possible role in the DNA damage-induced G2 checkpoint. *EMBO J* **17**, 2728-2735, doi:10.1093/emboj/17.10.2728 (1998).
173 Kõivomägi, M. *et al.* Cascades of multisite phosphorylation control Sic1 destruction at the onset of S phase. *Nature* **480**, 128-131, doi:10.1038/nature10560 (2011).
174 Bouchoux, C. & Uhlmann, F. A quantitative model for ordered Cdk substrate dephosphorylation during mitotic exit. *Cell*, doi:10.1016/j.cell.2011.09.047 (2011).
175 Basu, S., Greenwood, J., Jones, A. W. & Nurse, P. Core control principles of the eukaryotic cell cycle. *Nature* **607**, 381-386, doi:10.1038/s41586-022-04798-8 (2022).